Superconducting electronics

from Josephson effects to quantum computing

by Pascal Febvre and Paul Seidel

Superconducting electronics – Part 5 Digital electronics

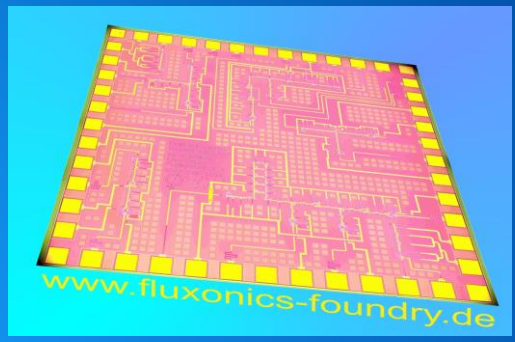

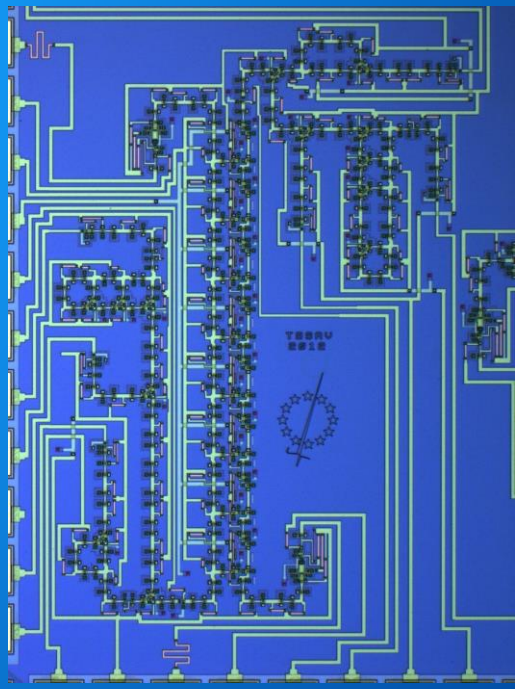

Outline

- Basic principles for superconducting electronics
- The Josephson junction
- The SQUID (Superconducting QUantum Interference Device)
- Digital electronics based on Josephson junctions
    1. The superconducting latching logic of the 80's
    2. The Rapid-Single-Flux-Quantum (RSFQ) logic
- Introduction to comparators
- Analog-to-digital conversion with Josephson junctions
    1. hysteretic junctions
    2. non-hysteretic junctions
- The DC-to-SFQ interface as a comparator
- The Quasi-One-Junction SQUID comparator
- The balanced comparator
- Applications of RSFQ logic

Vector potential & electrical potential

Maxwell equations + $\vec{B} = \vec{\nabla} \wedge \vec{A}$ & $\vec{E} = -\frac{\partial \vec{A}}{\partial t} - \vec{\nabla} U$

B & E uniques though the number of couples (A,U) is infinite (depends on the chosen gauge)

Lagrange function $L(r, \dot{r}, t) = \frac{1}{2} m \dot{r}^2 + q\, \dot{r}\, A(r,t) - q\, U(r,t)$

Hamilton function $H(r, p, t) = \frac{1}{2m} \left[p - q\, A(r,t) \right]^2 + q\, U(r,t)$

with time-dependent Schrödinger equation, lead to :

$\vec{J} = \frac{\rho \hbar}{2 m_e} \left(\vec{\nabla} \varphi - \frac{2\pi}{\Phi_0} \vec{A} \right)$ where $\Phi_0 = \frac{h}{2e}$ is the quantum of magnetic flux

Relation between magnetic flux & phase (1/2)

Case of normal metals:

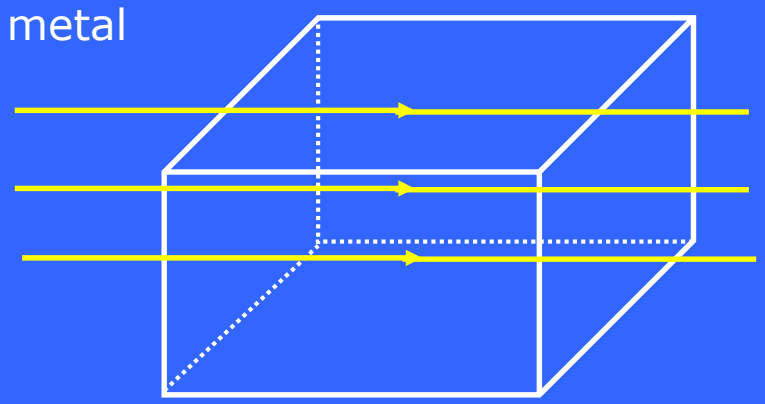

Faraday's law:

$$i_{induit} = \frac{1}{R}\frac{\P f(t)}{\P t}$$

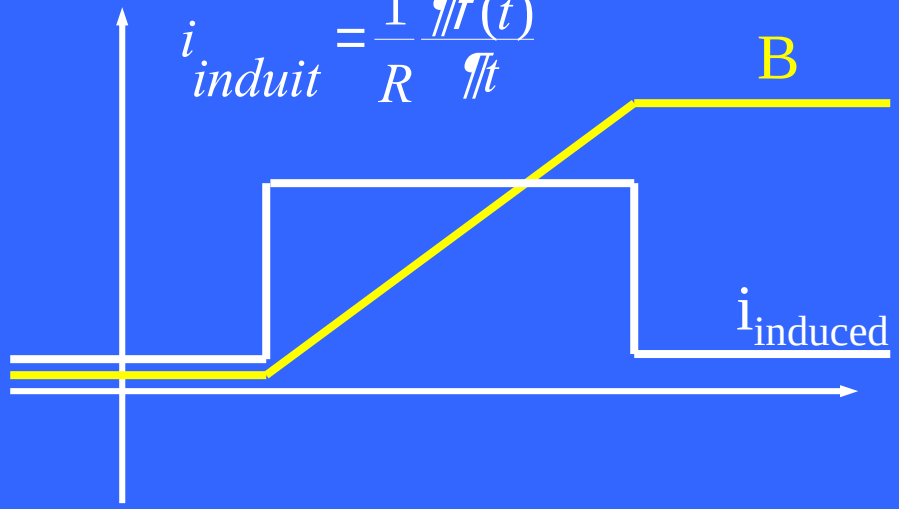

Relation between magnetic flux & phase (2/2)

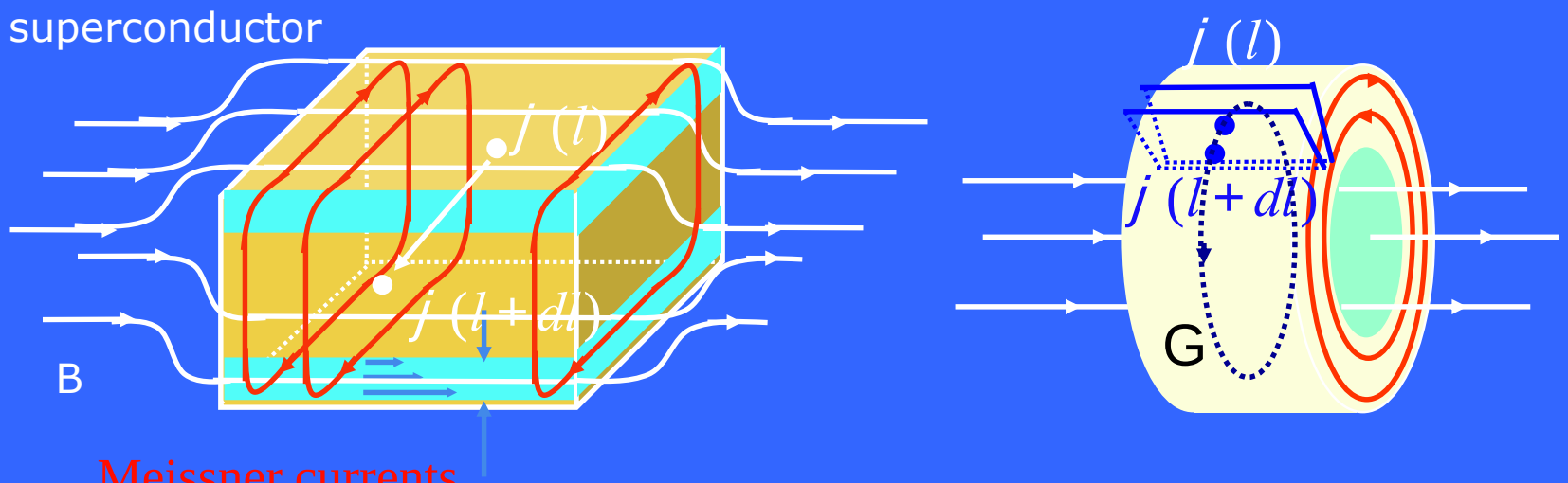

Meissner currents (diamagnetism)

λ_L : London penetration depth

$$\vec{J} = \frac{\rho \hbar}{2 m_e}\left(\vec{\nabla}\varphi - \frac{2\pi}{\Phi_0}\vec{A}\right) = \vec{0} \; on \; \Gamma \quad \Rightarrow \quad \oint_\Gamma \vec{\nabla}\varphi \cdot \vec{dl} = 2n\pi = \frac{2\pi}{\Phi_0}\Phi_{loop}$$

$$\Phi_{loop} = n\Phi_0$$

Flux quantization

$$j(l+dl) - j(l) = \frac{2p}{\Phi_0}\Phi_{length\ dl}$$

Phase – flux relation
Aharonov-Bohm effect

Phases, flux and inductances

$$j\,(l+dl) - j\,(l) = \frac{2p}{F_0} F_{dl}$$

$$F_{dl} = L_{dl}\, I$$

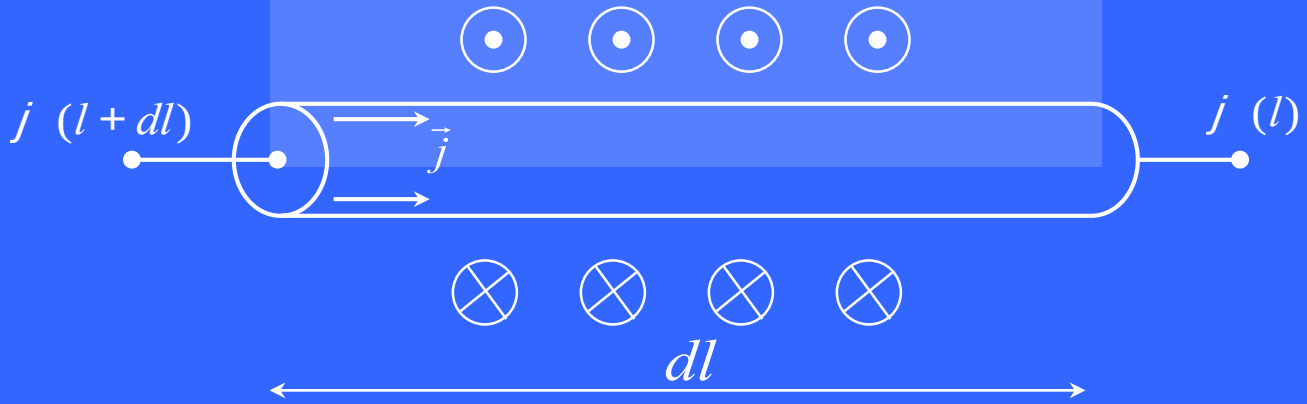

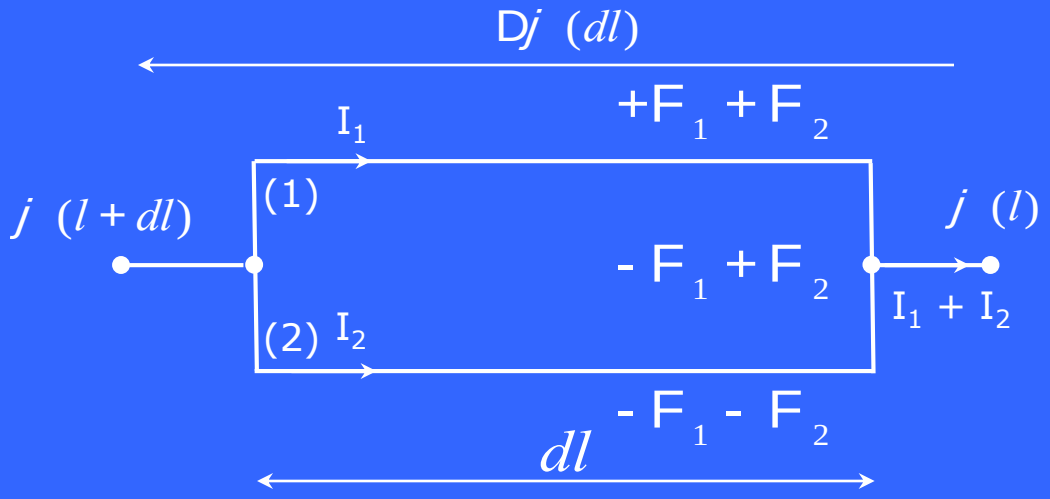

$$-F_1 + F_2 = 2np$$

$$\rightarrow L_1 I_1 = L_2 I_2$$

if no flux in the loop ; same current distribution as with

$$R_1 I_1 = R_2 I_2$$

The Josephson junction

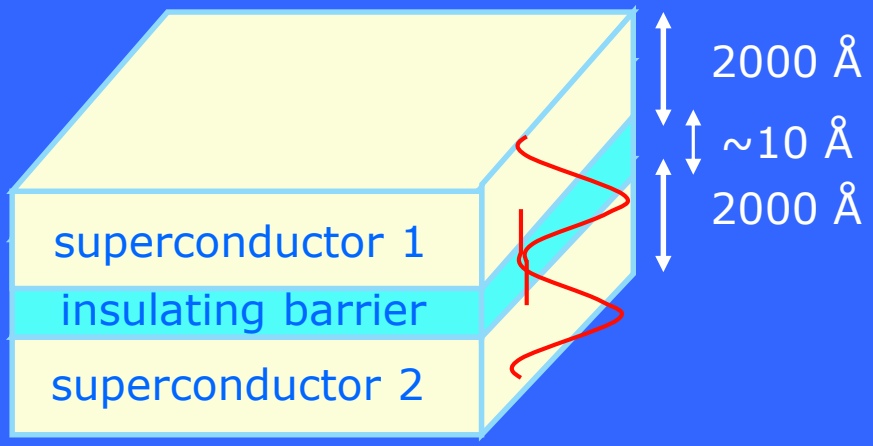

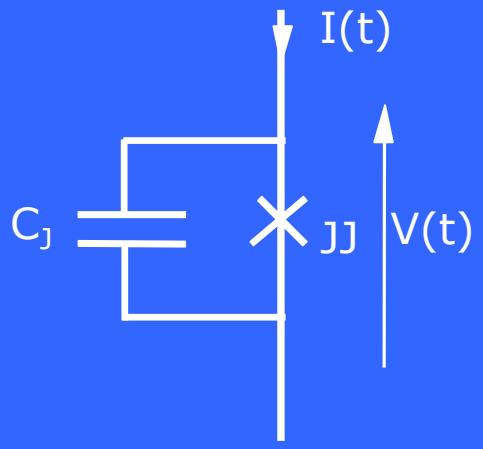

$\psi_i = \psi_{i_0} e^{i\varphi_i(t)}$ $\varphi = \varphi_1 - \varphi_2$: phase difference between the two wavefunctions

Josephson equations: $I_J = I_c \sin\varphi(t)$ $\frac{\partial\varphi(t)}{\partial t} = \frac{2\pi}{\Phi_0} V(t)$

DC Josephson effect at V = 0 :

$I_{J0} = I_c \sin\varphi_0$

ac Josephson effect at V_0 = cste :

$I_J = I_c \sin\left(\frac{2\pi}{\Phi_0} V_0 t\right) = I_c \sin\left(2\pi f_J t\right)$

with f_J = 484 GHz/mV (Josephson relation)

The Josephson junction

Josephson junction: equivalent to the transistor for semiconductor electronics

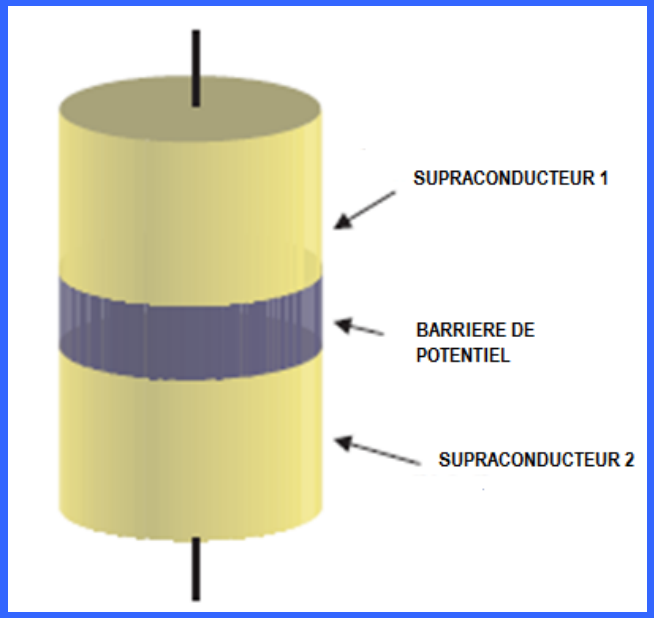

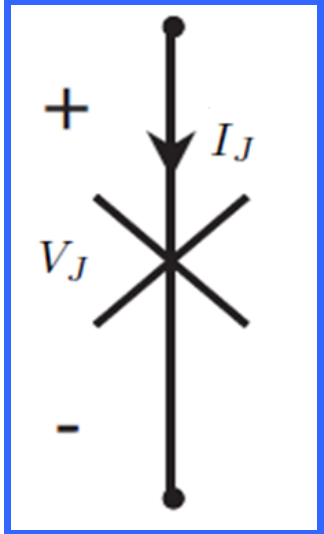

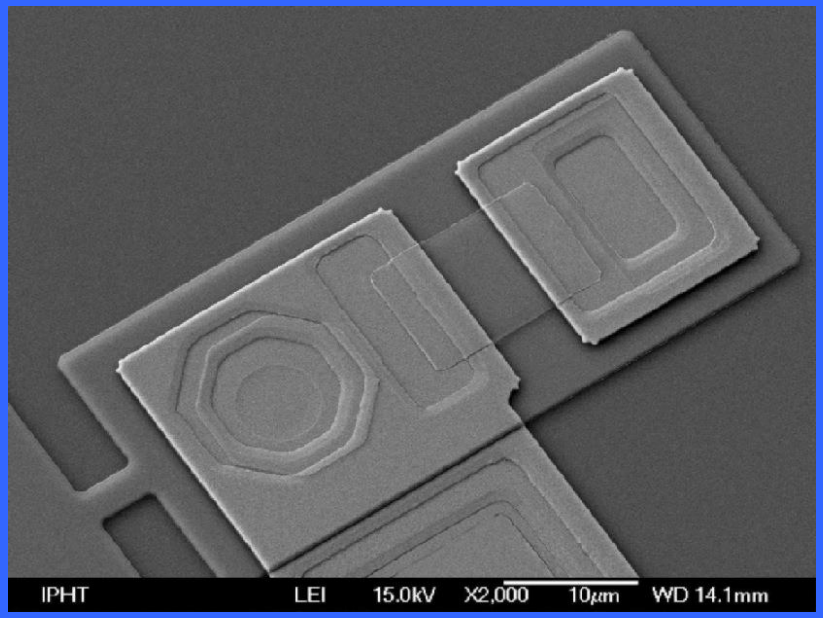

Materials commonly used: Nb/Al-AlOx/Nb @4.2 K

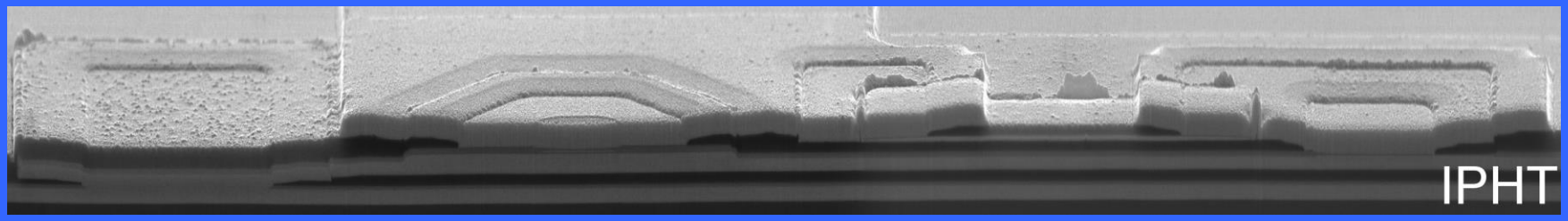

3 μm

I-V characteristic of a Josephson junction

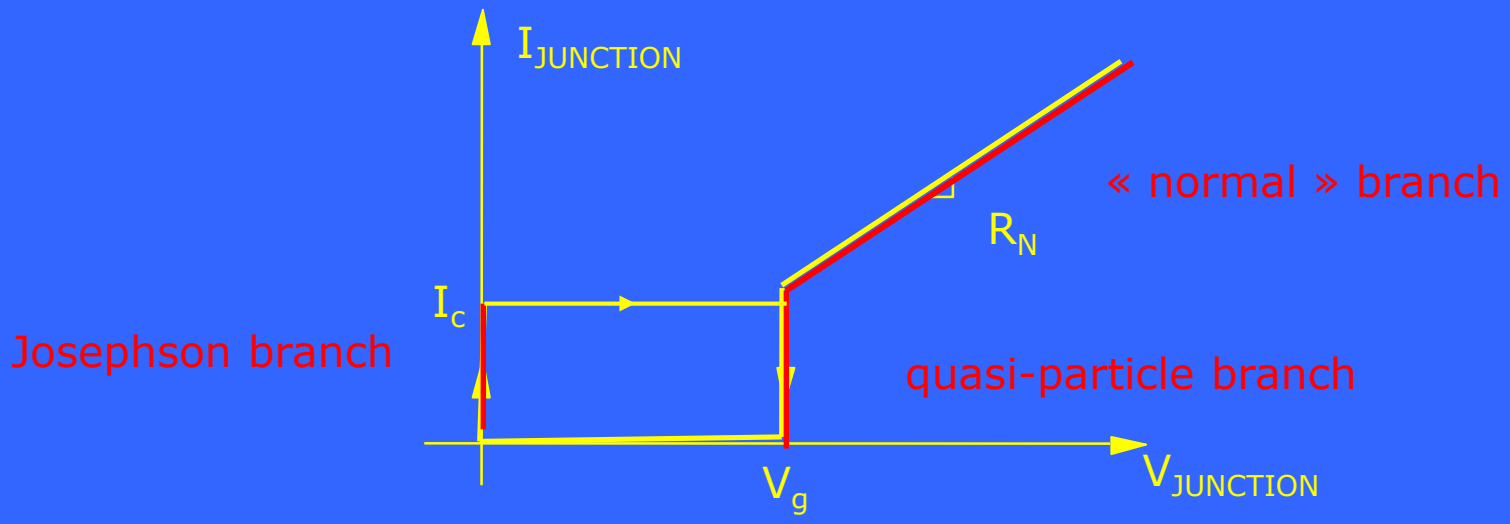

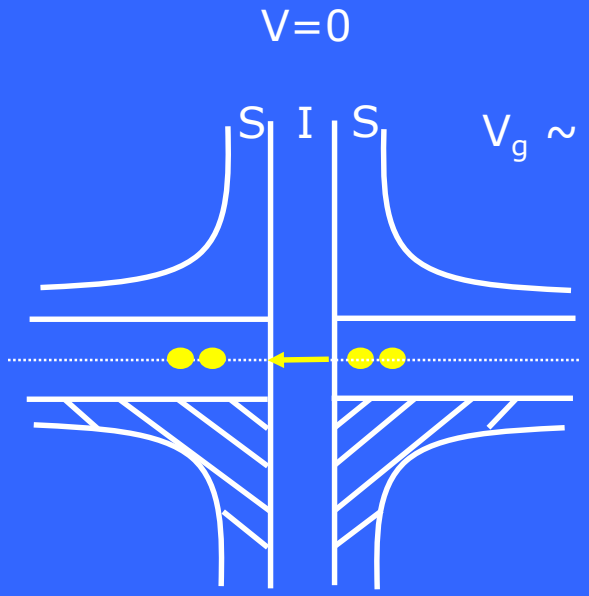

for niobium:
$V_g \sim 2.85$ mV and $f_g \sim 680$ GHz

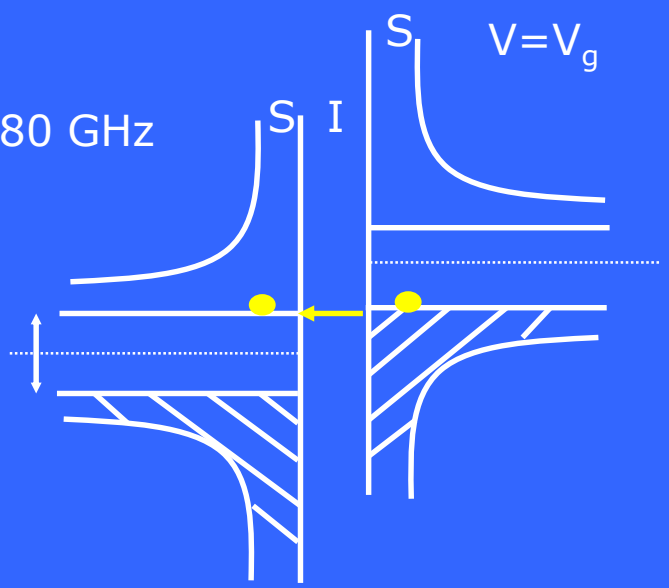

$$eV_g = 2\Delta$$

The superconducting latching logic of the 80's

Absence of resistance of superconductors combined with characteristic frequencies of a few hundreds GHz →

- development of a static logic in the eighties (IBM ; MITI)
- based on hysteretic Josephson junctions

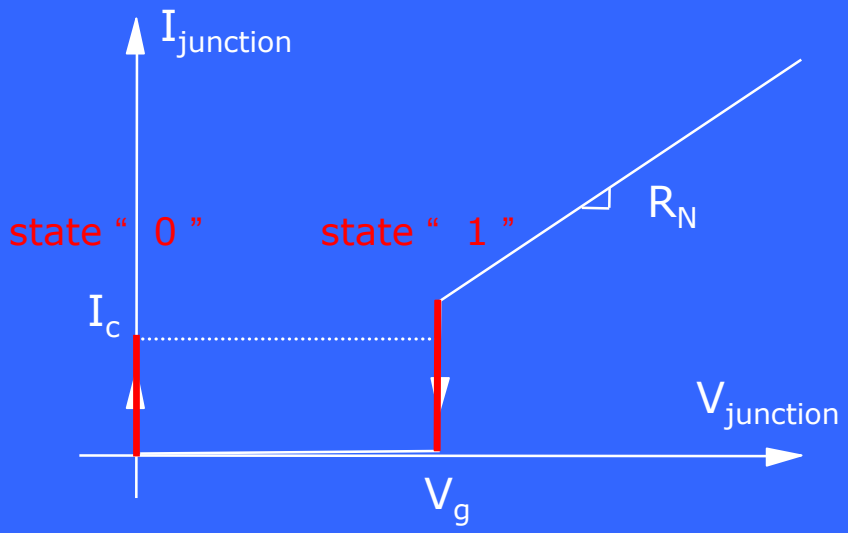

Outcome:

- clock frequencies of a few GHz limited by the punch-through effect
- with the drawback of cryogenic cooling
- period of intense research & development still used today

End of the eighties: Konstantin K. Likharev & his team (Moscow State University) proposed a superconducting logic based on quanta of magnetic flux :

a dynamic logic which relies on the use of shunted Josephson junctions

Josephson junction electrodynamics

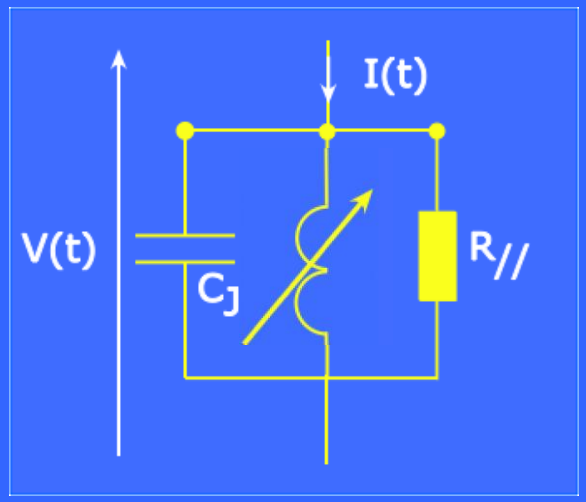

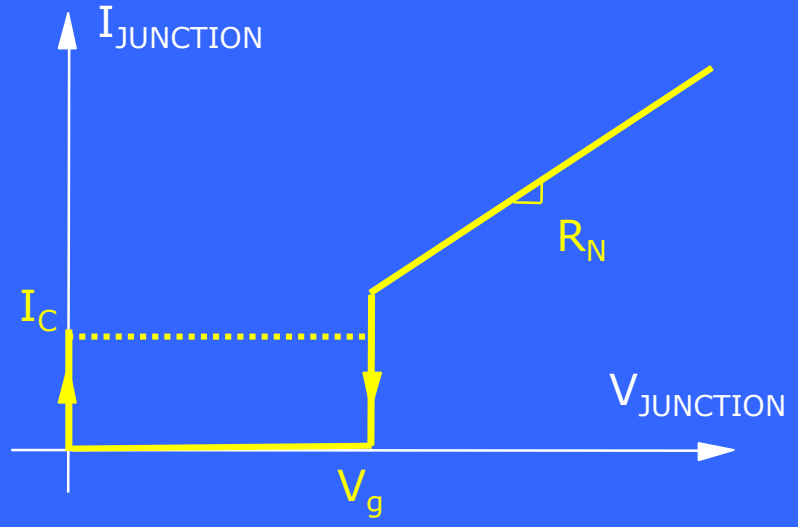

$$I(t) = I_C(t) + I_J(t) + I_R(t)$$

$$I_J(t) = I_c \sin j(t)$$

$$I_C(t) = C_J \frac{\P V(t)}{\P t}$$

$$I_R(t) = \frac{V(t)}{R_{//}}$$

2nd Josephson equation (Faraday's law): $V(t) = \frac{\Phi_0}{2p} \frac{\P j(t)}{\P t}$

$$\rightarrow V(t) = \frac{\Phi_0}{2p}\left[\frac{1}{I_c \cos j(t)} \frac{\partial I_J(t)}{\partial t}\right] = L_J \frac{\partial I_J(t)}{\partial t}$$

$$L_J = \frac{L_{J_0}}{\cos j(t)} \text{ with } L_{J_0} = \frac{\Phi_0}{2p I_c}$$ Josephson inductance

$\rightarrow$ JJ = non-linear parallel RLC circuit

Characteristic time constants & frequencies

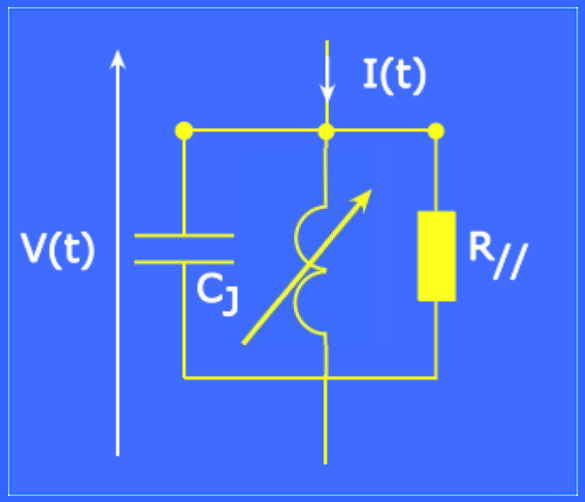

$$\frac{I(t)}{I_c} = L_{J_0} C_J \frac{\partial^2 j(t)}{\partial t^2} + \frac{L_{J_0}}{R_{//}} \frac{\partial j(t)}{\partial t} + \sin j(t)$$

Anharmonic oscillator

Electrical approach

Physical approach (BCS theory)

Plasma period of the L-C circuit :

$$t_p = 2\pi\sqrt{L_{J0} C_J}$$

$$t_p = \sqrt{\frac{2\pi \Phi_0 C_S}{j_C}}$$

L-R circuit time constant :

$$t_c = \frac{L_{J0}}{R_{//}}$$

$$t_c = \frac{2\Phi_0}{\pi^2 V_g}$$

Nb: 0.15 ps
NbN: 0.07 ps

R-C circuit time constant :

$$t_{RC} = R_{//} C_J$$

$$t_{RC} = \frac{\pi V_g C_S}{4 j_C}$$

Linearized approach

$$If\ j(t) \ll 1 \qquad \frac{I(t)}{I_c} = L_{J_0} C_J \frac{\partial^2 j(t)}{\partial t^2} + \frac{L_{J_0}}{R_{//}} \frac{\partial j(t)}{\partial t} + j(t)$$

Damping coefficient: $x = \frac{1}{2R_{//}} \sqrt{\frac{L_{J_0}}{C_J}}$

Quality factor: $Q = \frac{1}{2x} = R_{//} \sqrt{\frac{C_J}{L_{J_0}}}$

For damped oscillatory regimes, transients evolve as: $e^{-\frac{t}{2R_{//}C_J}} = e^{-\frac{t}{2t_{RC}}}$

Example:
SIS junction used in radio-astronomy:
R_N=12 οημσ ; C_J = 190 fF ; I_c = 200 μA

$$t_{LR} = 0.13 ps$$
$$t_p = 3.5 ps$$
$$t_{RC} = 2.3 ps$$

Criteria : $f_{\max} = \frac{1}{12\, t_{RC}}$

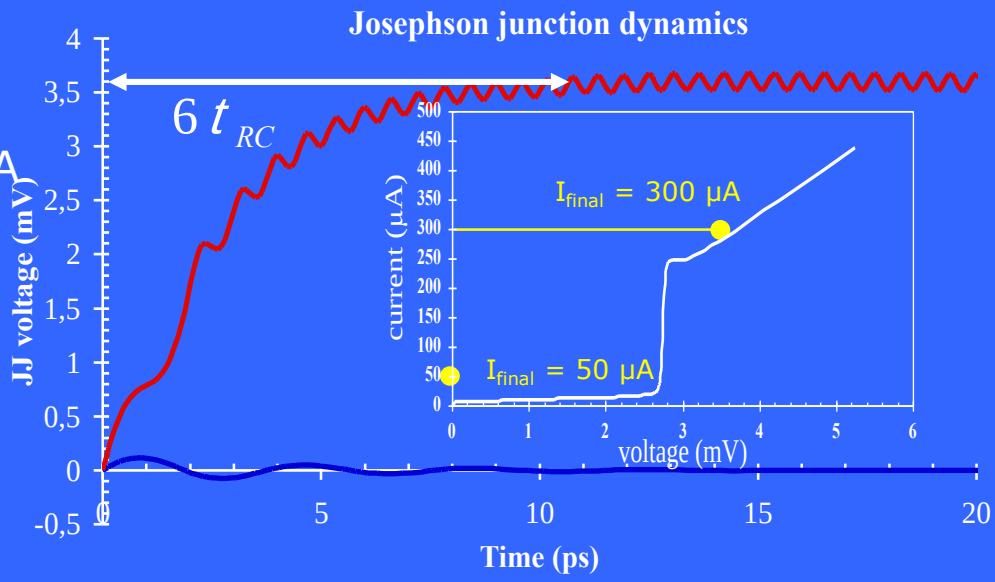

Limitations of the static logic

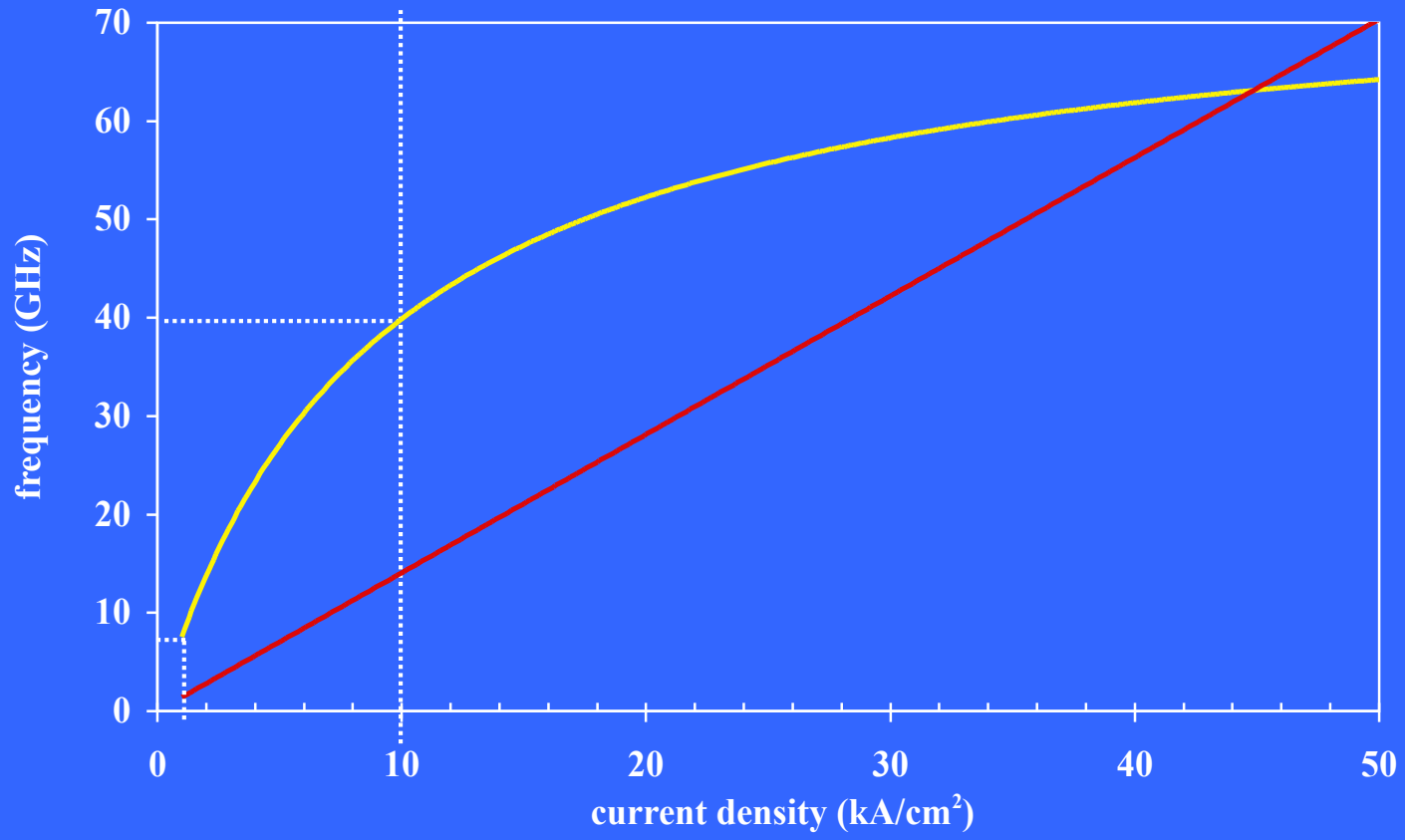

Reduce the switching time

→ Reduce the R-C time constant

→ Reduce R

Minimising the switching time

$$t_p = 2p\sqrt{L_{J0}C_J}$$

L-C circuit plasma period

$$t_{LR} = \frac{L_{J0}}{R_{//}}$$

L-R circuit time constant

$$t_{RC} = R_{//}C_J$$

R-C circuit time constant

McCumber parameter defined by: $$b_c = \frac{t_{RC}}{t_{LR}} = \frac{R_{//}^2 C_J}{L_{J_0}} = \frac{2p R_{//}^2 C_J I_c}{\Phi_0}$$

Minimum switching time obtained for : $$t_{RC} = t_{LR}\left(= \frac{t_p}{2p}\right) : b_c = 1$$

$$R_{//} \gg R_{shunt}$$

New time constant

$$t_0 = \sqrt{\frac{\Phi_0 C_S}{2p j_c}} = \frac{\Phi_0}{2p R_{shunt} I_c}$$

$$t_0(ps) \gg \frac{1}{pV_c(mV)} \text{ with } V_c = R_{shunt} I_c$$

Criteria: $f_{max} = 1/(2\pi\tau_0)$

f_{max}(GHz) = 500 x V_c(mV)

Maximum frequency of operation

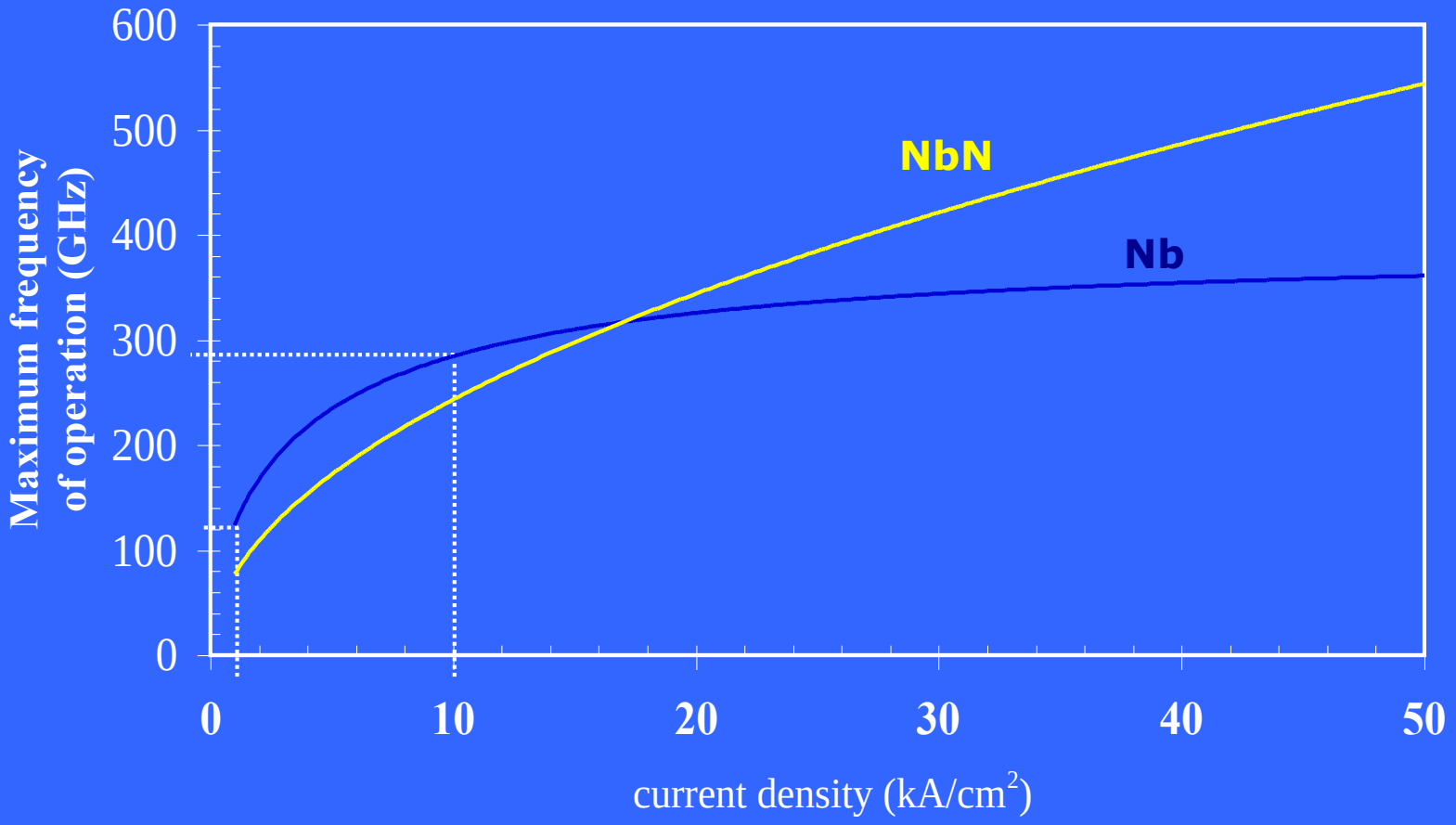

Valid for externally-shunted SIS junctions

Influence of the McCumber parameter

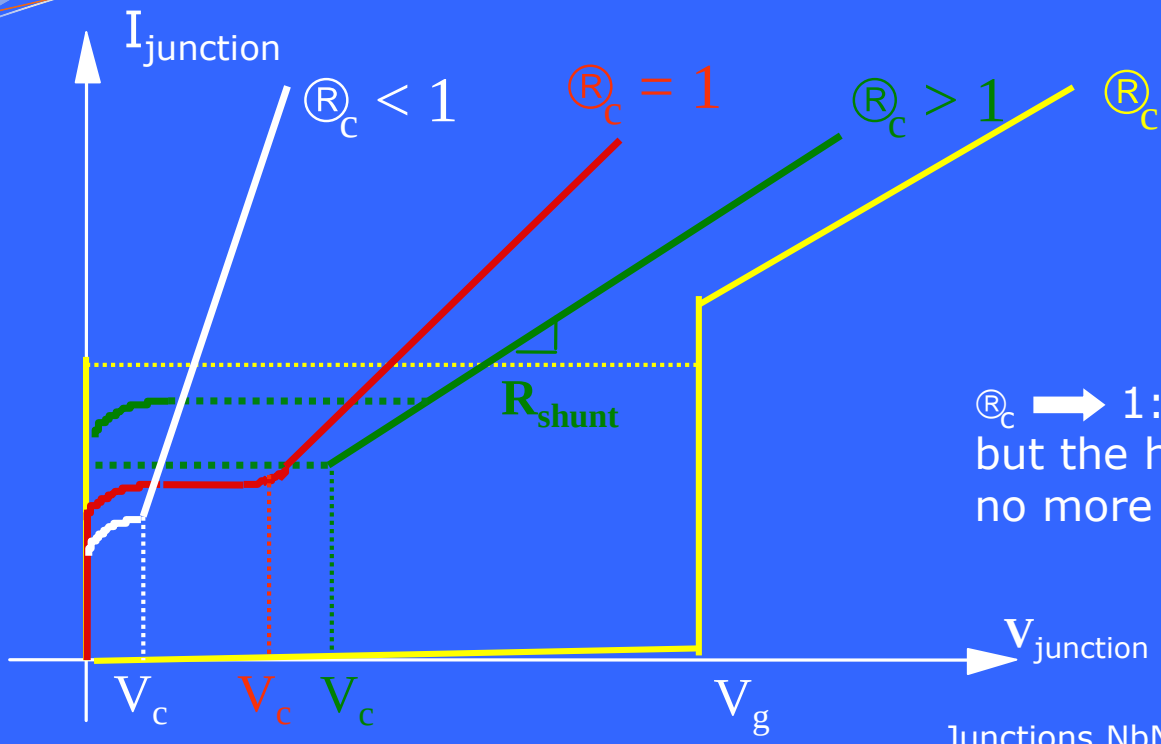

$®_c \rightarrow 1$: f_{max} ↗
but the hysteresis disappears:
no more switching between 2 states

Junctions NbN/MgO/NbN - CEA-INAC Grenoble

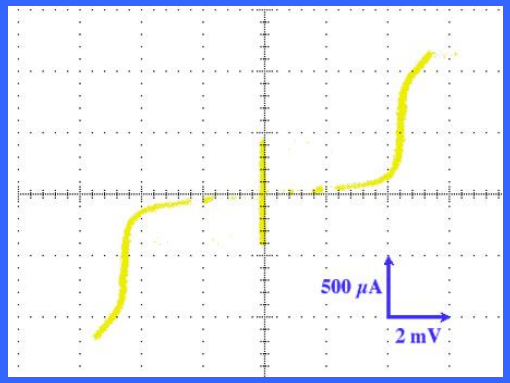

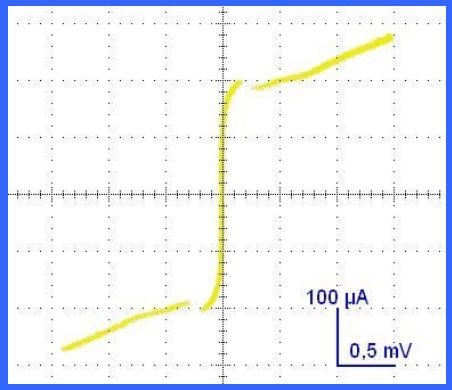

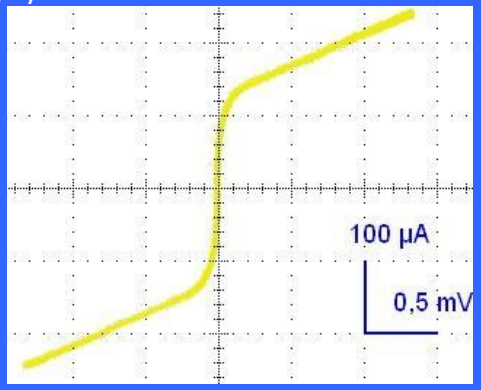

I-V characteristics of Josephson junctions

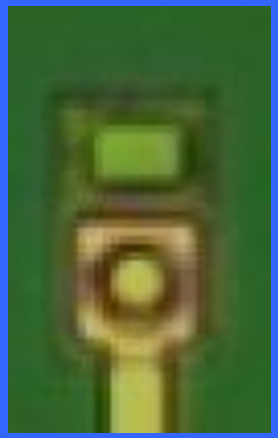

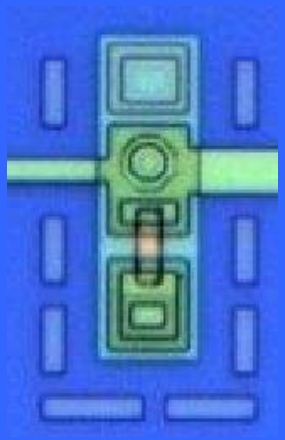

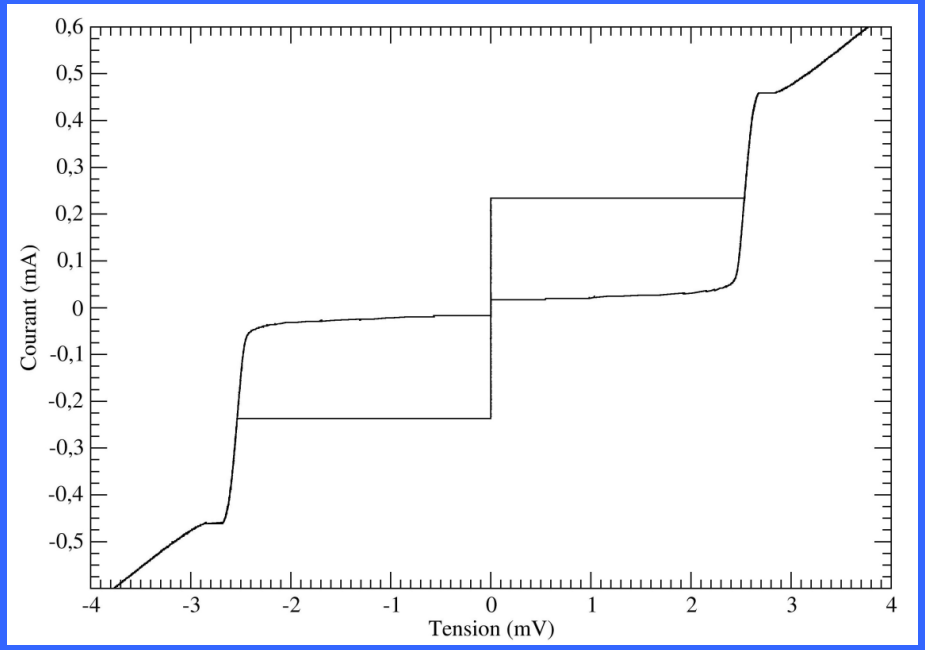

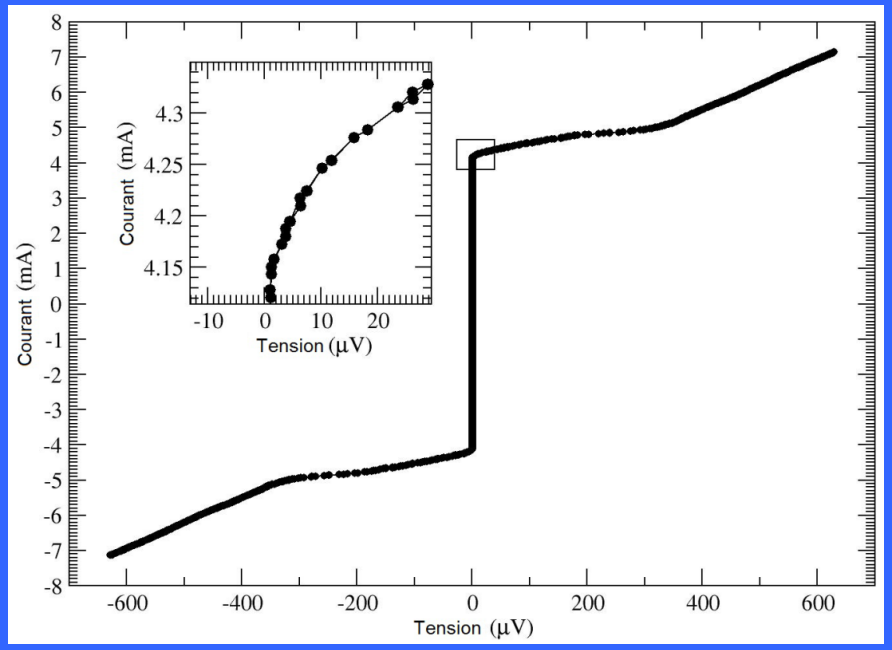

Josephson junction dynamics

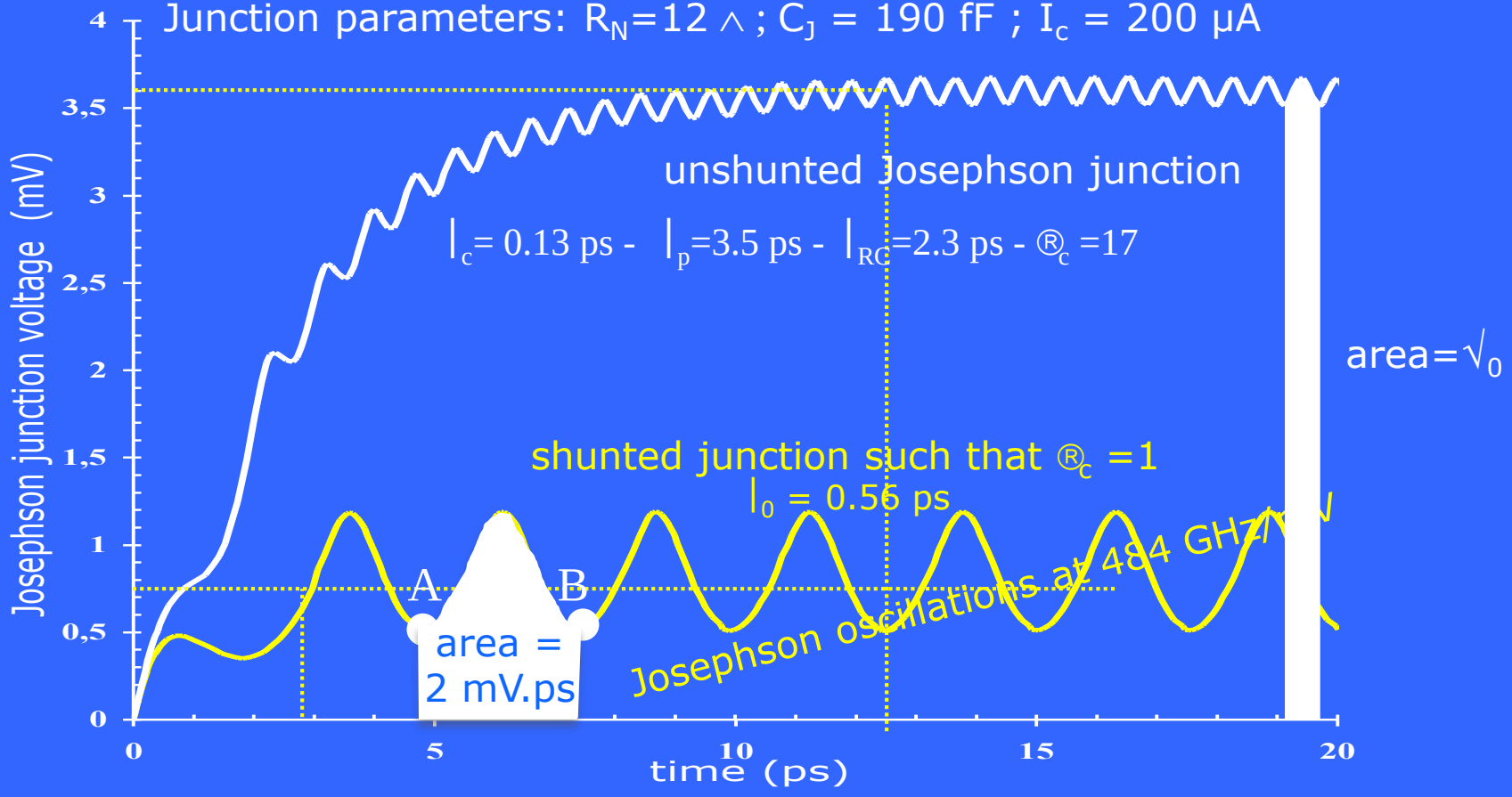

$$I = C_J \frac{\P V(t)}{\P t} + \frac{1}{R_{shunt}} V(t) + I_c \sin j\,(t) \quad \rightarrow \quad \begin{cases} \mathrm{D}j = 2p \\ \int_A^B V(t)\,dt = \mathrm{F}_0 \end{cases}$$

Dynamics of shunted Josephson junctions

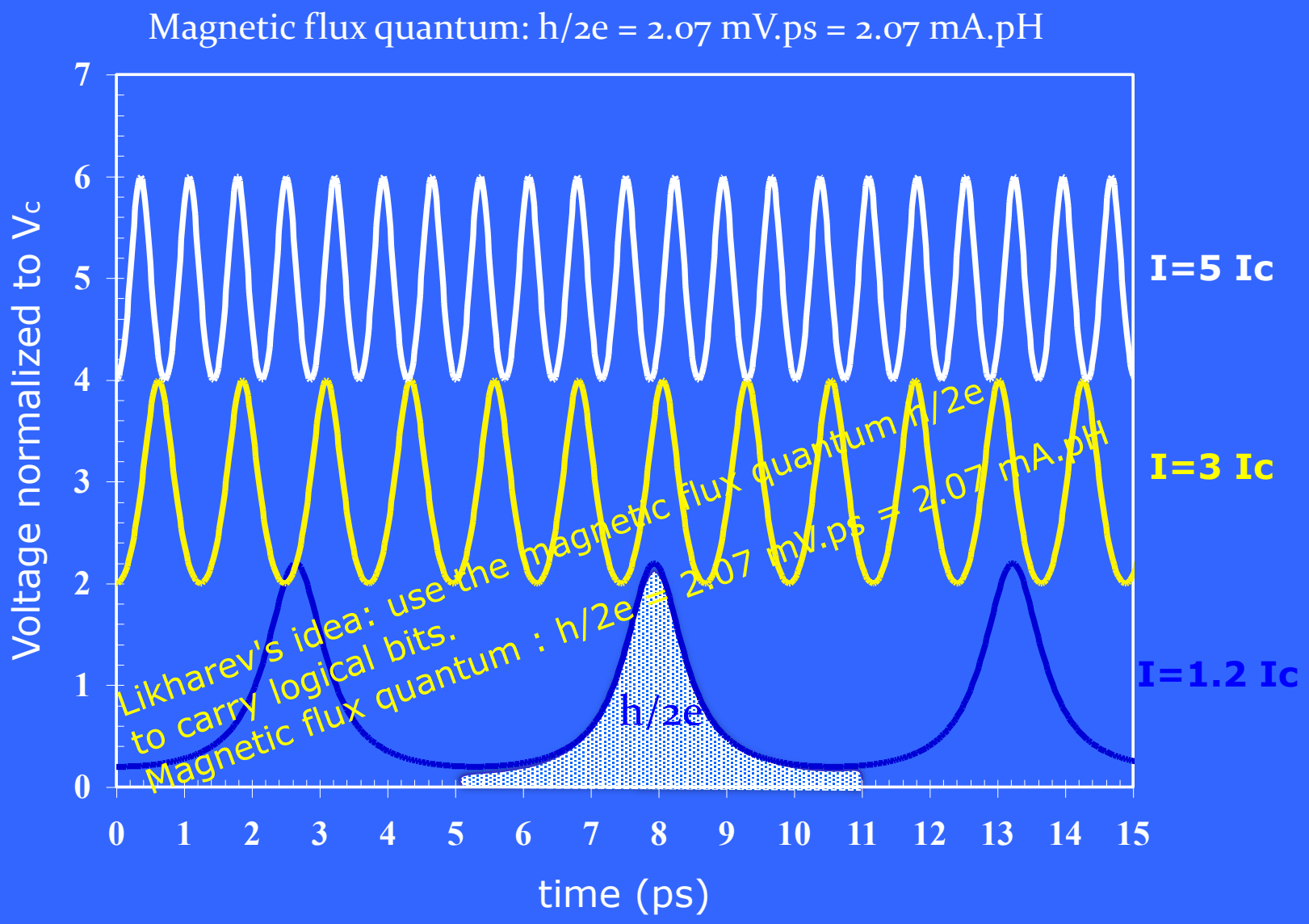

This dynamic logic is called Rapid Single Flux Quantum (RSFQ)

On-chip RSFQ clock

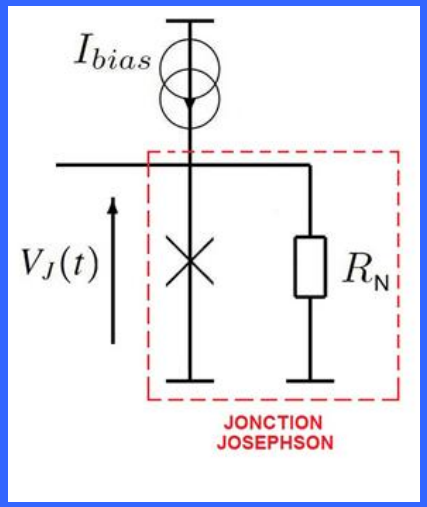

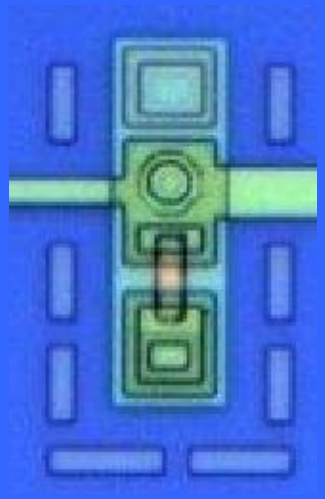

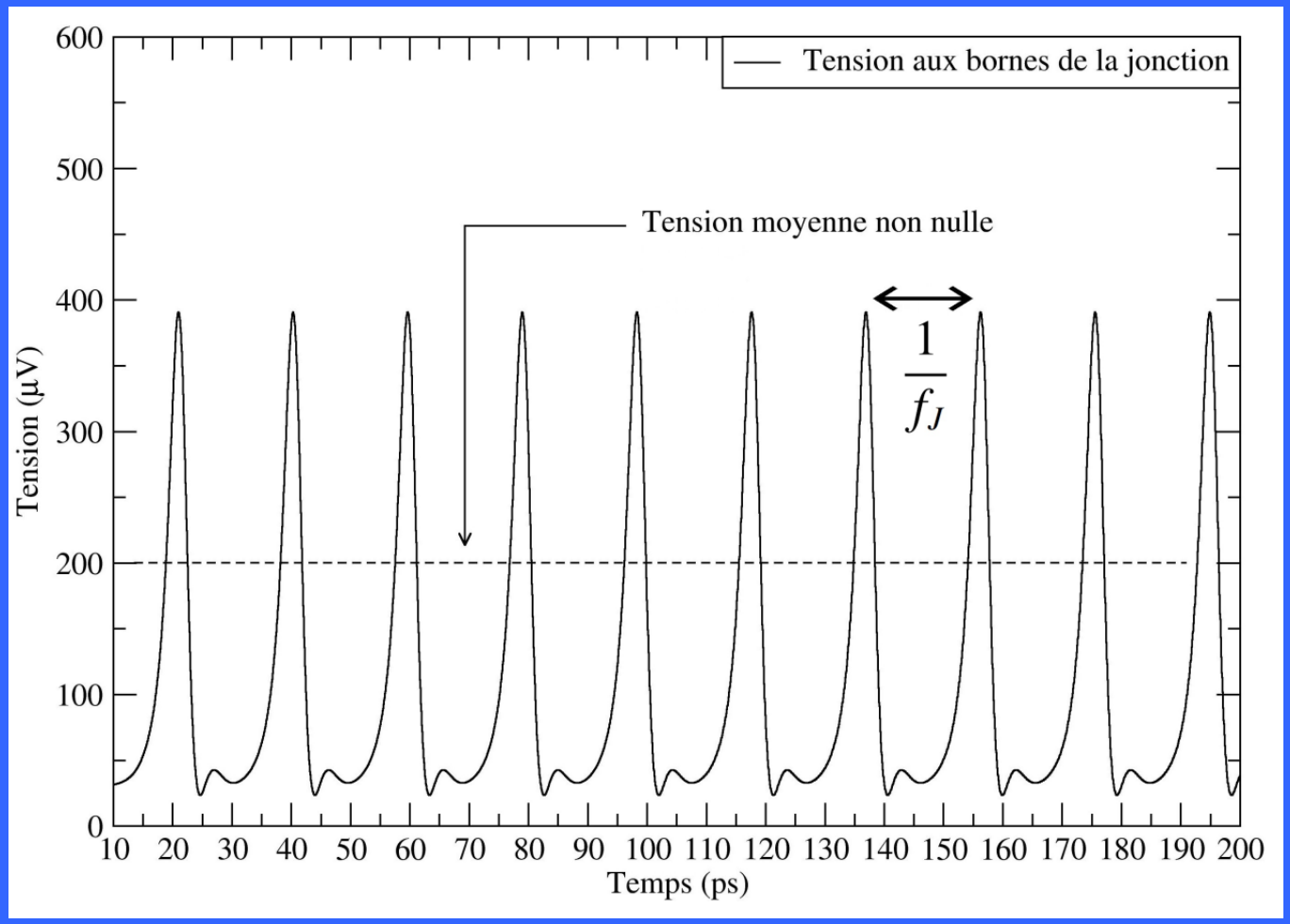

Technological status

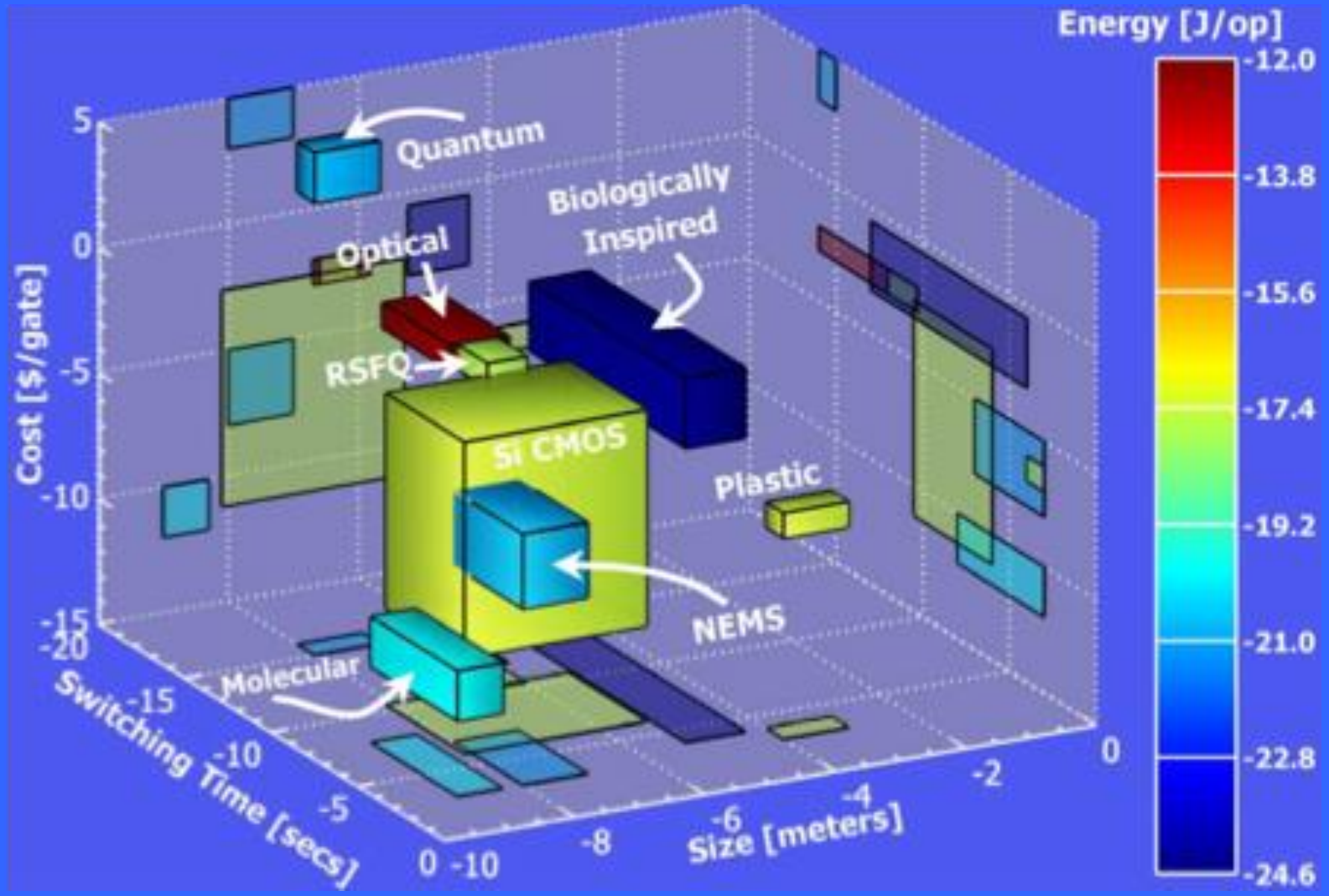

Source: ITRS 2004

How to manage single pulses?

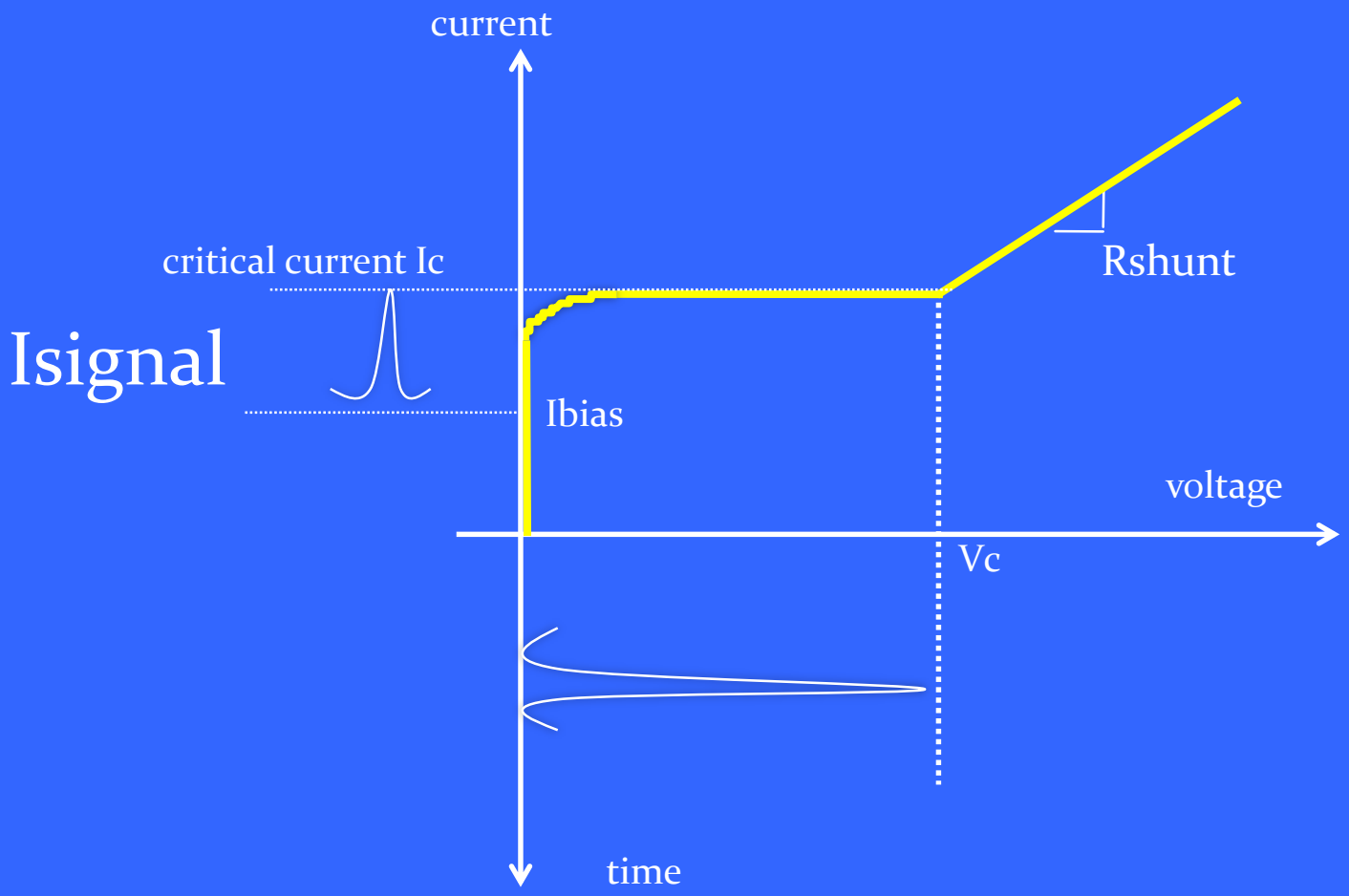

Processing magnetic flux quanta

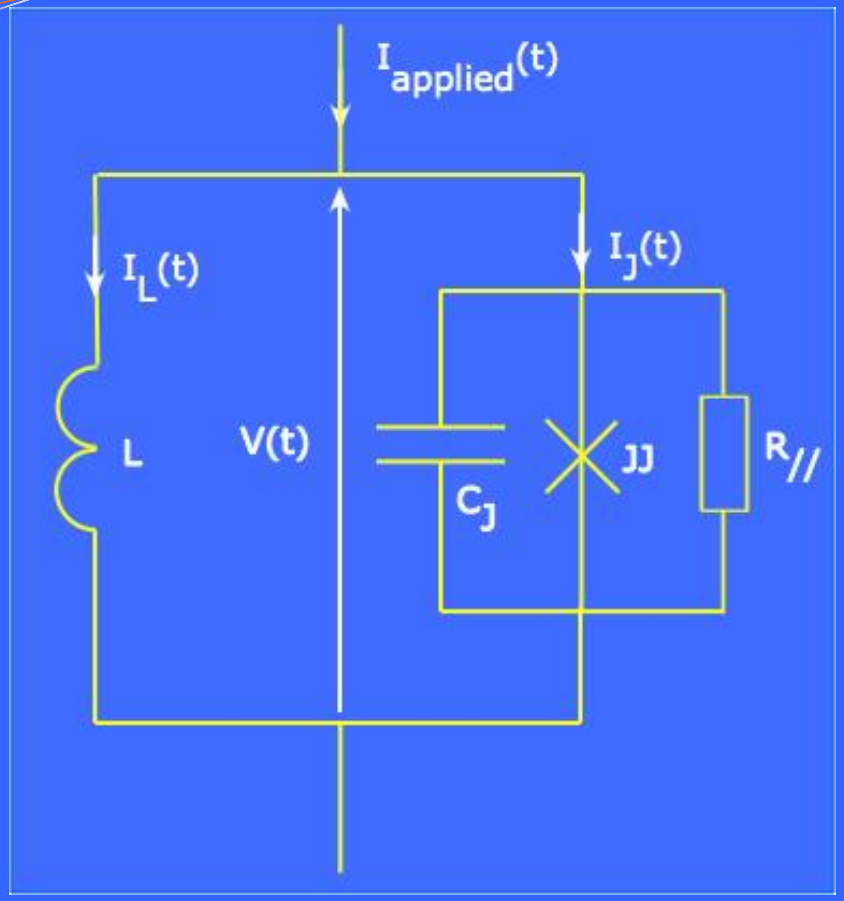

Kirchhoff's laws:

Nodal rule: $I_{applied} = I_L + I_J$

Loop rule: $\sum_{loop} V_i = 0$

Integration over a loop:

$$\int \left(\sum_{loop} V_i \right) dt = \int 0\, dt = \text{constant , " time interval}$$

$$\sum_{loop} \int V_i\, dt = \frac{\Phi_0}{2\pi} \sum_{loop} \Delta\varphi_i = \text{constant} = n\Phi_0$$

Modified Kirchhoff's law (law of phases): $\sum_{loop} \Delta\varphi_i = 2n\pi$

Processing flux quanta - static analysis (1/2)

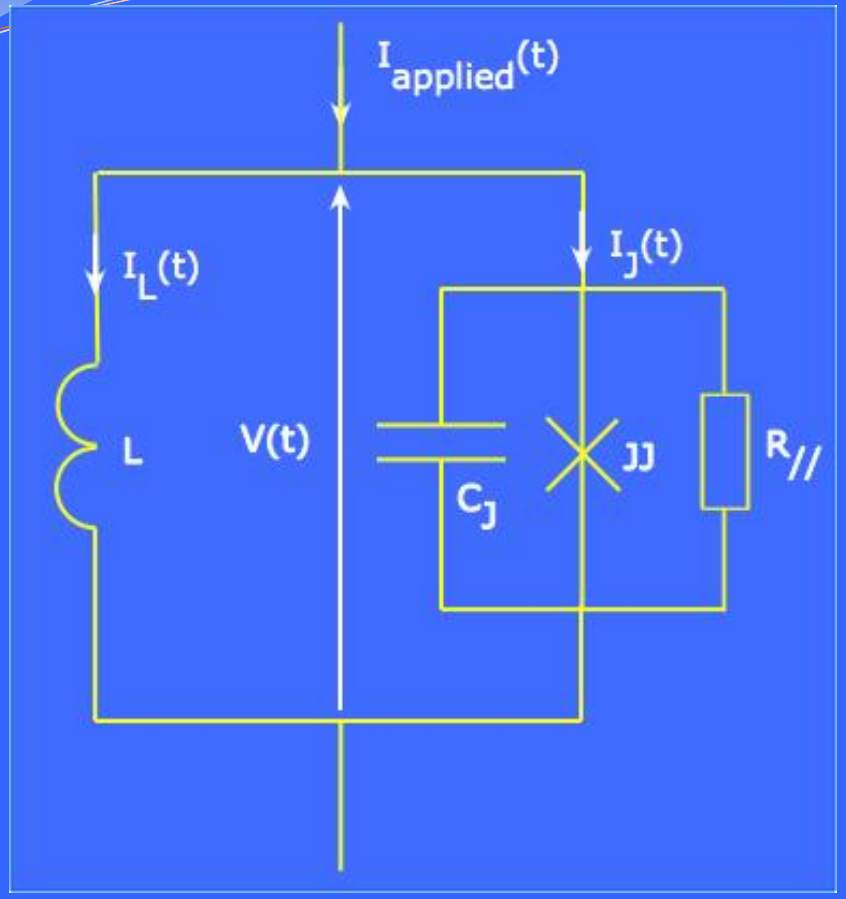

DC-SFQ converter
or
ac SQUID (e.g. rf SQUID)
or
Schmidt trigger

Nodal rule : $I_{applied} = I_L + I_C \sin j$

$$\frac{2p\,LI_{applied}}{F_0} = \frac{2p\,LI_L}{F_0} + \frac{2p\,LI_c}{F_0} \sin j$$

$$j_{ext} = \frac{2p}{F_0} L\,I_{applied} \qquad j_L = \frac{2p}{F_0} F_L$$

$$l = \frac{2p\,L\,I_c}{F_0}$$

2□ * maximum number of flux quanta storable before JJ switching

$$\rightarrow \quad j_{ext} = j_L + l \sin j$$

Loop rule : $j_L - j = 2np$

$$\boxed{j_{ext} = 2np + j + l \sin j}$$

Processing flux quanta - static analysis (2/2)

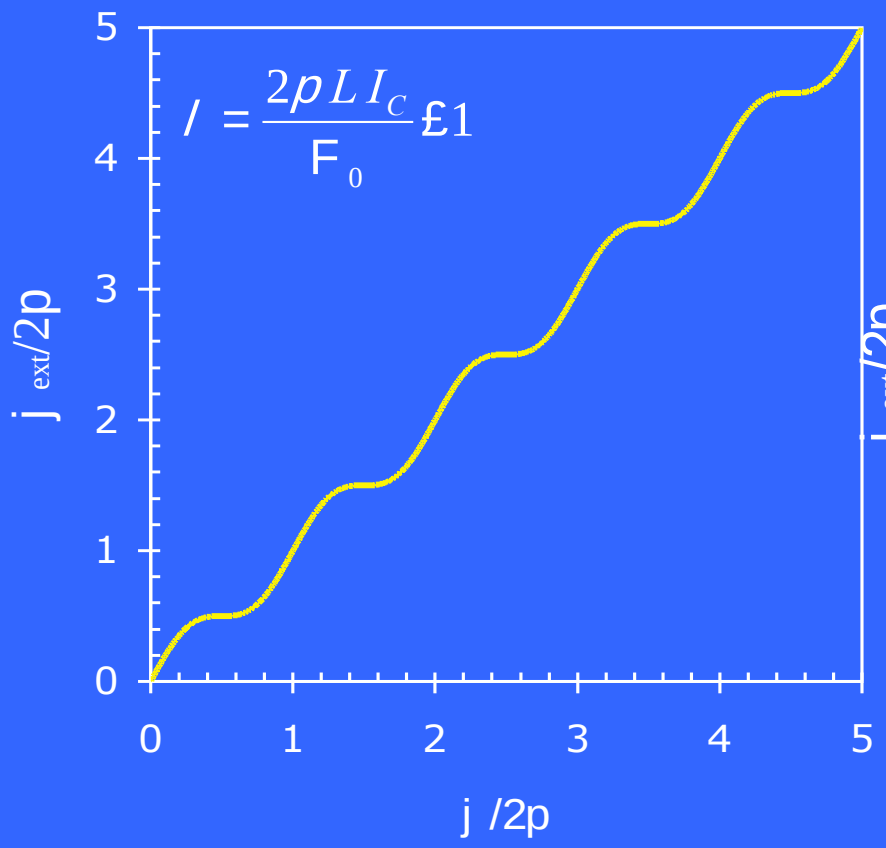

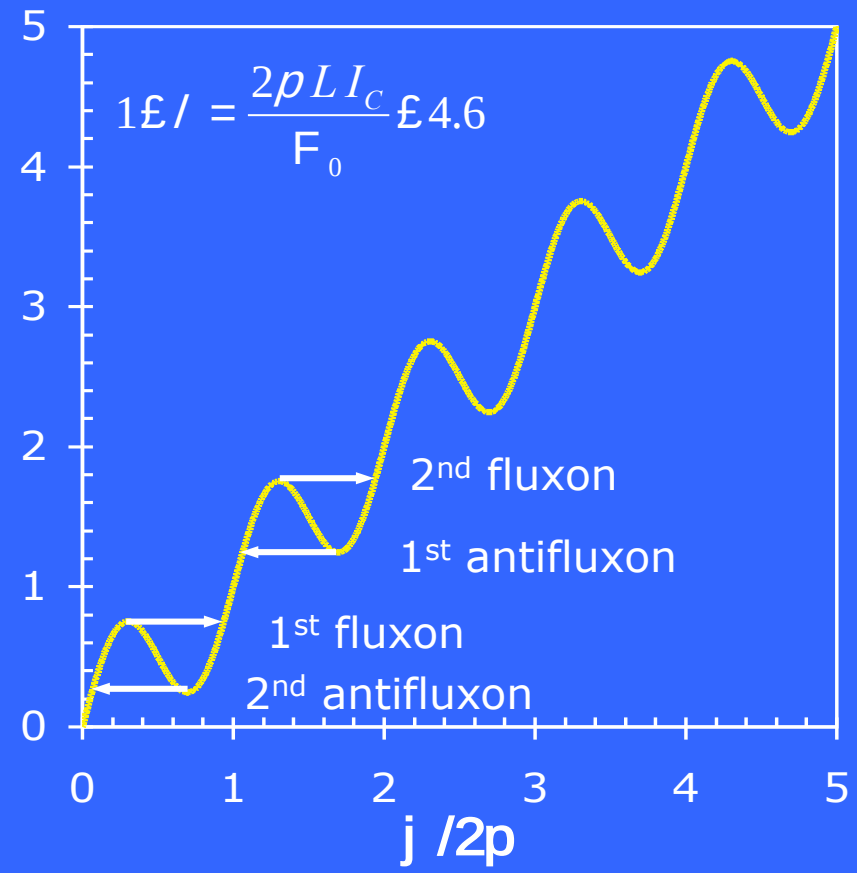

Generation of quantized pulses (1/2)

The first fluxon enters the loop for:

$$j_{ext}\left(1^{st}\ fluxon\right) = \arccos\left(-\frac{1}{l}\right) + \sqrt{l^2 - 1}$$

The second fluxon enters the loop for:

$$j_{ext}\left(2^{nd}\ fluxon\right) = j_{ext}\left(1^{st}\ fluxon\right) + 2\pi$$

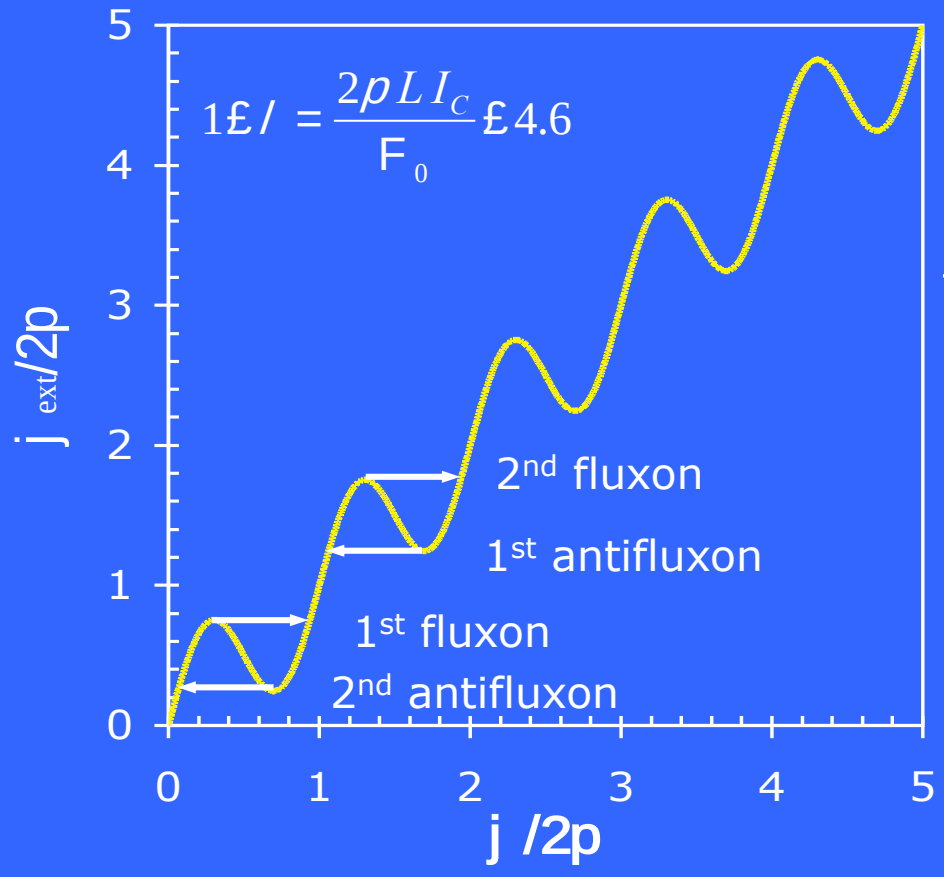

The first antifluxon enters the loop for:

$$j_{ext}\left(1^{st}\ antifluxon\right) = 2\pi - \arccos\left(-\frac{1}{l}\right) - \sqrt{l^2 - 1}$$

The second antifluxon enters the loop for:

$$j_{ext}\left(2^{nd}\ antifluxon\right) = j_{ext}\left(1^{st}\ antifluxon\right) - 2\pi$$

Generation of quantized pulses (2/2)

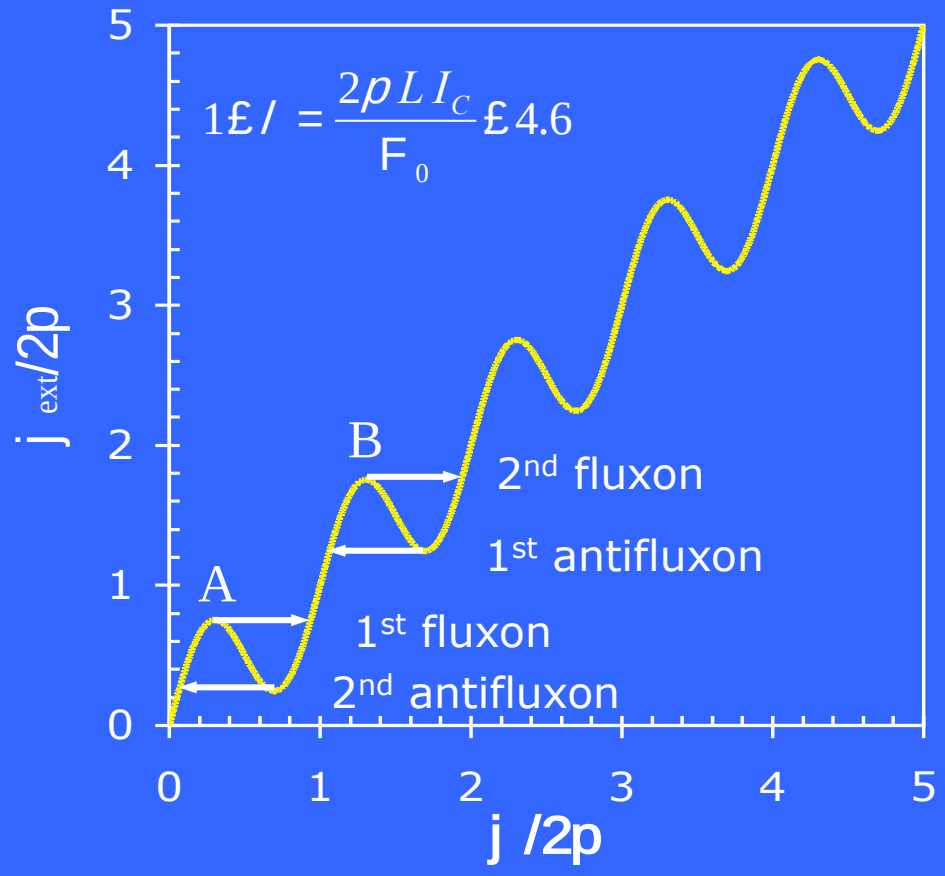

$$\frac{I_{ext}}{I_C}(\text{pointA}) = \frac{1}{l}\left[\arccos\left(-\frac{1}{l}\right) + \sqrt{l^2 - 1}\right]$$

$$\frac{I_{ext}}{I_C}(\text{point B}) = \frac{I_{ext}}{I_C}(\text{point A}) + \frac{2\pi}{l}$$

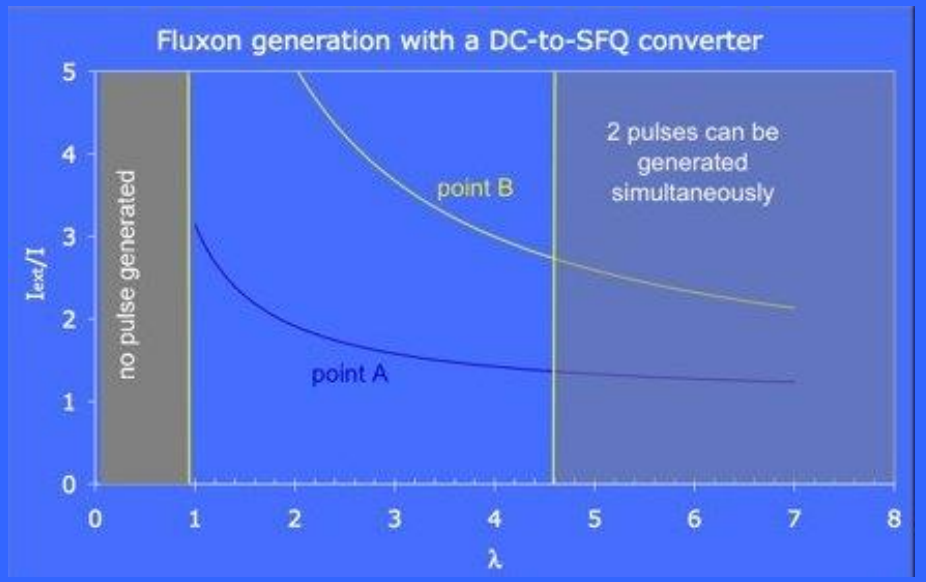

Picosecond pulse and magnetic flux quantum

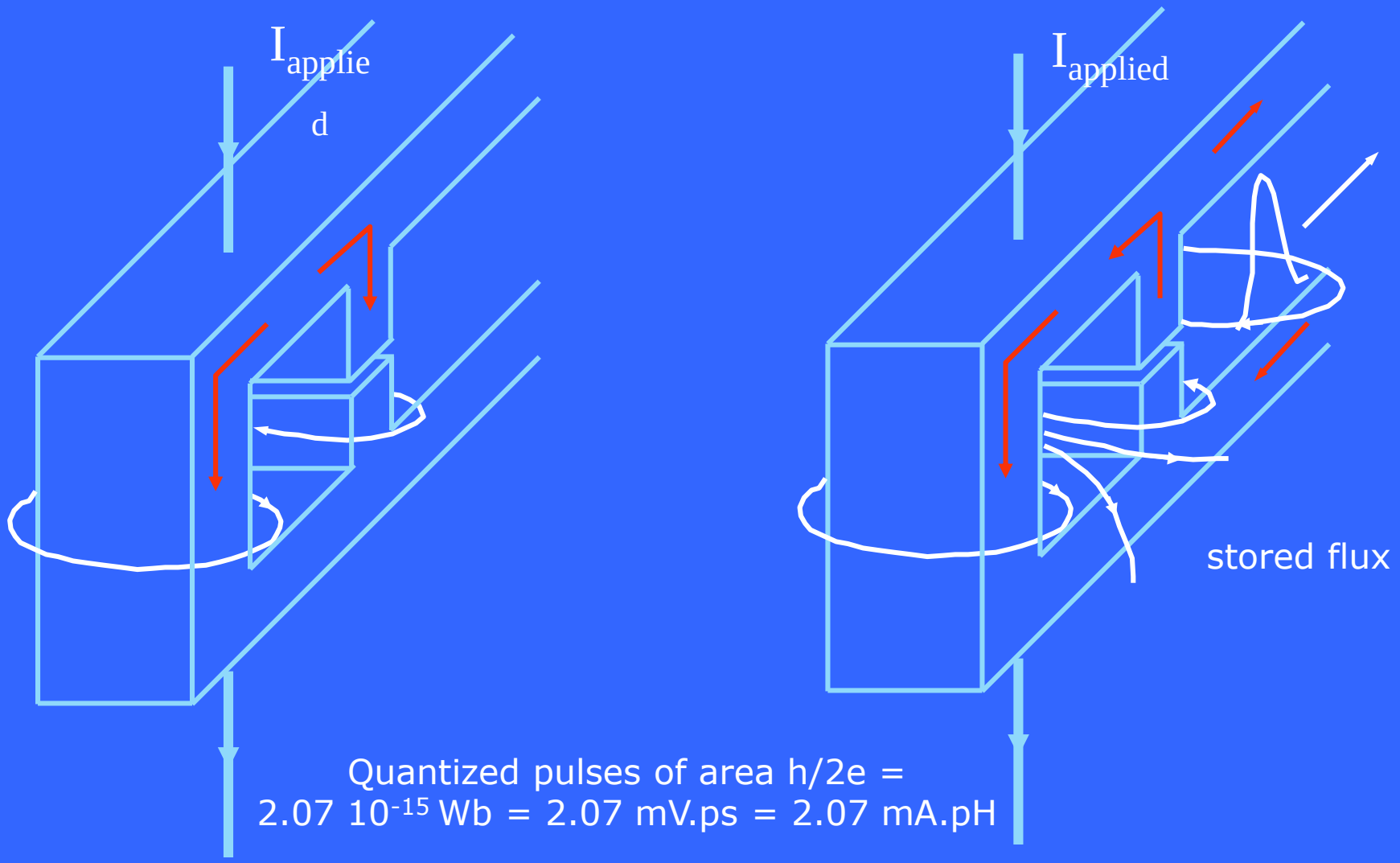

Quantized pulses of area h/2e =
2.07 10^{-15} Wb = 2.07 mV.ps = 2.07 mA.pH

Simulation of a pulse generator

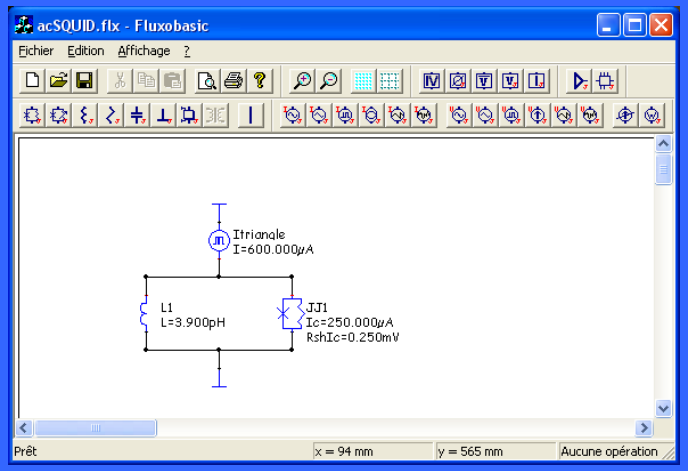

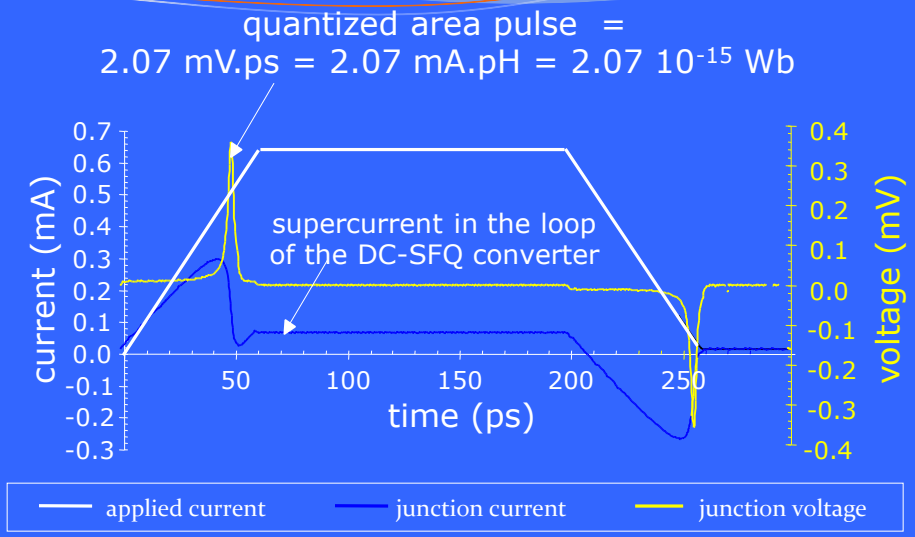

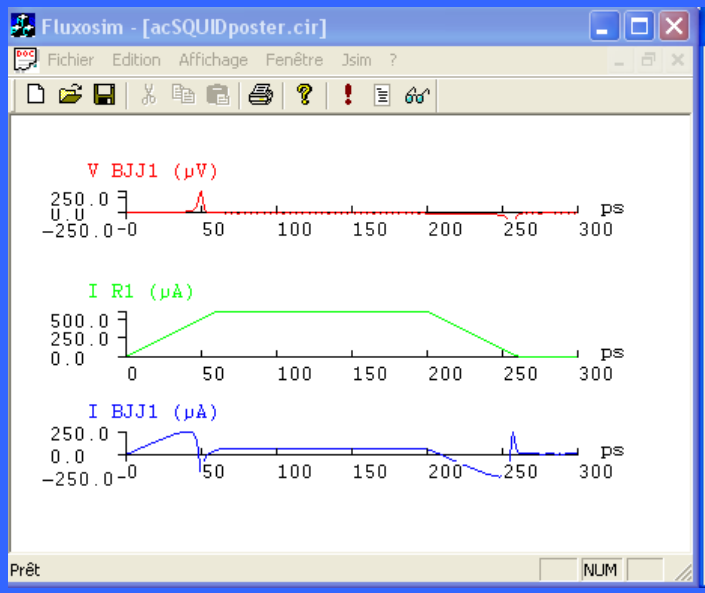

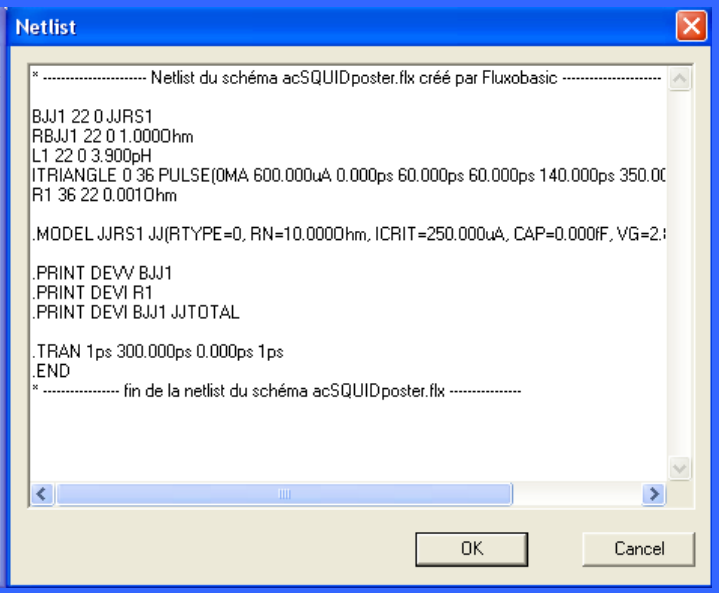

Pulse transmission

$L \cdot I_c < \Phi_0$

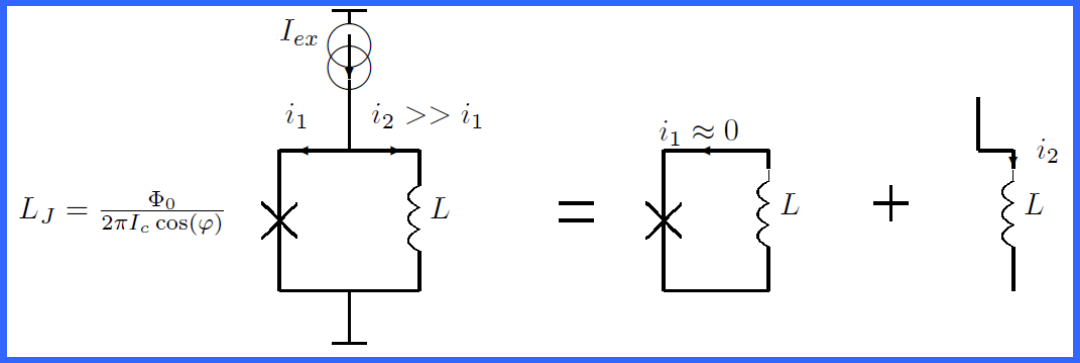

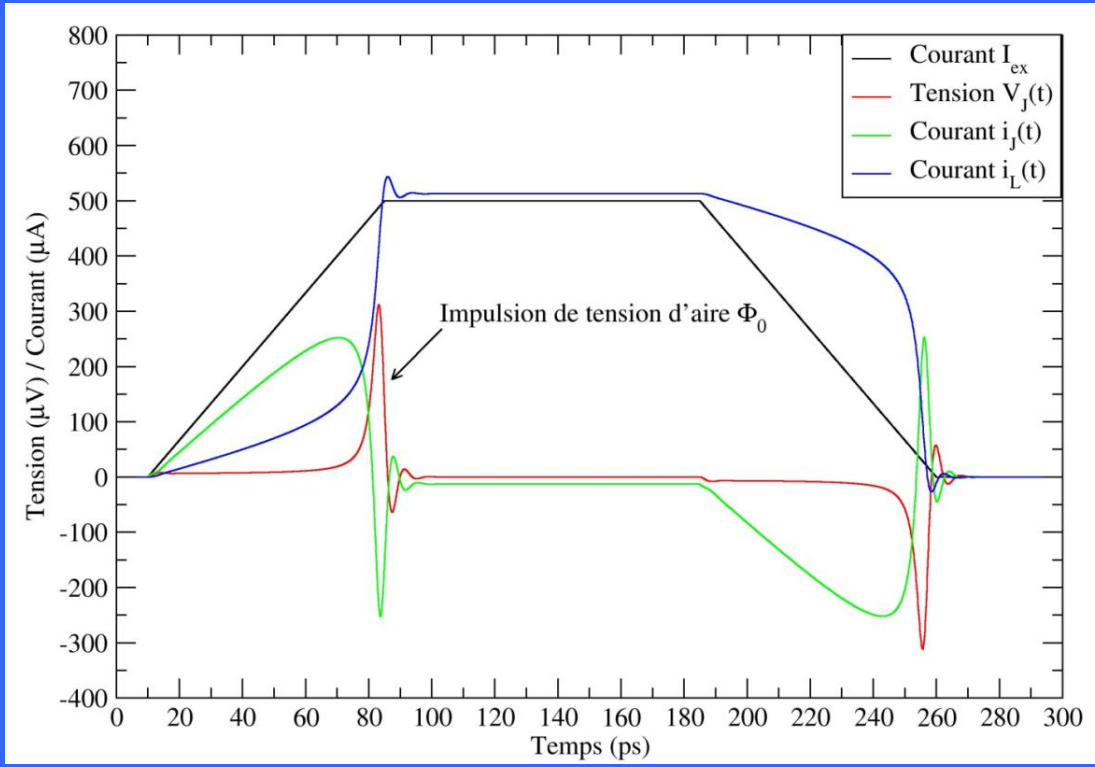

Pulse storage

$L . I_c > \Phi_0$

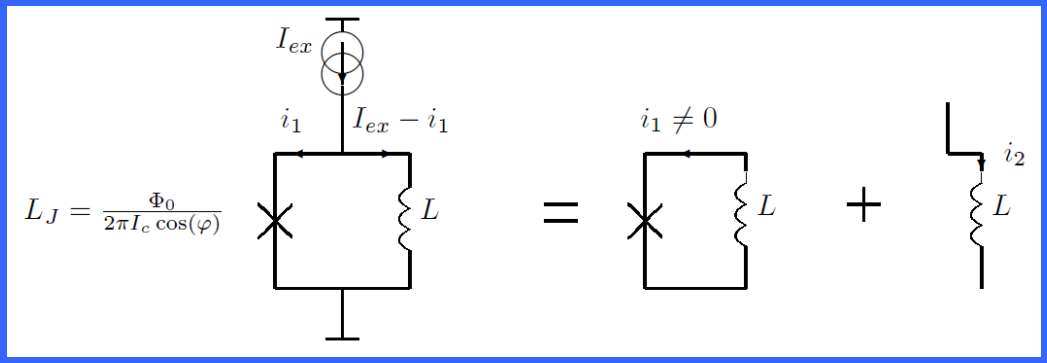

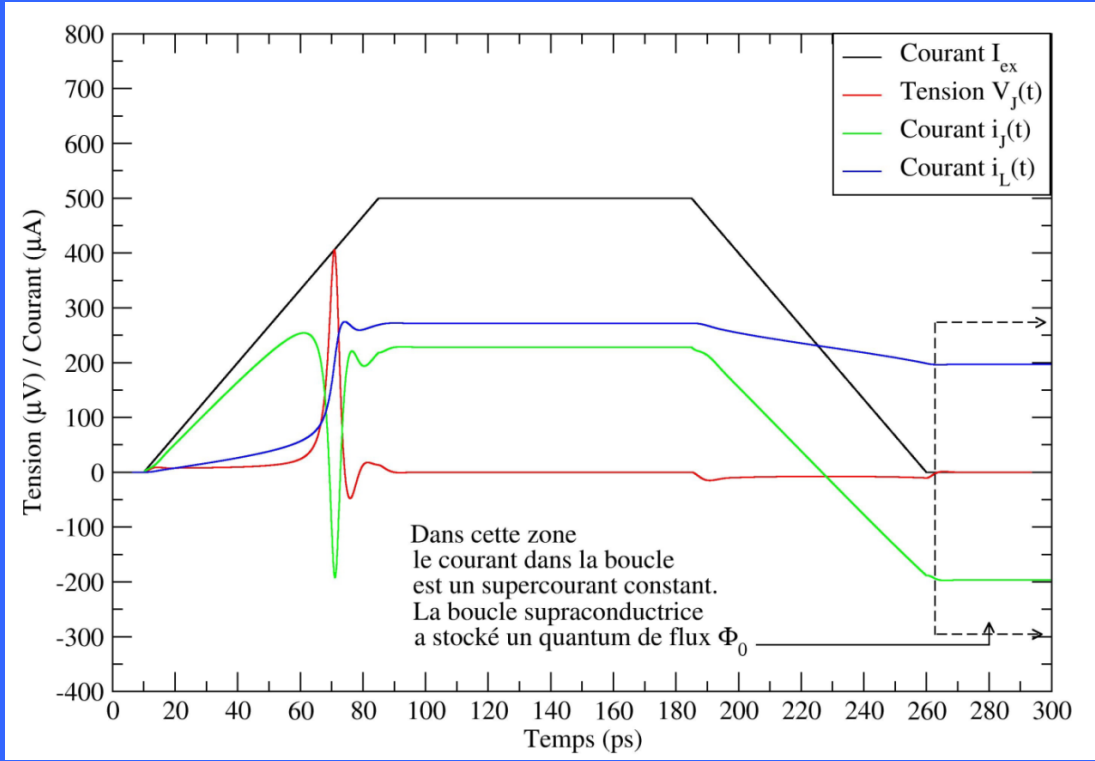

Example of SFQ gate: the Delay-Flip-Flop (DFF)

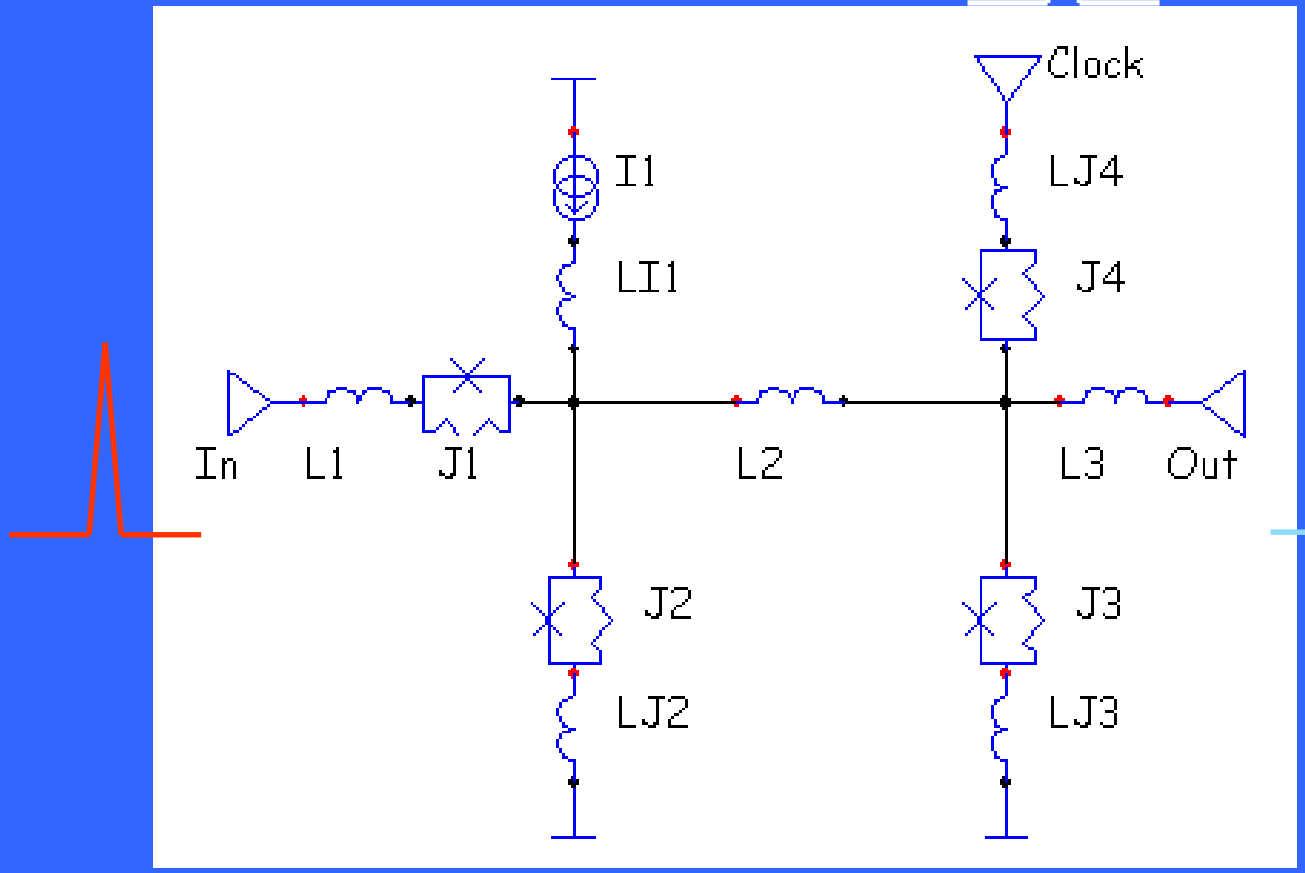

The digital signal is coded with 2 states, between two clock pulses :

- '0' : no pulse
- '1' : one quantized pulse (SFQ pulse)

Schematics of the Delay-Flip-Flop cell FLUXONICS Cell Library

www.FLUXONICS.eu

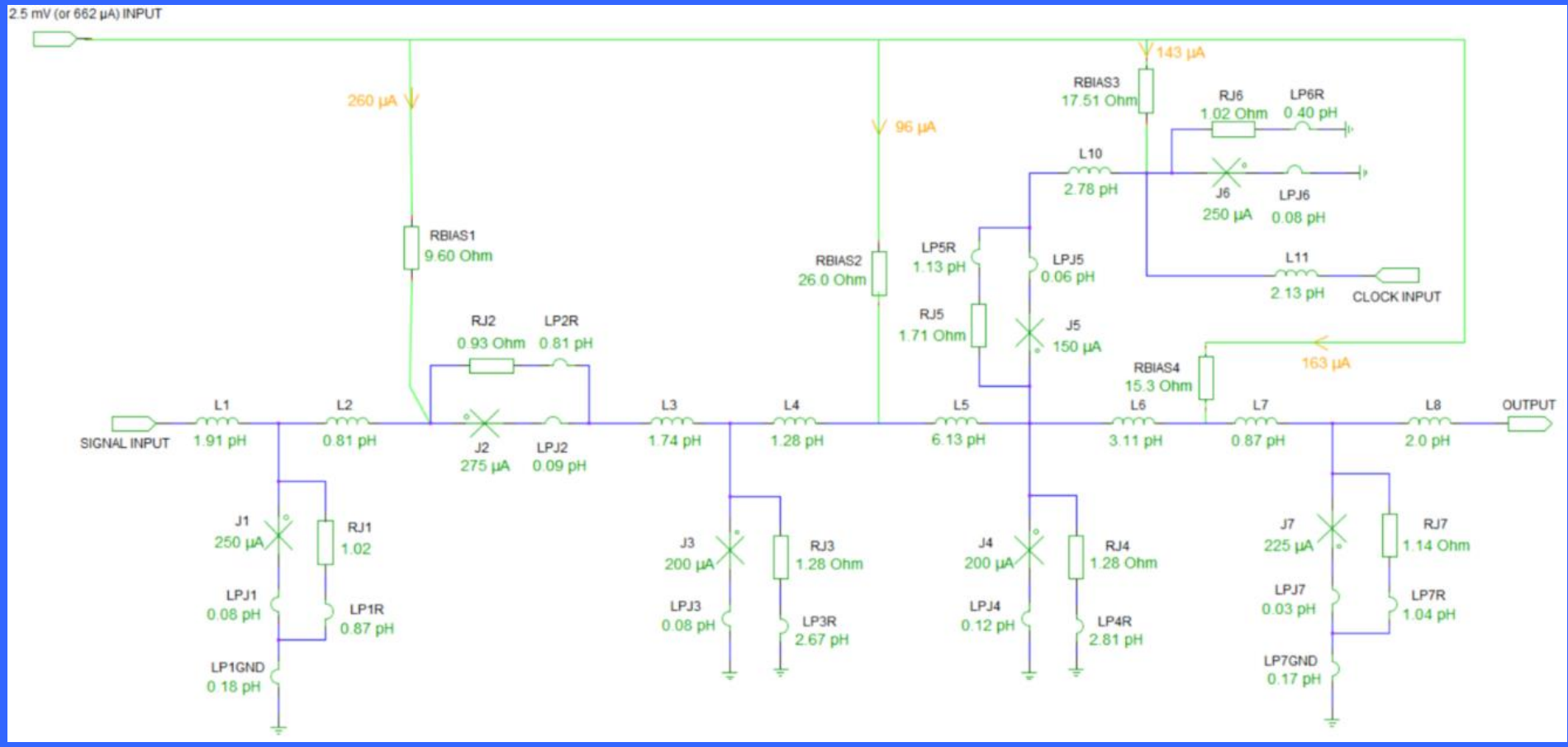

Layout of the Delay-Flip-Flop cell FLUXONICS Cell Library

Layout for the Nb/Al-AlOx/Nb technology – FLUXONICS Foundry – IPHT Jena - Germany

www.FLUXONICS.eu

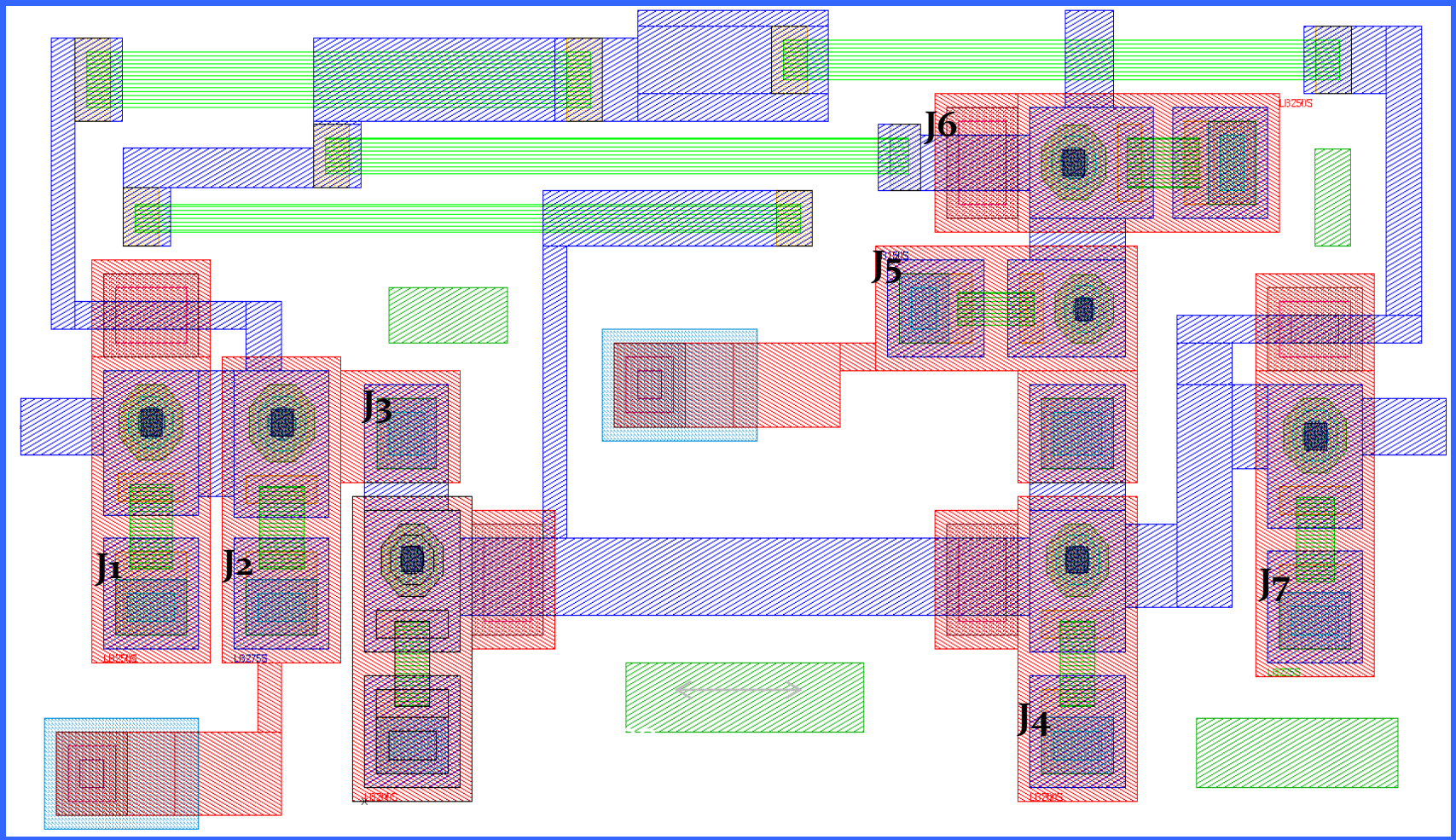

Simulation of the Delay-Flip-Flop cell FLUXONICS Cell Library

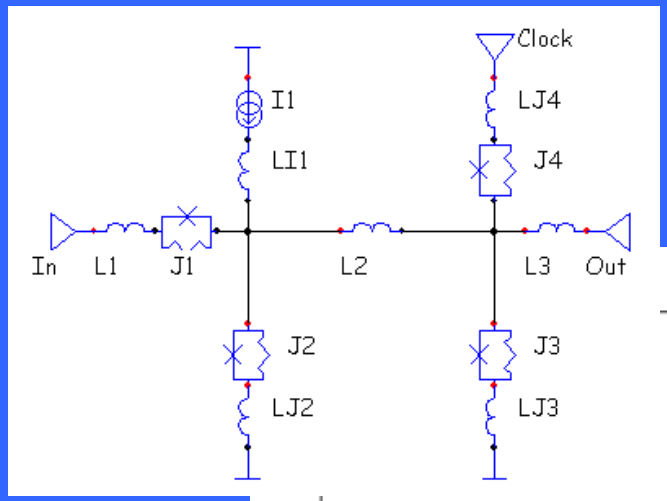

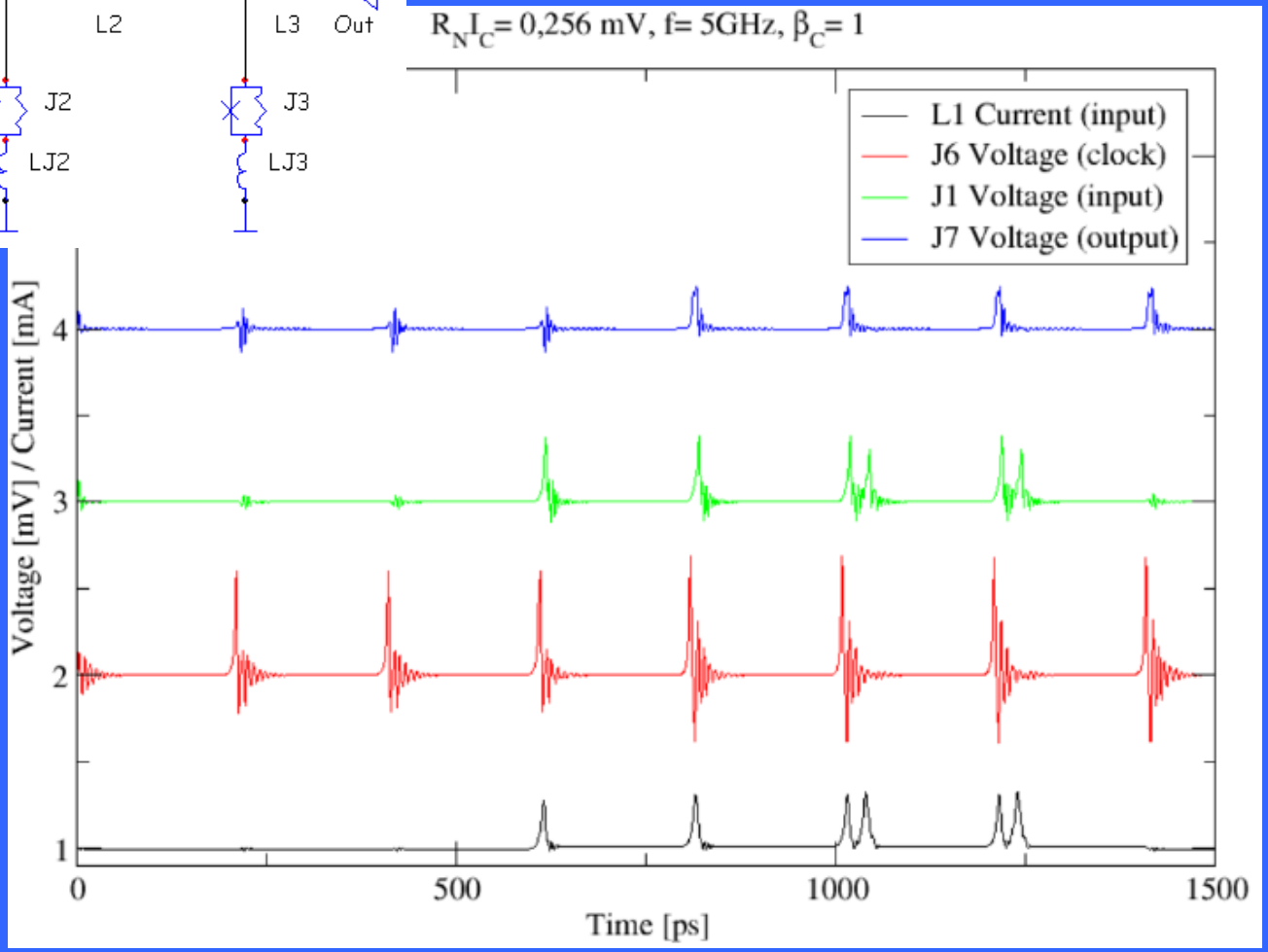

www.FLUXONICS.eu

Margins of the Delay-Flip-Flop cell FLUXONICS Cell Library

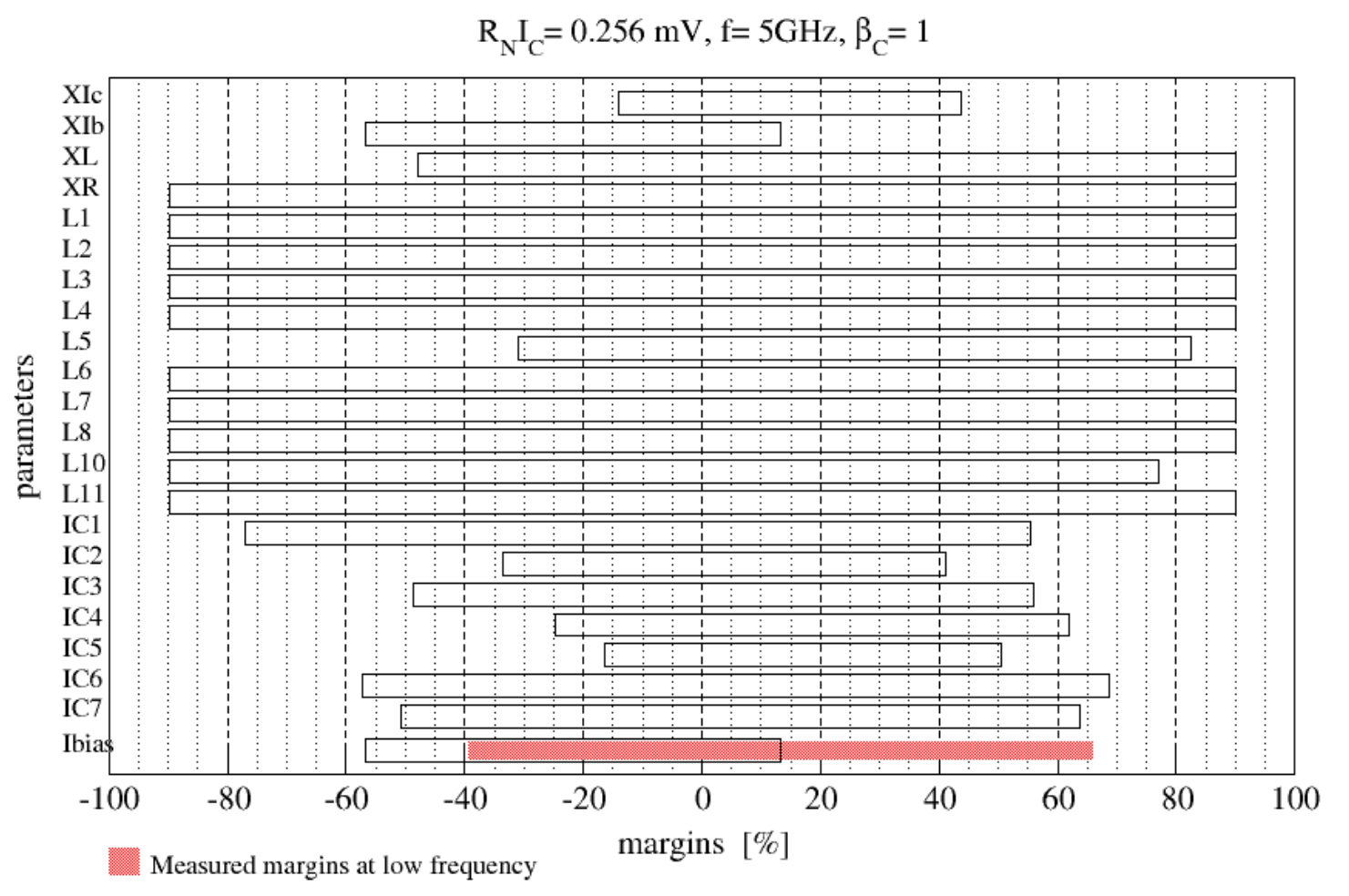

www.FLUXONICS.eu

Yield of the Delay-Flip-Flop cell FLUXONICS Cell Library

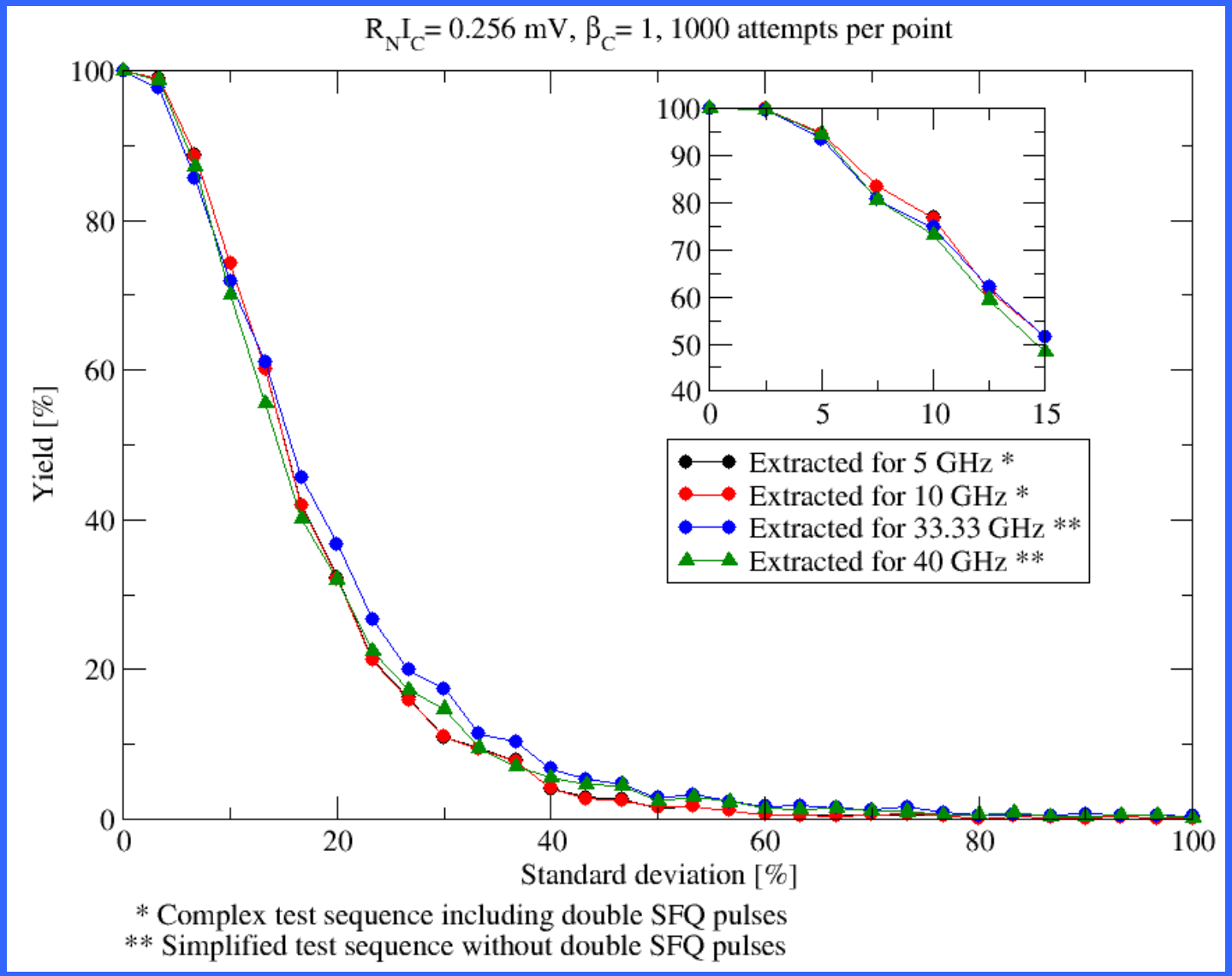

www.FLUXONICS.eu

RSFQ process cross-section
FLUXONICS Foundry

RSFQ process – cross section

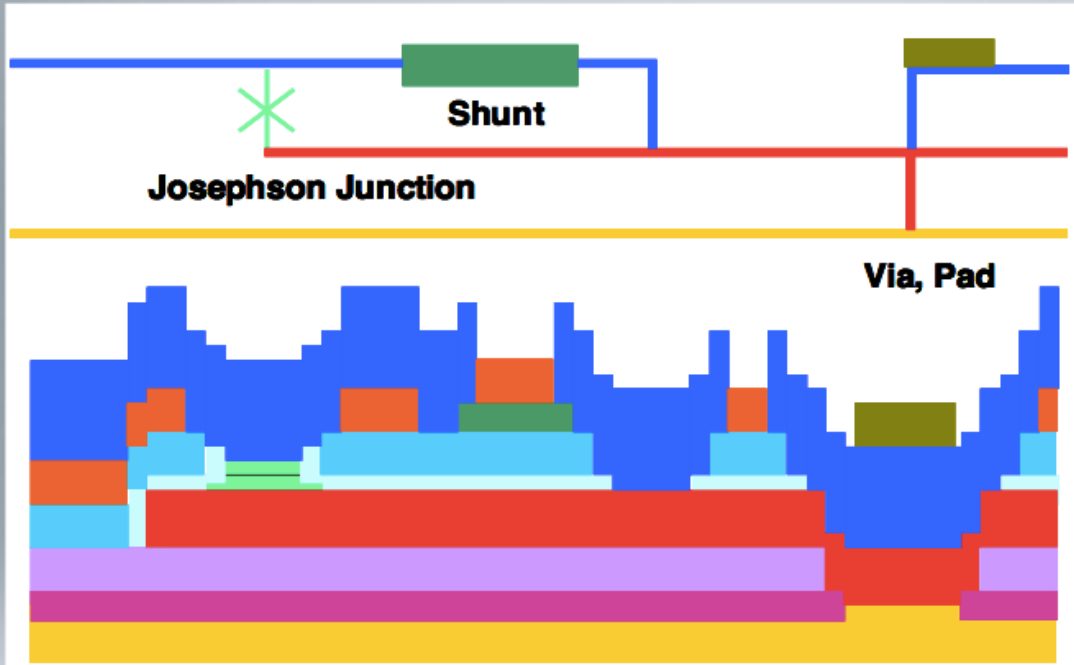

Layer	Thickness	Material
R2	50 nm	Au
M2	350 nm	Nb
I2	150 nm	SiO
R1	80 nm	Mo
I1B	150 nm	SiO
I1A	70 nm	Nb_2O_5
T1	60 nm 12 nm 30 nm	Nb Al_2O_3 Nb
M1	250 nm	Nb
I0B	200 nm	SiO
I0A	50 nm	Nb_2O_5
M0	200 nm	Nb

RSFQ technology parameters and tolerances FLUXONICS Foundry

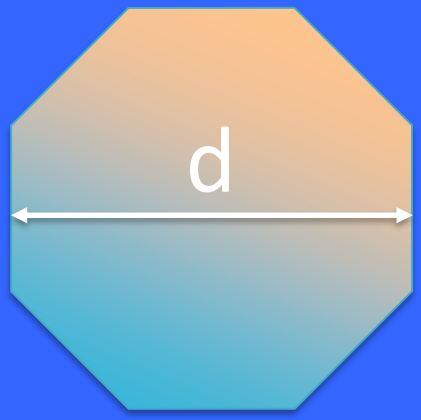

Josephson junction
specific capacitance :
50±2 fF/μm^2

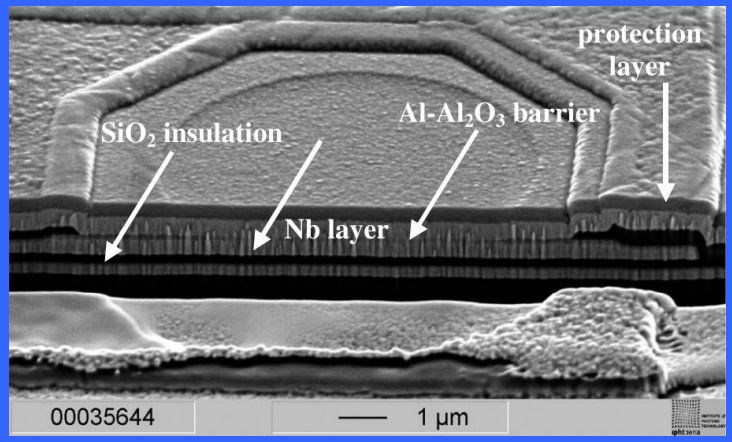

FLUXONICS octagonal Josephson junctions

RSFQ technology parameters and tolerances FLUXONICS Foundry

- Current density of 1 kA/cm² based on Nb/Al-AlOx/Nb tri-layers
- 3 metal layers M0, M1 & M2 : 1st for ground plane and 2nd/3rd for wiring
- Characteristic voltage V_c=256 μV
- McCumber parameter βc = 1
- 13 shunted octagonal Josephson junctions for digital operation

Junction	Lb100	Lb125	Lb150	Lb175	Lb200	Lb225	Lb250	Lb275	Lb300	Lb325	Lb350	Lb375	Lb400
Ic (μA)	100	125	150	175	200	225	250	275	300	325	350	375	400
area (μm²)	9.94	12.44	15.11	17.59	20.09	22.54	25.13	27.59	29.99	32.47	35.03	37.42	40.18
d (μm)	3.4	3.8	4.3	4.7	4.9	5.2	5.5	5.9	6.1	6.3	6.5	6.8	7.0
R_{shunt} (Ω)	2.58	2.06	1.69	1.46	1.27	1.14	1.02	0.93	0.85	0.79	0.73	0.68	0.64

RSFQ technology parameters and tolerances FLUXONICS Foundry

www.FLUXONICS.eu

Parameter	Nominal Value	Inter Wafer tolerance	On wafer tolerance	On chip tolerance
Josephson current density J_C	1000 A/cm^2	± 20 %	± 15 %	± 5 %
Sheet Resistance R_{square}	1.0 Ω	± 20 %	± 10 %	± 5 %
Inductance L_{10} M1-M0	0.52 pH	± 10 %	± 5 %	± 2 %
Inductance L_{21} M2-M1	0.64 pH	± 10 %	± 5 %	± 2 %
Inductance L_{20} M2-M0	0.81 pH	± 10 %	± 6 %	± 2 %

The Toggle Flip-Flop cell

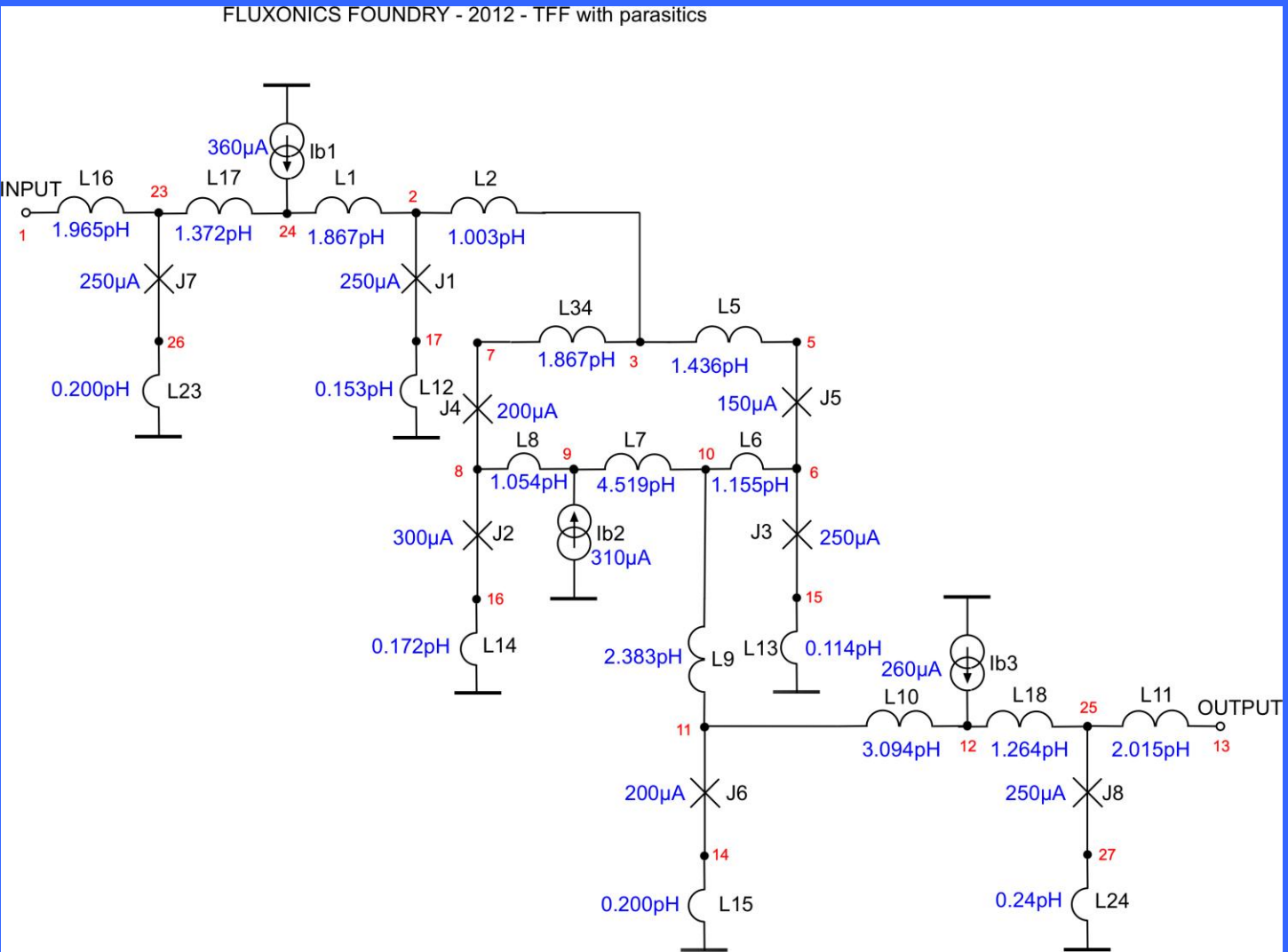

www.FLUXONICS.eu

The Toggle Flip Flop (TFF) cell delivers an SFQ output pulse once every two SFQ pulses sent to its input.

For an SFQ clock signal at a given frequency, the output pulse train is an SFQ clock at half-frequency.

The Toggle Flip-Flop cell

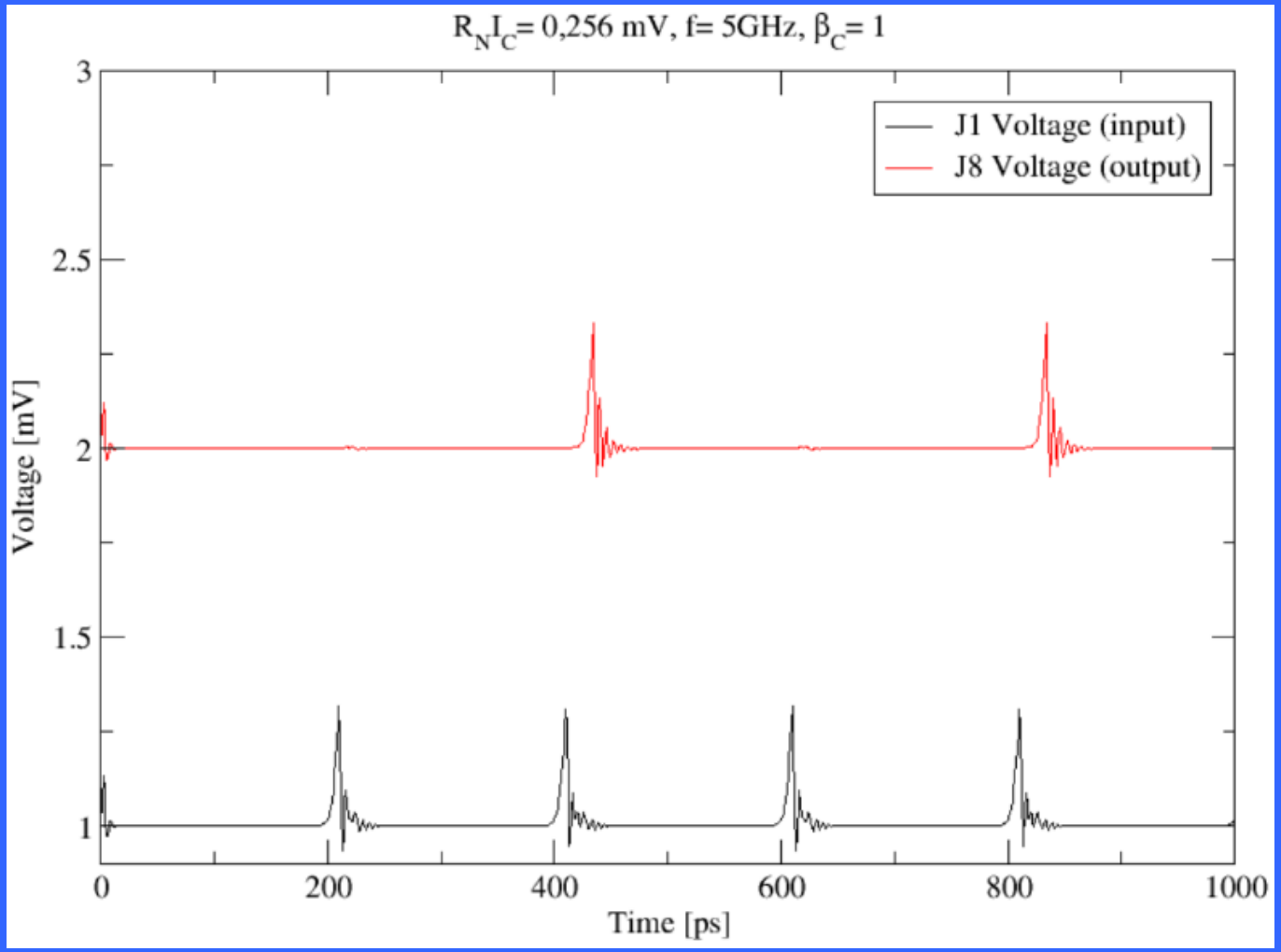

www.FLUXONICS.eu

The FLUXONICS Toggle Flip-Flop cell margins and yield

www.FLUXONICS.eu

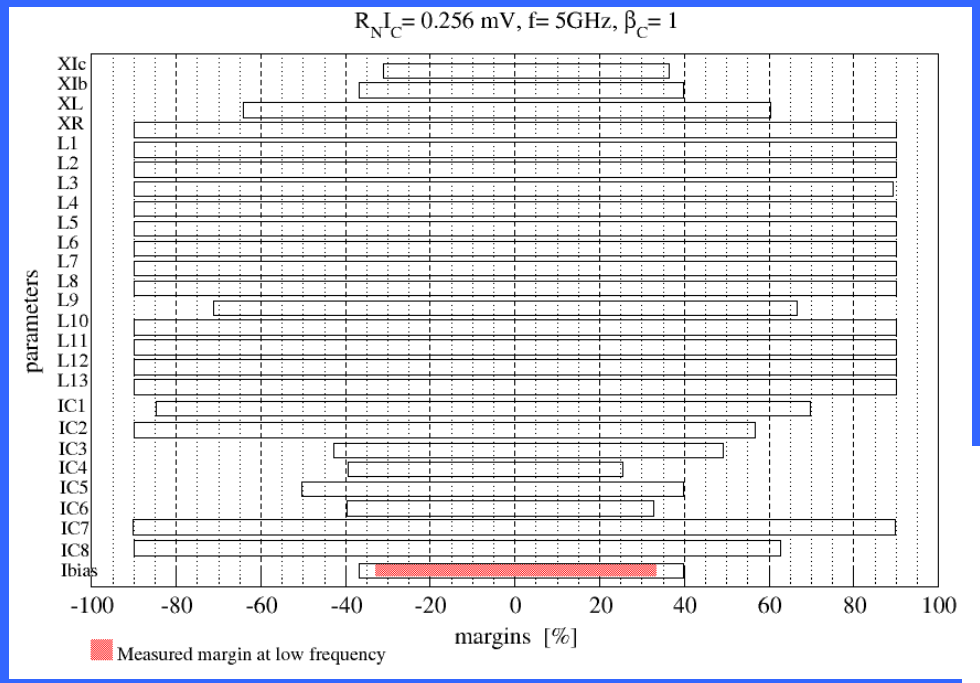

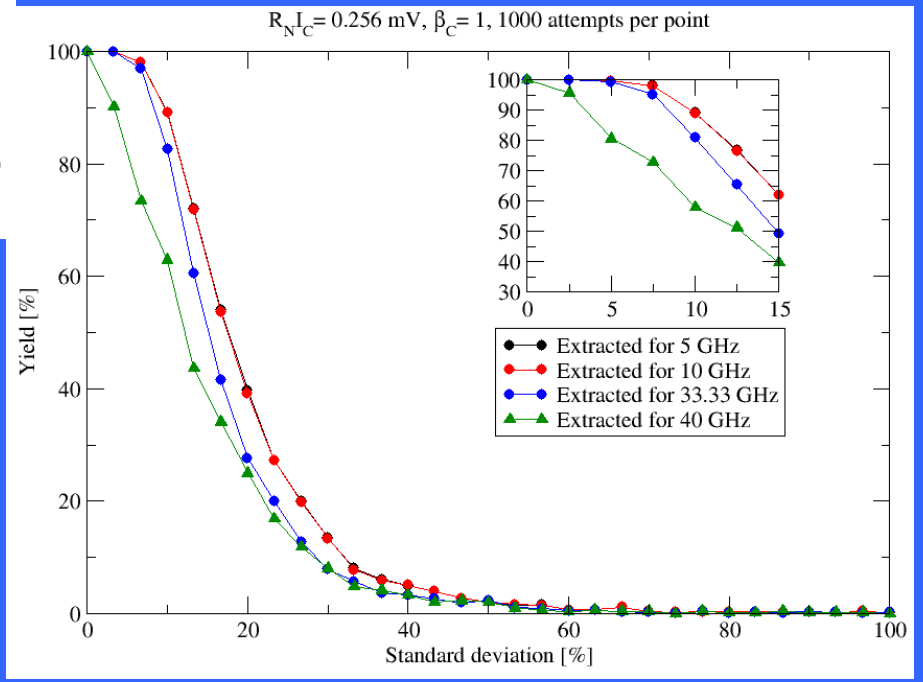

Picture of Toggle Flip-FLop cell

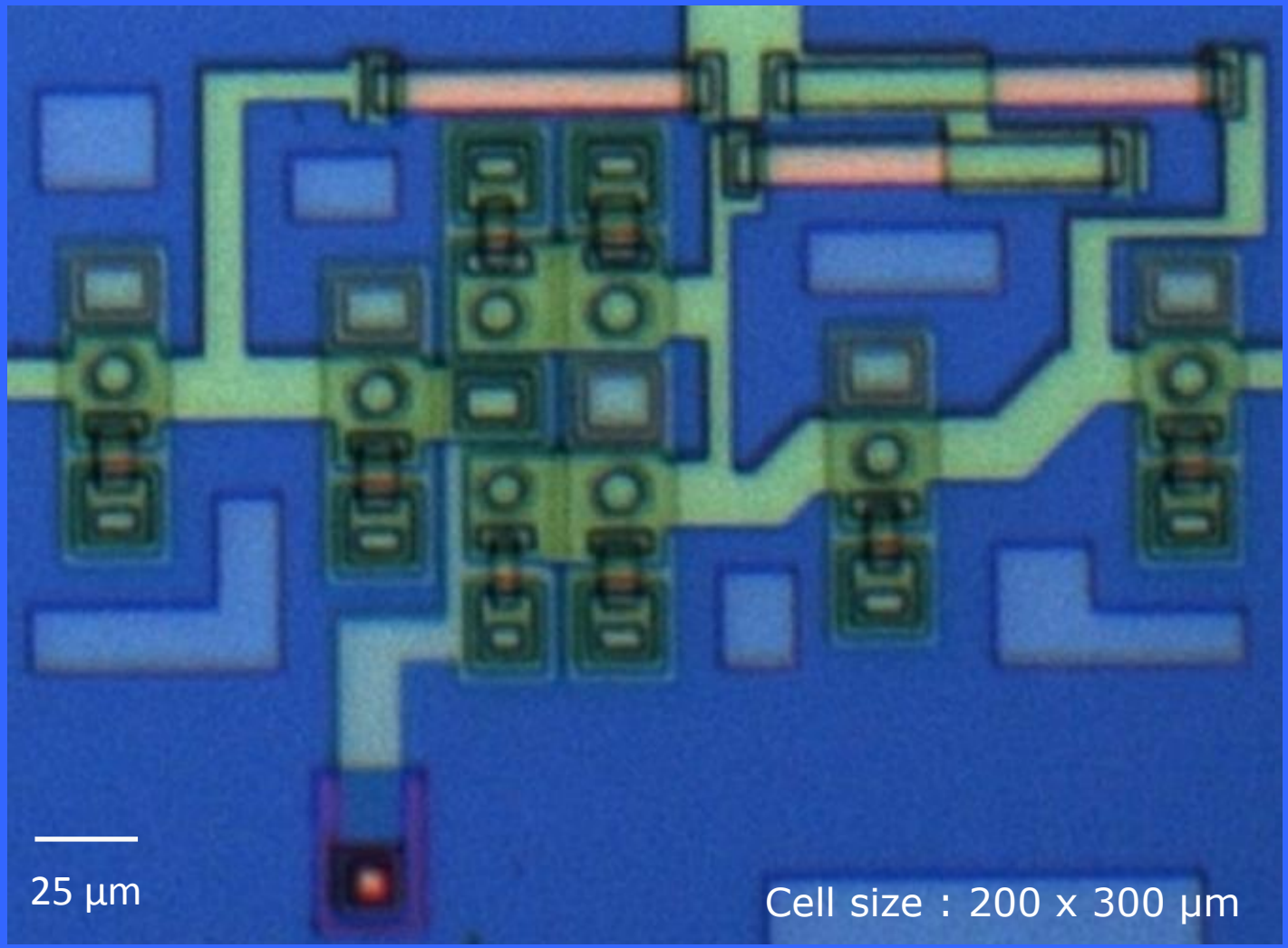

www.FLUXONICS.eu

Toggle Flip-FLop experimental results

www.FLUXONICS.eu

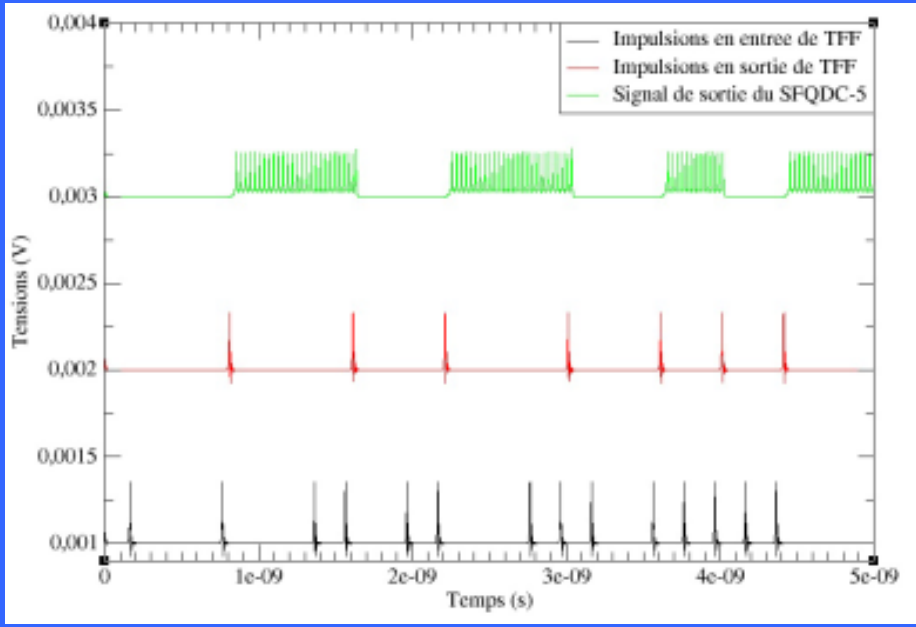

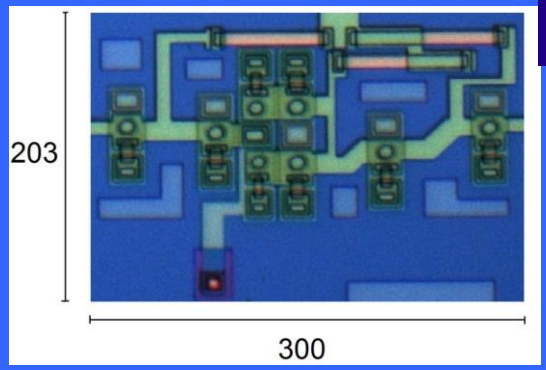

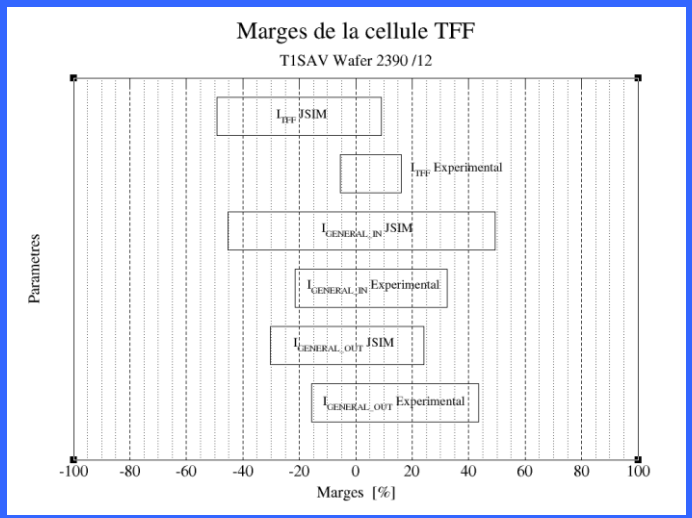

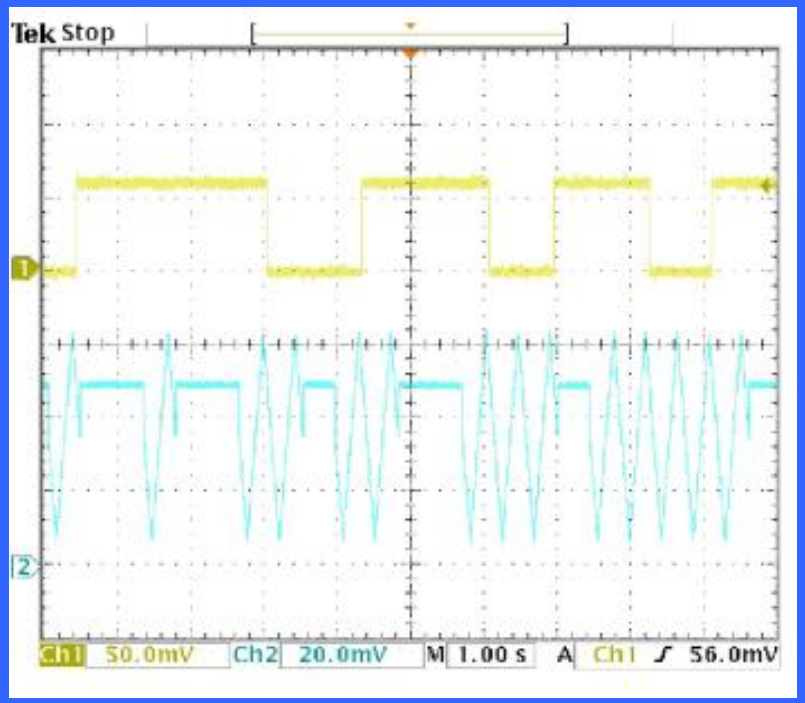

FLUXONICS cell library

www.FLUXONICS.eu

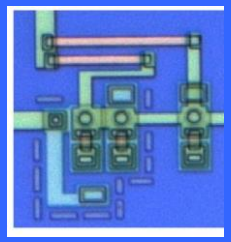

DCSFQ

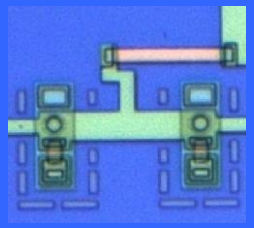

JTL

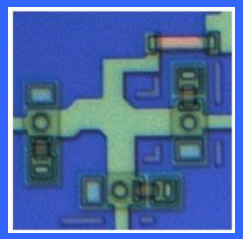

SPLITTER

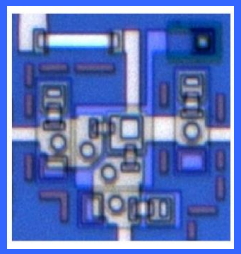

MERGER-1

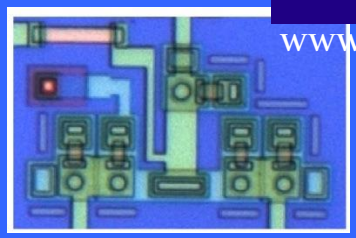

MERGER-2

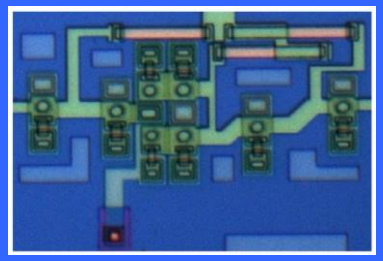

TFF

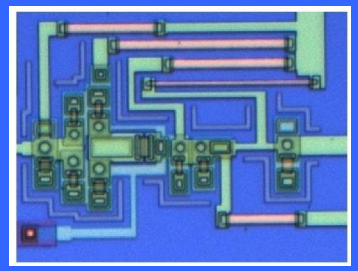

SFQDC

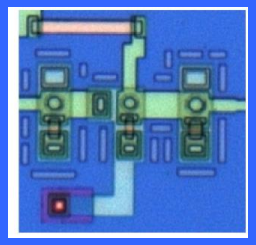

BUFFERJTL

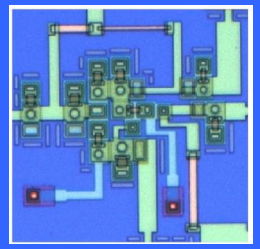

DFFC

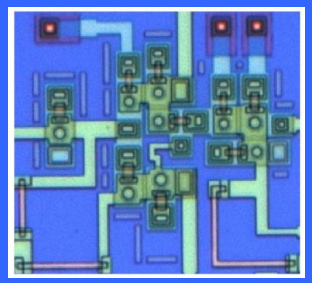

TFFC-A

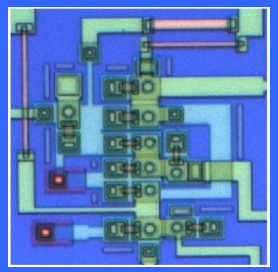

TFFC-B

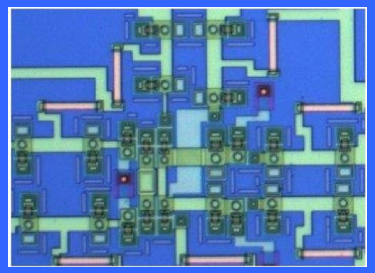

NDRO

Experimentally-verified frequency limit

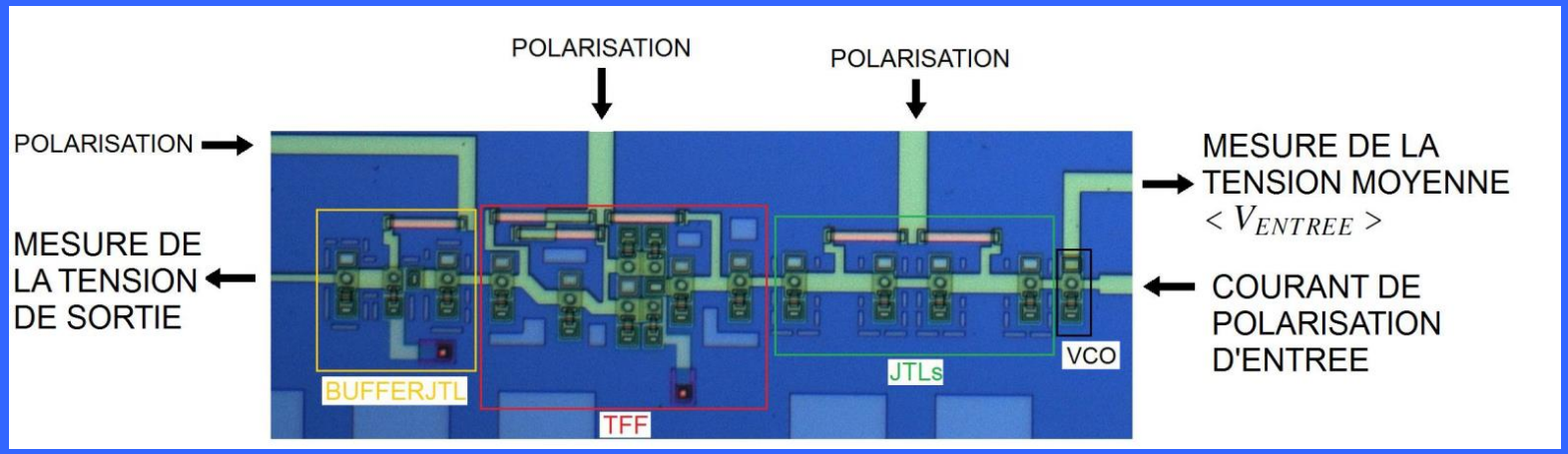

The physics of the Josephson junction gives easy access to the frequency of oscillations

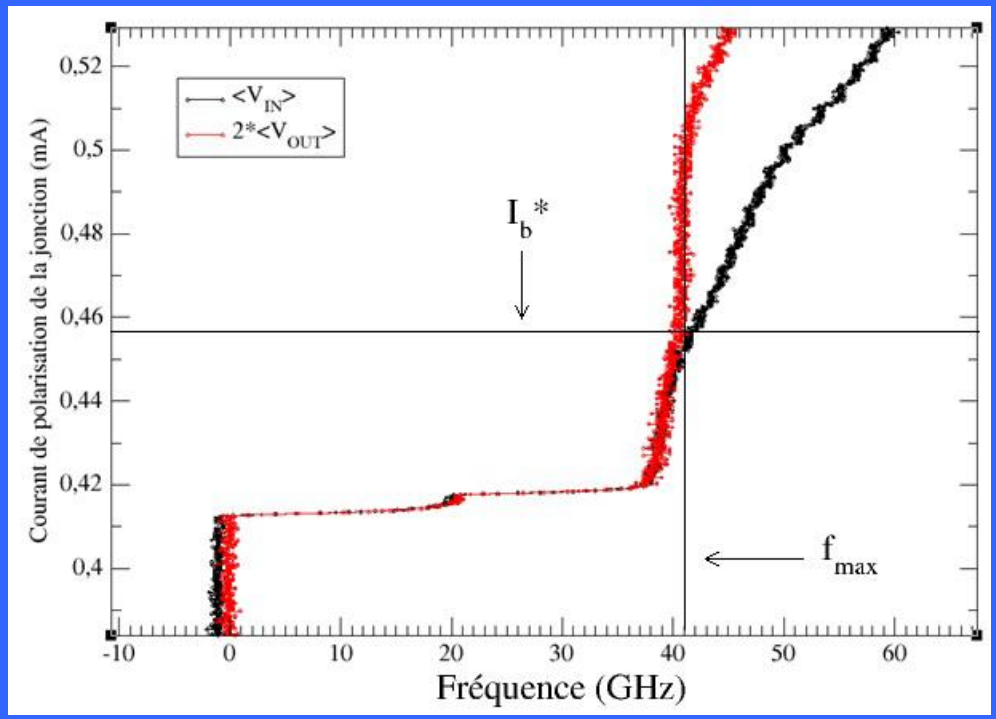

Performances & applications of RSFQ logic

Performances:

- clock frequencies in the 30-110 GHz range (state-of-the-art)
- ultimate clock frequencies up to 770 GHz : demonstrated on simple circuit
- clock frequency objective for the next decade: 160-300 GHz
- very low consumption with new eSFQ and eRSFQ concepts

Applications:

Telecommunication domain:

- analog-to-digital converters
- routers
- base-station of mobile phones

Security & intelligence:

- analog-to-digital converters
- super-computers
- software-defined radio - SDR

Science:

- super-computers
- astronomy: signal processing of imagers
- geophysics: study of Earthquakes, geophysical prospection
- (bio)-medical: encephalo- & cardio- magnetography
- archeology

Analog-to-Digital Converters

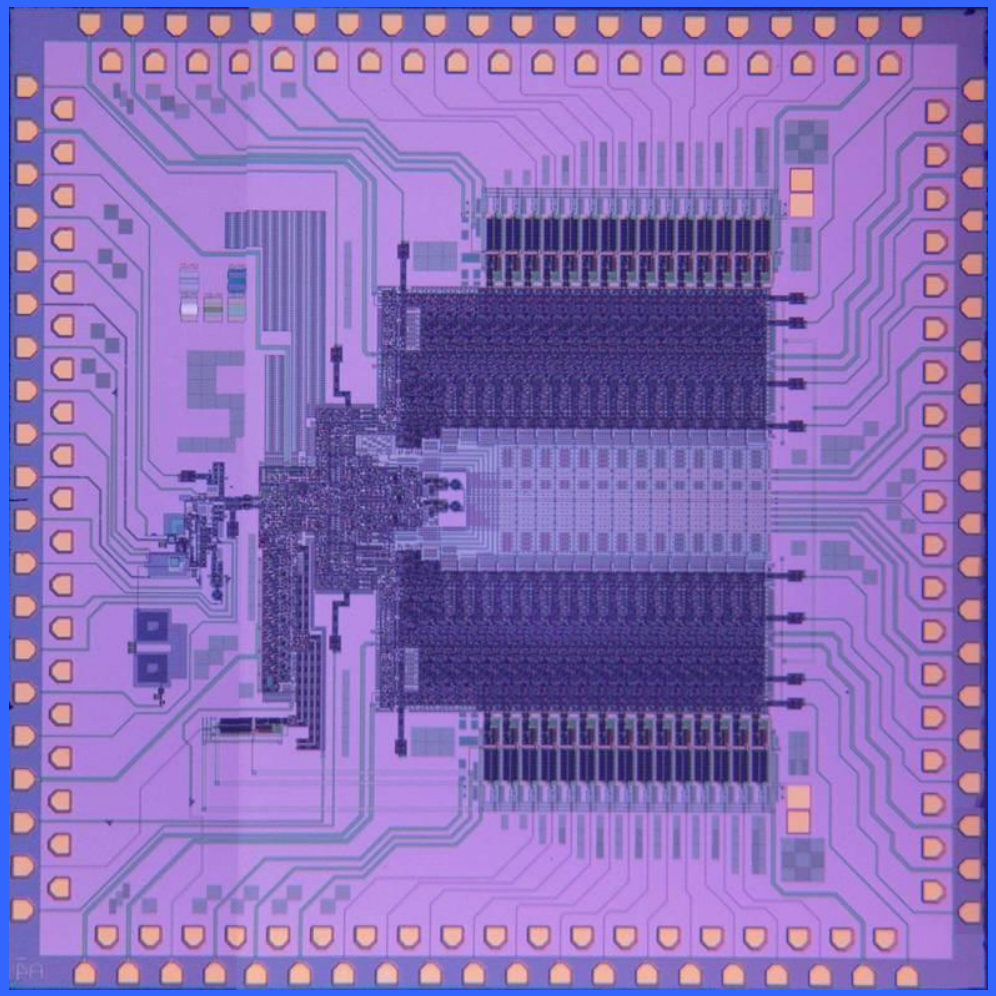

1 cm^2 chip, fabricated with HYPRES' standard Nb process with Jc = 4.5 kA/cm^2.

It contains :
- a bandpass delta-sigma ADC,
- a digital channelizer,
- output drivers.

5000 - 10 000 Josephson junctions.

Courtesy of Deep Gupta - HYPRES

Floating-point units (Japan)

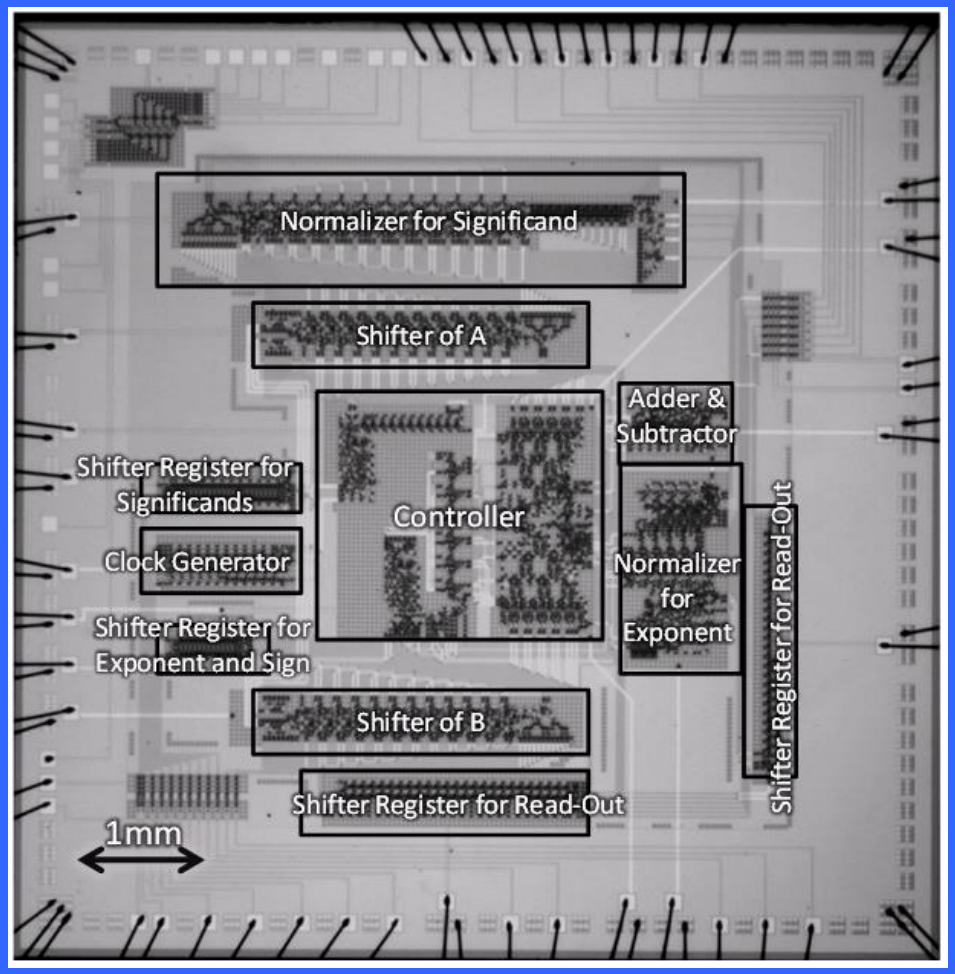

RSFQ half-precision floating-point adder (FPA) successfully demonstrated at 20 GHz.

Circuit size is 5.9 mm × 5.7 mm.

10224 Josephson junctions.

Performance is 1.67 GFLOPS.

Total power consumption is 3.5 mW.

Courtesy of Noboyuki Yoshikawa - University of Yokohama - Japan

Superconducting digital electronics integrated systems

Courtesy of Deep Gupta - HYPRES

Complete cryocooled digital-RF receiver system prototype, assembled in a standard 1.8-meter tall 0.5-meter wide equipment rack.

Using the modular packaging approach, the system can currently host variety of chips.

The system includes a two-stage 4-K Gifford-McMahon cryocooler manufactured by Sumitomo, two sets of interface amplifiers for connecting chip outputs to an FPGA board (placed behind the vacuum enclosure, on the metal tray) for further digital processing and computer interface. The system also includes a current source and a temperature controller.

An introduction to comparators

- **Semiconductor technology:** comparators based on operational amps have specifications that depend weakly on environment

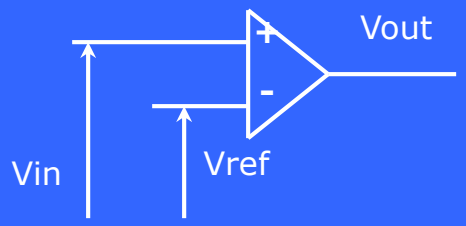

- **Superconductor technology:** comparators are based on Josephson junctions whose high non-linearity involves a design that is fully environment-dependent

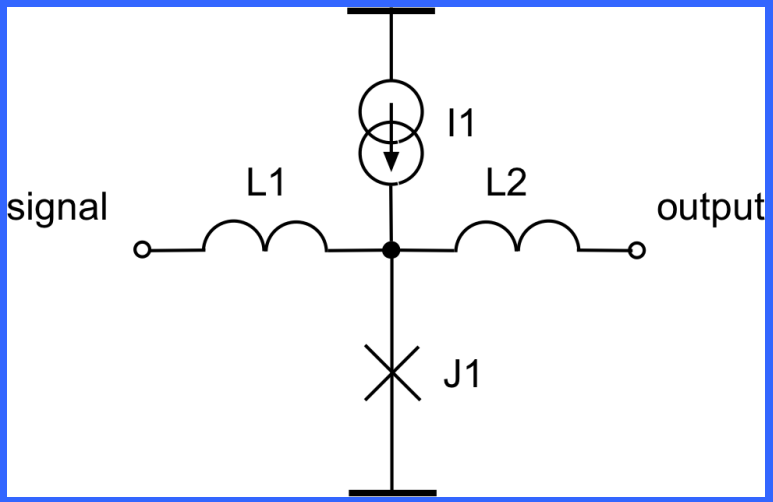

Analog-to-digital conversion with Josephson junctions

When Josephson junctions are shunted to be non-hysteretic and faster, digital information is stored in the magnetic flux quantum and requires a superconducting loop to be generated.

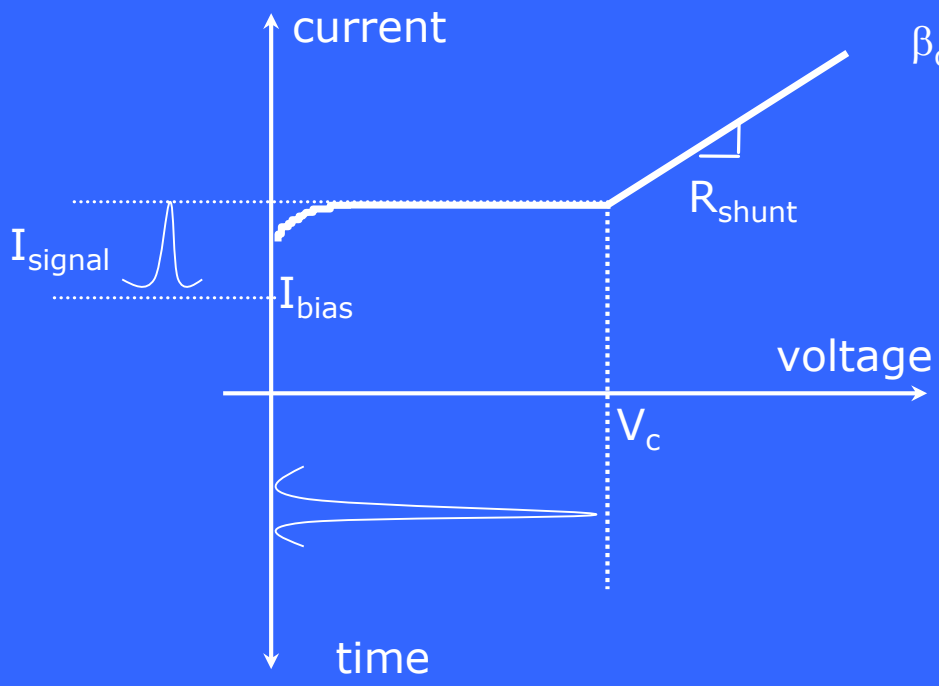

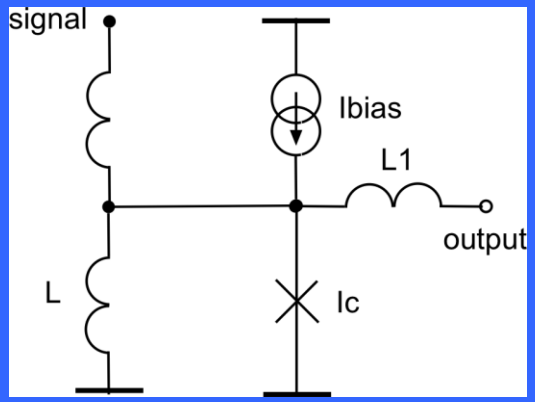

- Digital signal is based on two states, for a given time interval:
  - '0' : no pulse
  - '1' : one SFQ pulse
- Much faster than switching logic if shunt resistance is correctly chosen

The DC-to-SFQ interface used as a comparator

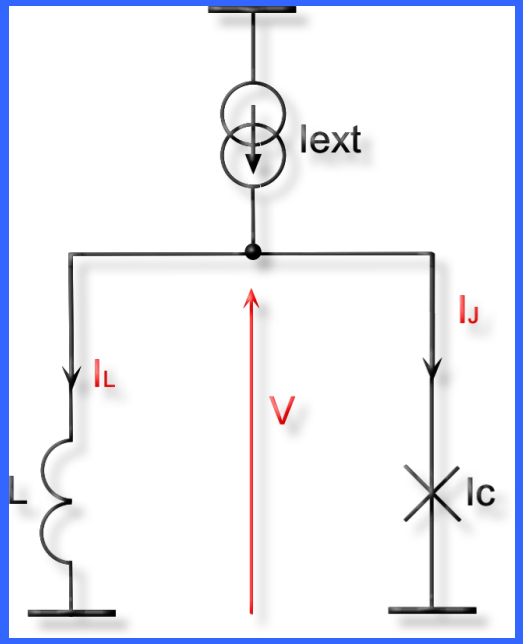

- The Josephson junction switches for specific values of I_{ext};
- It can be used to know I_{ext} at the switching instants;
- If the temporal form of I_{ext} is complex, the pulses are not equally spaced in time and the post-processing of digital data is complex.

- A pulse added to the signal to sense, and chosen to force triggering of the Josephson junction at a regular rate, transforms the DC-to-SFQ converter into a comparator.
- Then the generated pulse needs to be measured and processed.

The DC-to-SFQ interface used as a comparator

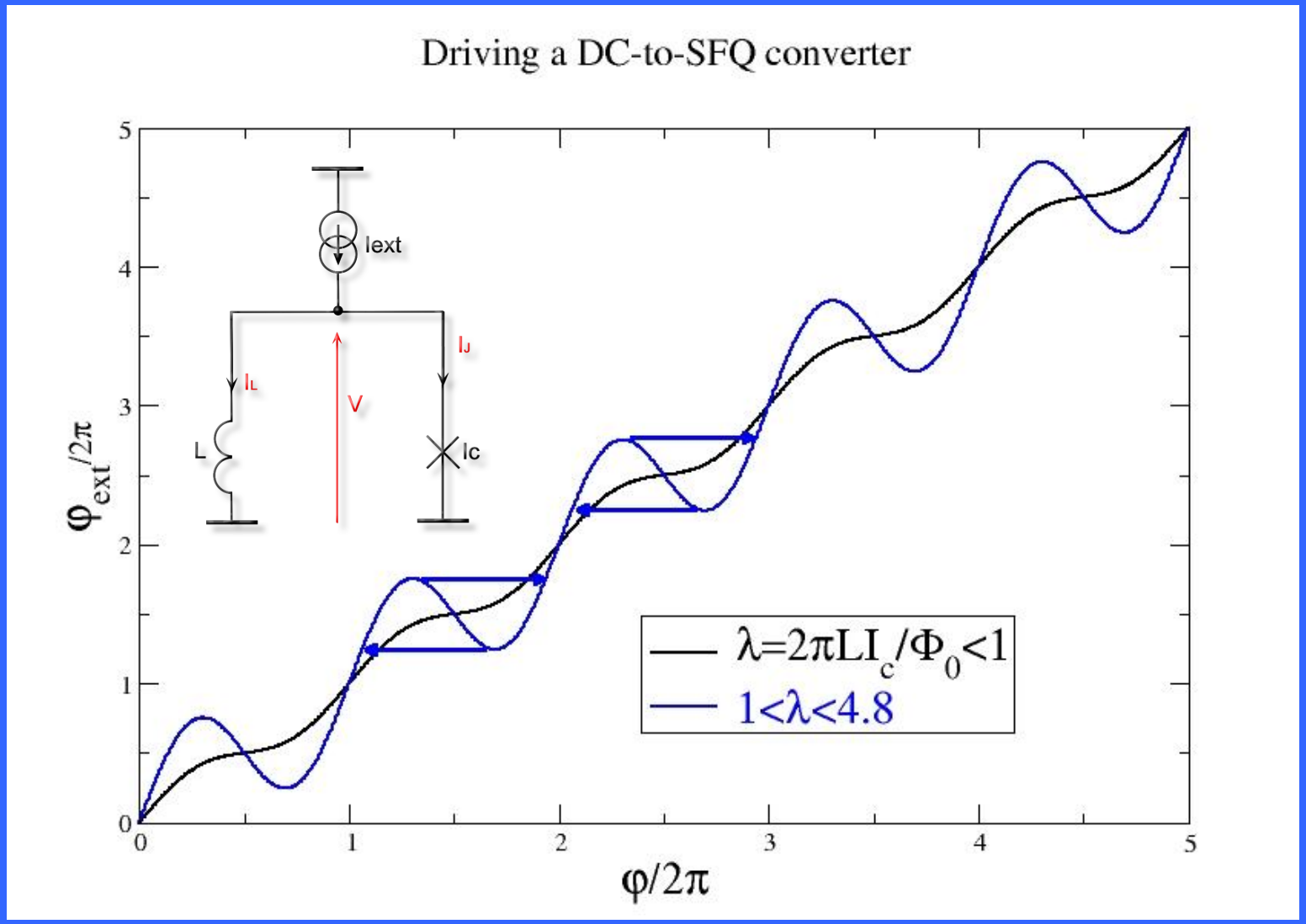

The DC-to-SFQ interface used as a QOJ comparator

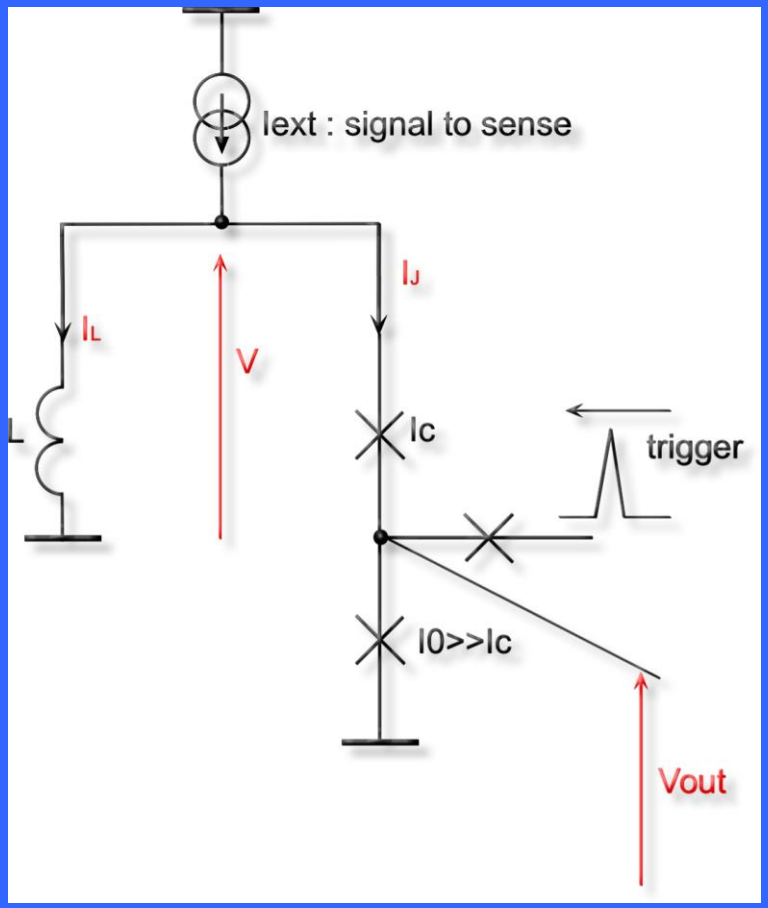

- The second junction is chosen to have a critical current much higher that the one of the comparator junction
- The device is a quasi-one-junction SQUID (QOJS): Ko & Van Duzer, 1988
- It is biased so that P(switching) = 50% in absence of signal
- Ko & Van Duzer, 1988
- Networks of such QOJS made for flash ADCs

- 6-bit ADC demonstrated (4 bits at 5 GHz and 3 bits at 10 GHz) : Bradley (1993)

The DC-to-SFQ interface used as a QOJ comparator

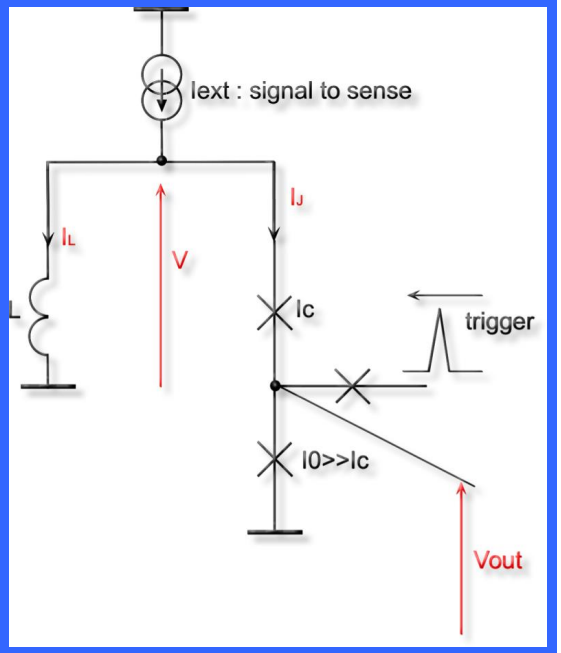

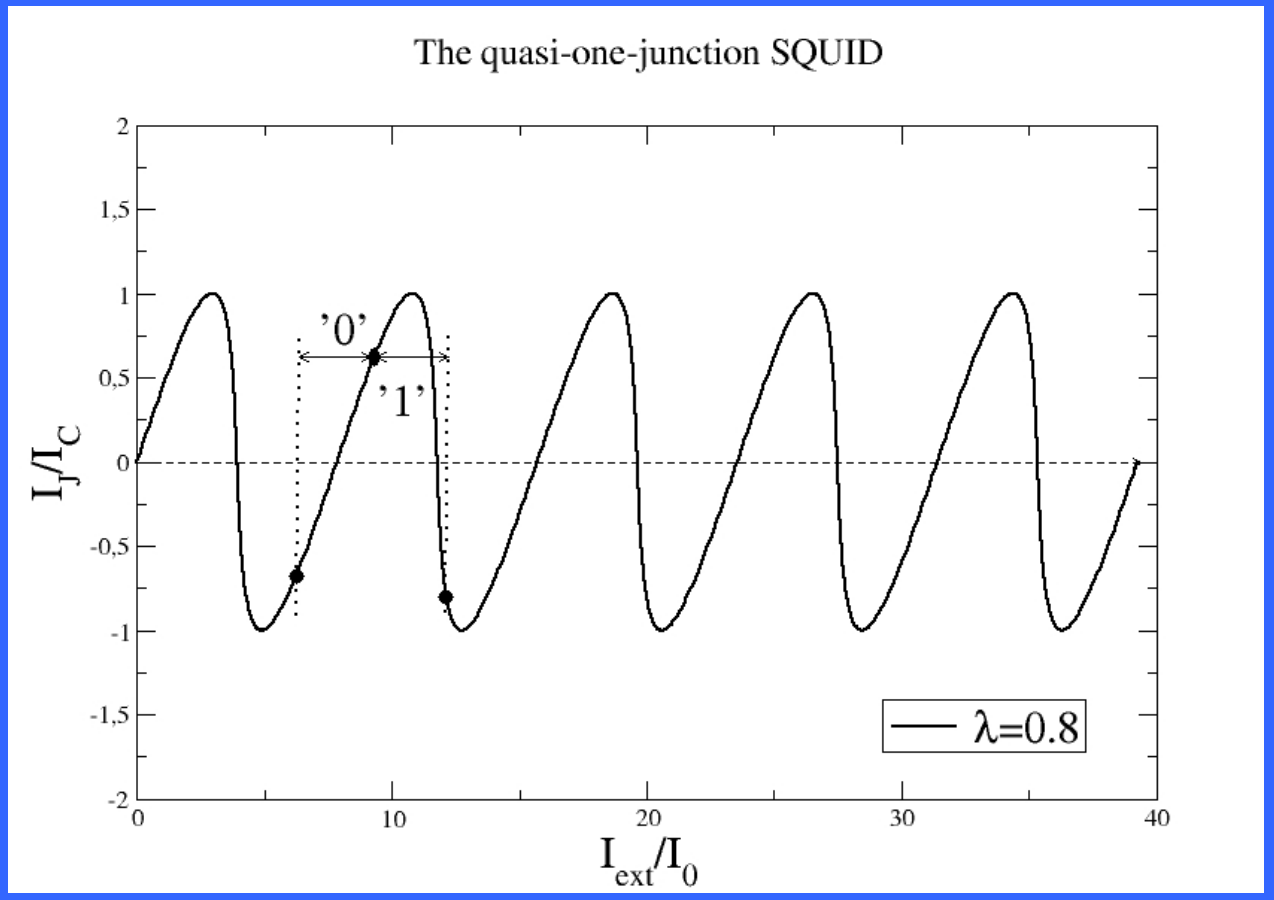

- 6-bit ADC demonstrated (4 bits at 5 GHz and 3 bits at 10 GHz) : Bradley (1993)

The SQUID comparator

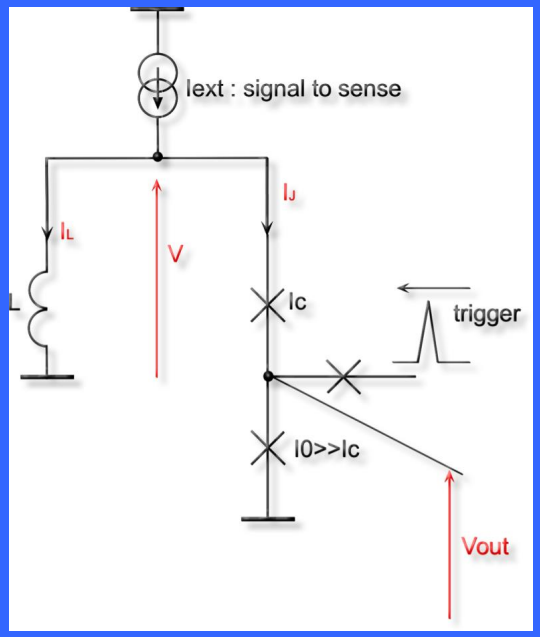

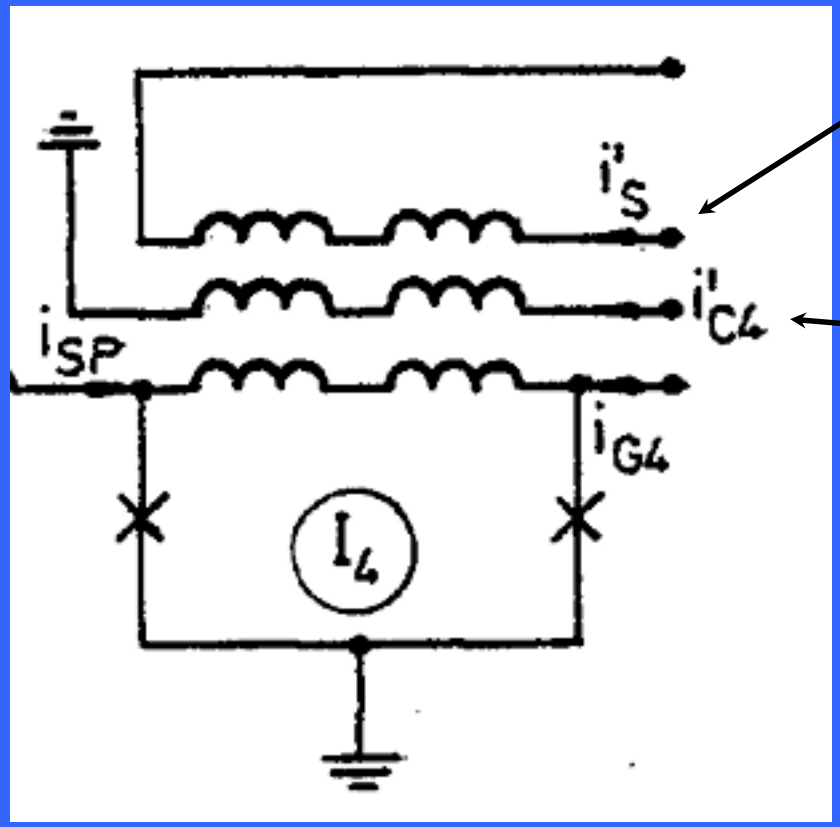

Kratz & Jutzi, 1985

The balanced comparator

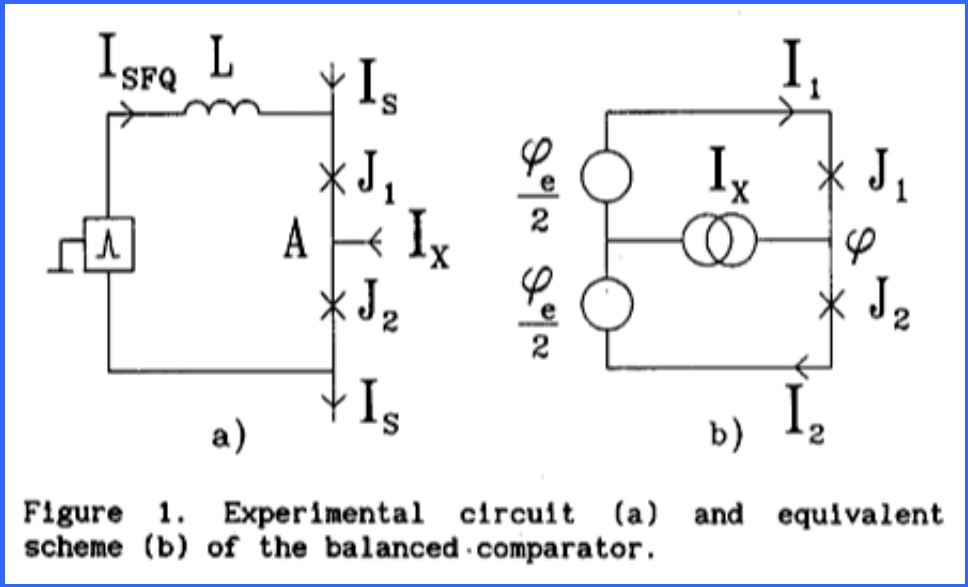

Figure 1. Experimental circuit (a) and equivalent scheme (b) of the balanced comparator.

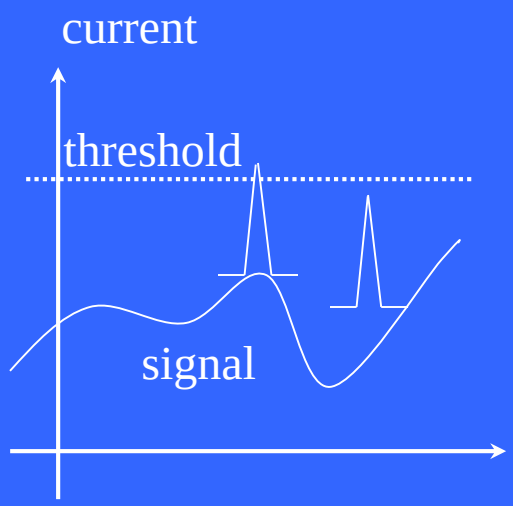

Filippov & Kornev, 1991

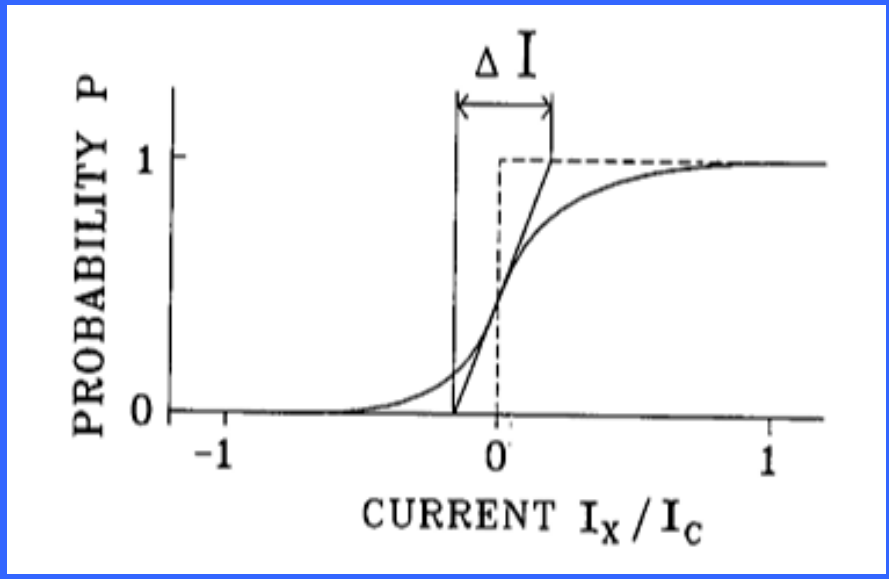

$$DI = \left| \frac{\partial P}{\partial I} \right|_{I=0}^{-1}$$

Parameters influencing the comparator resolution

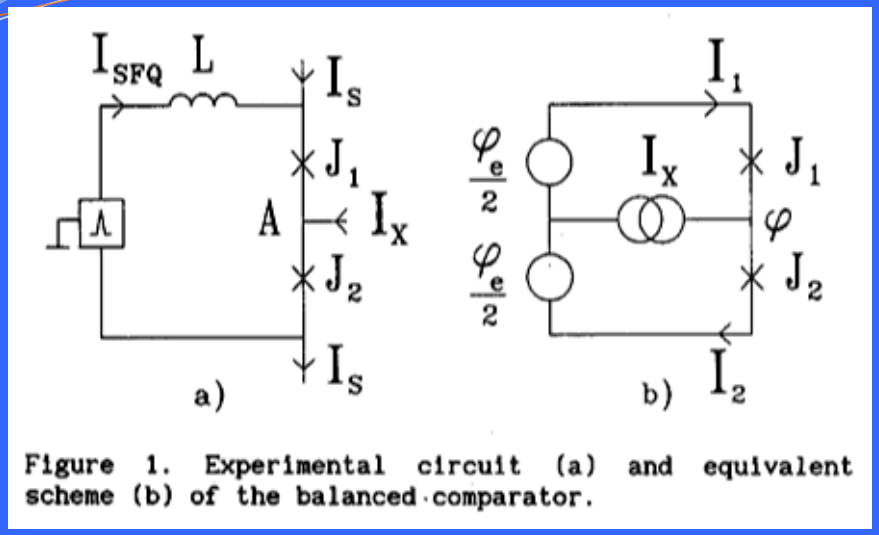

Figure 1. Experimental circuit (a) and equivalent scheme (b) of the balanced comparator.

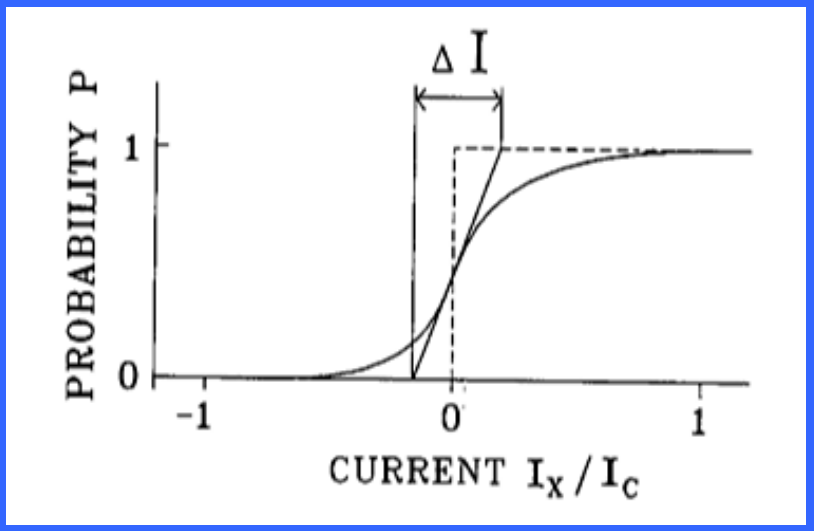

ΔI depends on:
- noise in the system (<-- temperature)
- trigerring pulse shape: time rise,…(<-- frequency of operation)
- JJ parameters (capacitance, McCumber parameter)
- loop inductances (and stray inductances)
- bias current
- environment impedance in a wide frequency range

The balanced comparator resolution

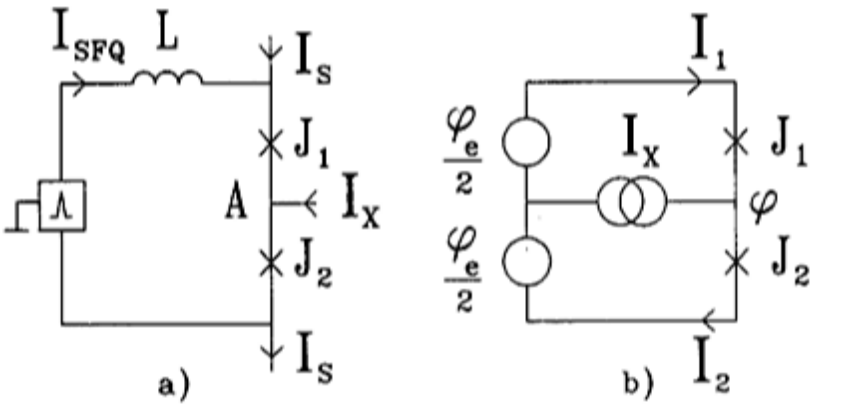

Figure 1. Experimental circuit (a) and equivalent scheme (b) of the balanced comparator.

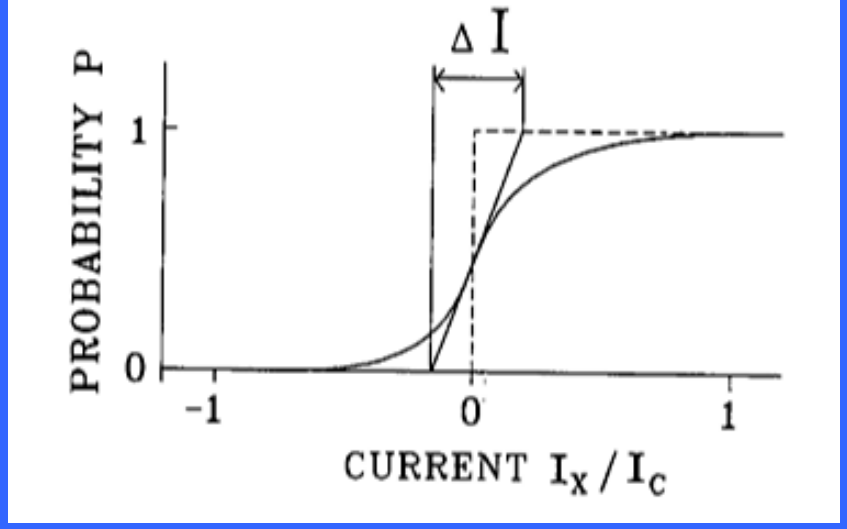

$$DI \propto I_c^{1/3} I_T^{2/3} \ln\left(a \frac{R_N I_c T}{a}\right)^{-1/3}$$

α is the switching rate

$$I_T = \frac{2ek_BT}{\hbar} = 0.04\mu A / K$$

The balanced comparator resolution

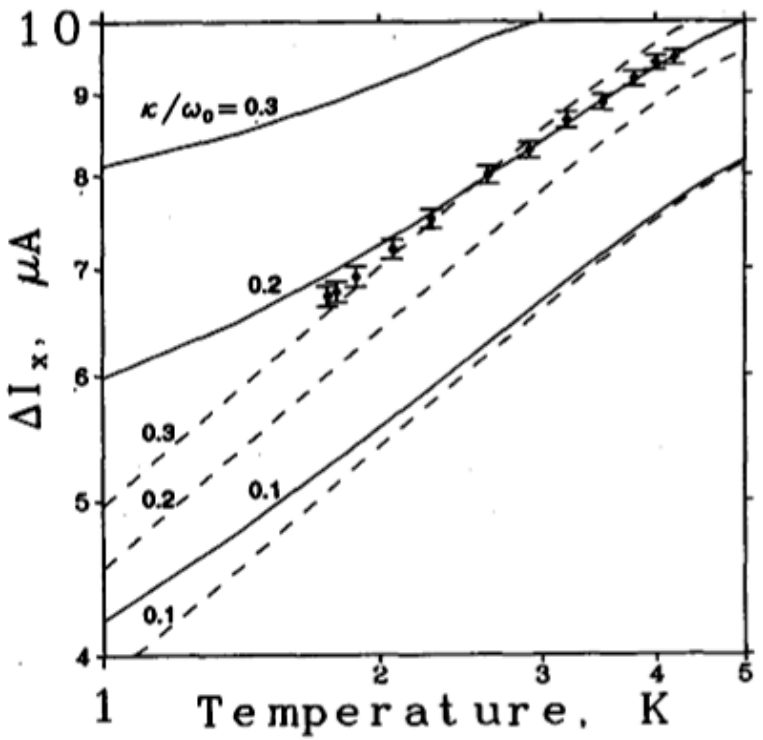

Fig. 4. Width of the switching probability distribution as a function of temperature. Points: experiment for chip# USB99, wafer 2440H, I_c(4.2K)=145 μA. Solid lines: theory for various values of the ratio κ/ω_0. Dashed lines: the same for purely thermal fluctuations ($\hbar\omega_0 << k_B T$).

Filippov et al, 1995

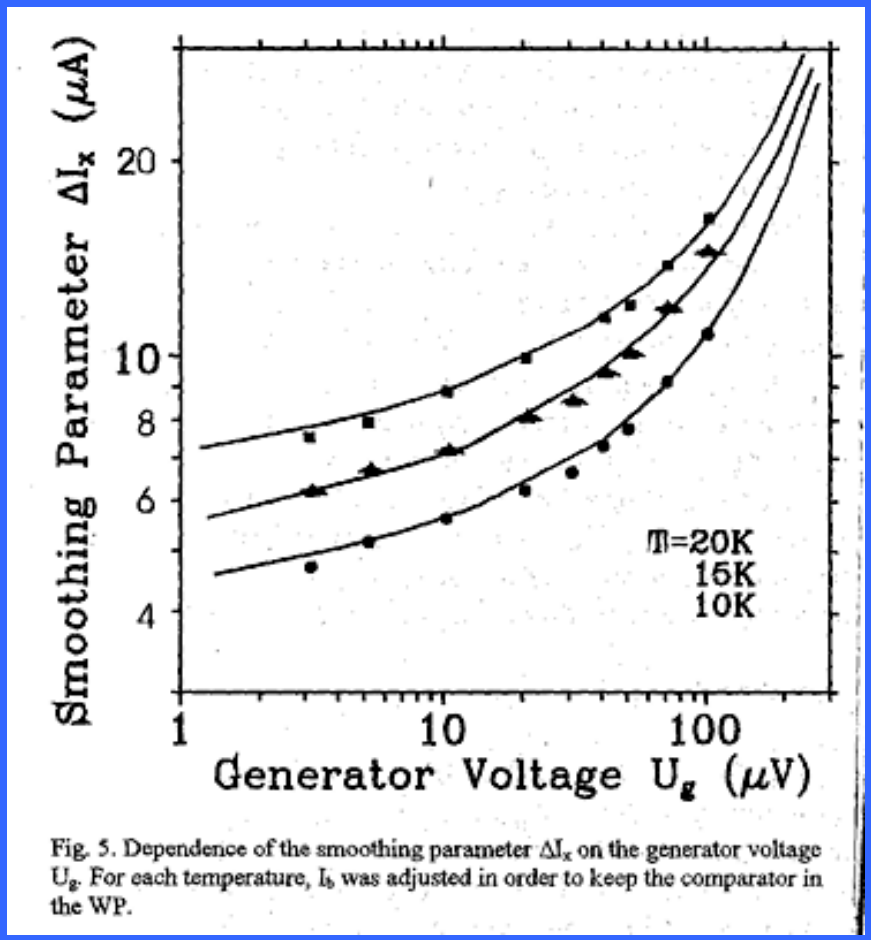

Fig. 5. Dependence of the smoothing parameter ΔI_x on the generator voltage U_g. For each temperature, I_b was adjusted in order to keep the comparator in the WP.

Oelze et al, 1997

The balanced comparator resolution

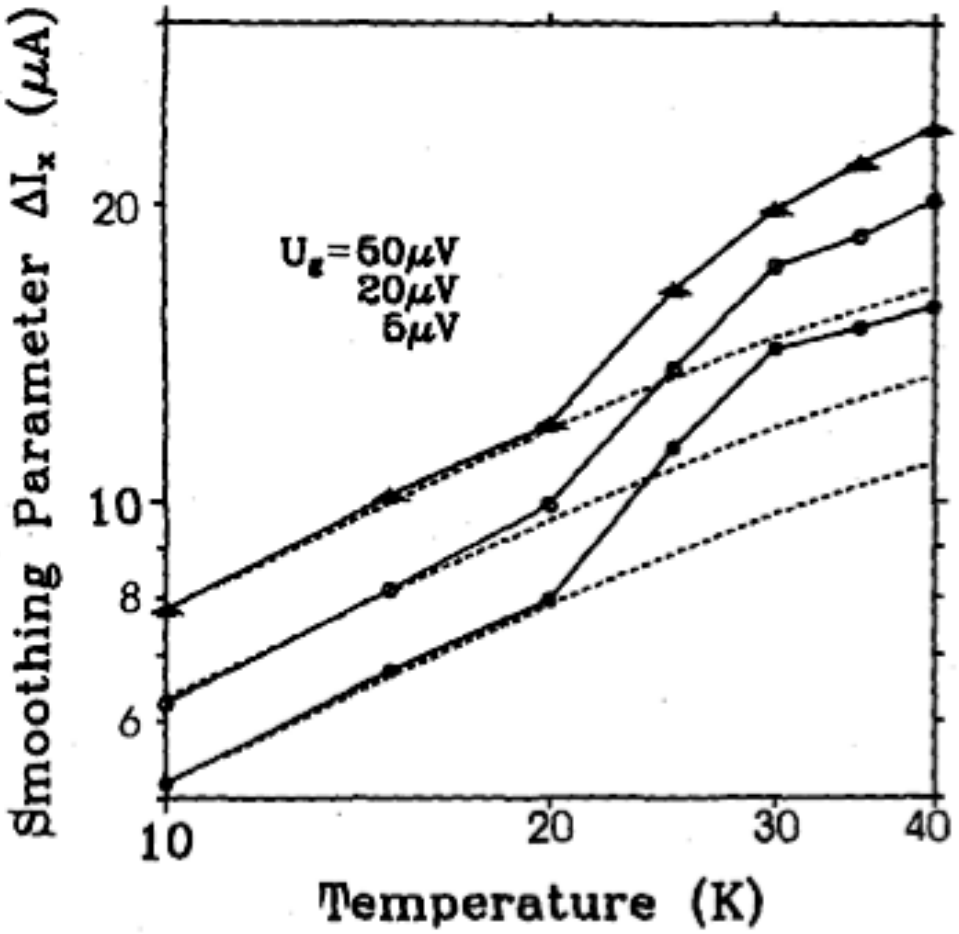

Fig. 6. Temperature dependence of the smoothing parameter; experimental data (solid lines, points) and theoretical results (dashed lines).

Oelze et al, 1997

The current knowledge on balanced comparators

- The influence of noise, shape of triggering pulse and speed is fully understood, even versus the input signal inductance

- The jitter of the device can be derived from this analysis

- Experiments and theory are in very good agreement regarding noise considerations (no extra noise needs to be added)

- The influence of the sensing impedance (in particular inductance) and of other parasitic elements in the sensing loop is still not totally sorted out (Gordeeva & Pankratov, JAP2008)

Sources of knowledge about Superconducting Electronics

Websites

The European Superconductivity News Forum (ESNF): http://www.ewh.ieee.org/tc/csc/europe/newsforum

http:// www.quantarctic.eu (under construction)

http:// www.fluxonics.eu (under reconstruction)

Books

A. Barone, G. Paternó, Physics and Applications of the Josephson Effect, John Wiley & Sons, 1982. ISBN: 0-471-01469-9.

T. Van Duzer, C.W. Turner, Principes of Superconductive Devices and Circuits, second ed., Prentice Hall PTR, Upper Saddle River, NJ, USA, 1998. ISBN: 0-13-262742-6.

K.K. Likharev, Dynamics of Josephson Junctions and Circuits, Gordon and Breach Publ., New York, 1986.

The SQUID Handbook, by John Clarke and Alex Braginski

Michael Tinkham, Introduction to Superconductivity, second ed., Dover Books on Physics, 2004. ISBN: 0-486-43503-2 Paperback.

Sources of knowledge about Superconducting Electronics

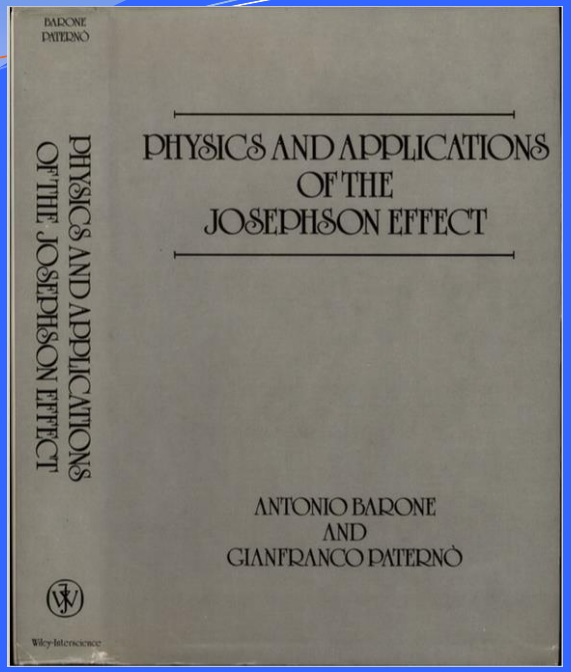

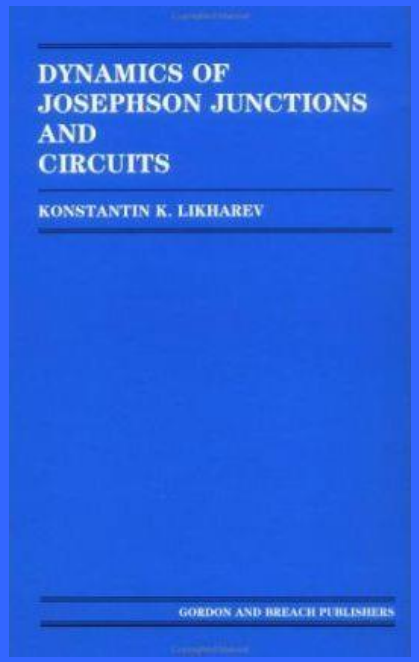

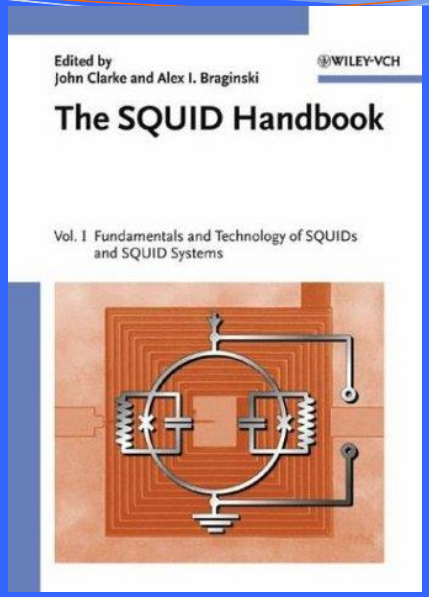

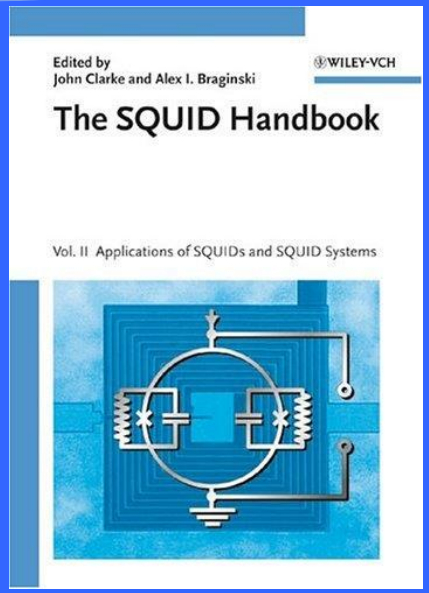

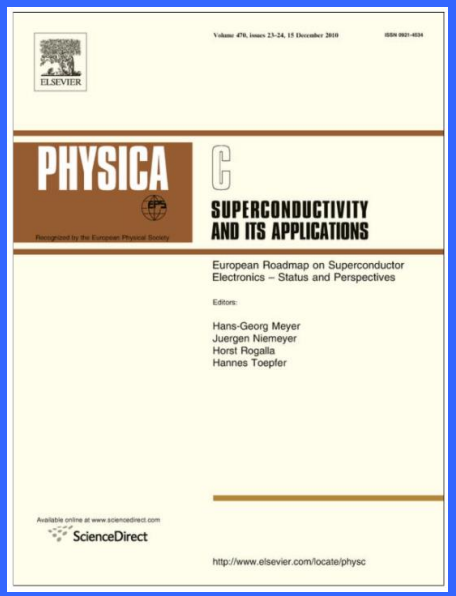

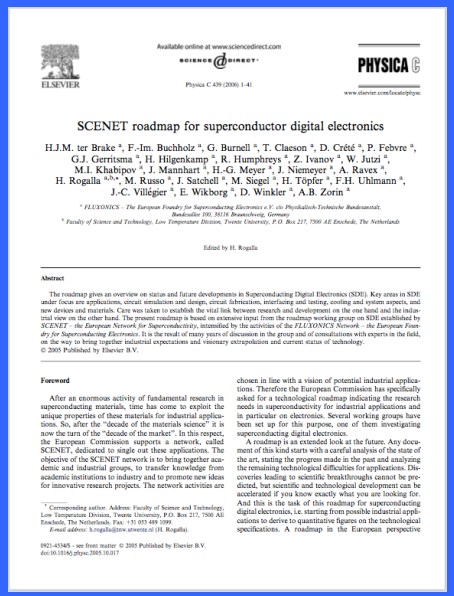

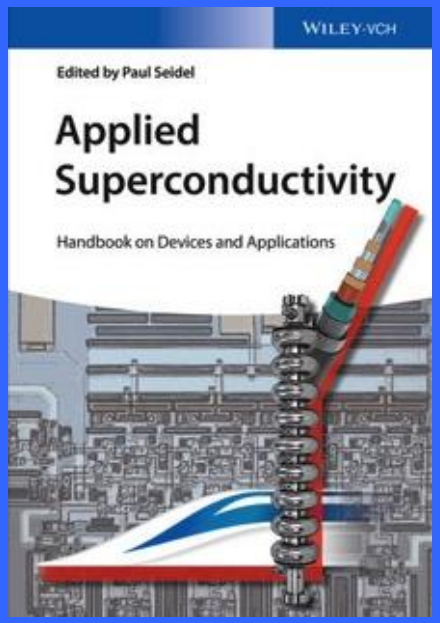

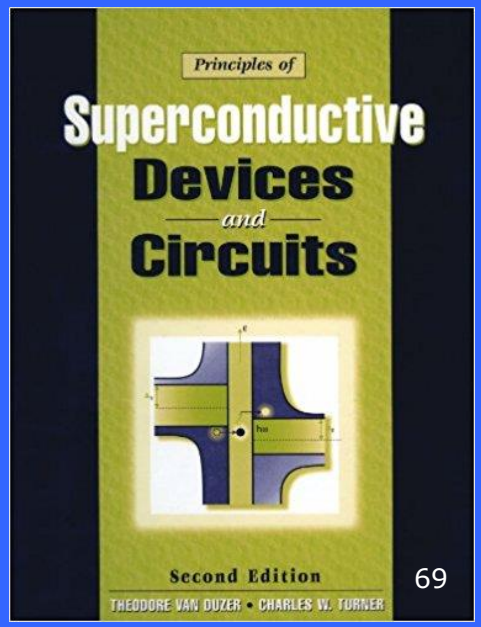

Sources of knowledge about SQUIDs

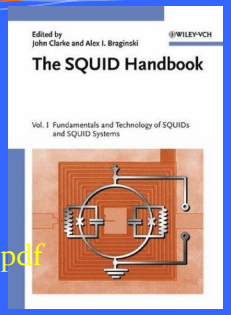

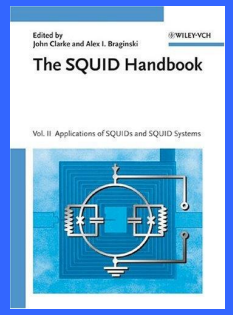

The SQUID Handbook, by John Clarke and Alex Braginski

The European Superconductivity News Forum (ESNF):
http://www.ewh.ieee.org/tc/csc/europe/newsforum

Volume 1 - Issue 1 - July 2007: *High-Performance dc SQUID Sensors and Electronics* by D. Drung et al
http://www.ewh.ieee.org/tc/csc/europe/newsforum/pdf/Drung_ESNF_PTB_Magnicon_final_0626071.pdf

Volume 2 - Issue 6 - October 2008: *section about SQUIDs, SQUIFs and related* -
http://www.ewh.ieee.org/tc/csc/europe/newsforum/Contents06.html

Volume 3 - Issue 8 - April 2009: *Recent SQUID Activities in Europe, Part I: Devices* by A. I. Braginski & G. B. Donaldson -
http://www.ewh.ieee.org/tc/csc/europe/newsforum/pdf/CR-12.pdf

Volume 3 - Issue 9 - July 2009: *Recent SQUID Activities in Europe, Part II: Applications* by A. I. Braginski & G. B. Donaldson -
http://www.ewh.ieee.org/tc/csc/europe/newsforum/pdf/CR12-II_Final_073009.pdf

Volume 4 - Issue 12 - April 2010: *Simplified Analysis of Direct SQUID Readout Schemes* by D. Drung
http://www.ewh.ieee.org/tc/csc/europe/newsforum/pdf/MT-21_ST188.pdf

Volume 5 - Issue 15 - Jan. 2011: *SQUIFs, Bi-SQUIDs & R-SQUIDs* - http://www.ewh.ieee.org/tc/csc/europe/newsforum/Contents15.html

Volume 5 - Issue 18 - Oct. 2011: *dc SQUID & SQIF Sensor with High Transfer Function Based on Sub-micrometer Cross-type Josephson Tunnel Junctions* by T. Schönau et al - http://www.ewh.ieee.org/tc/csc/europe/newsforum/pdf/KRYO-Schonau.pdf

Volume 6 - Issue 19 - Jan. 2012: *SQUID-based Systems for Co-registration of Ultra-Low Field Nuclear Magnetic Resonance Images and Magnetoencephalography* by A. Matlashov - http://www.ewh.ieee.org/tc/csc/europe/newsforum/pdf/ST289.pdf

Volume 6 - Issue 20 - April 2012: *SQUIDs: Then and Now* by John Clarke
http://www.ewh.ieee.org/tc/csc/europe/newsforum/pdf/issue20-Clarke.pdf

---

Superconductor Science and Technology - Volume 22 - no. 6 - June 2009 - *Special section: focus on nanosquids and their applications* -
http://iopscience.iop.org/0953-2048/22/6

Thank you for your attention !

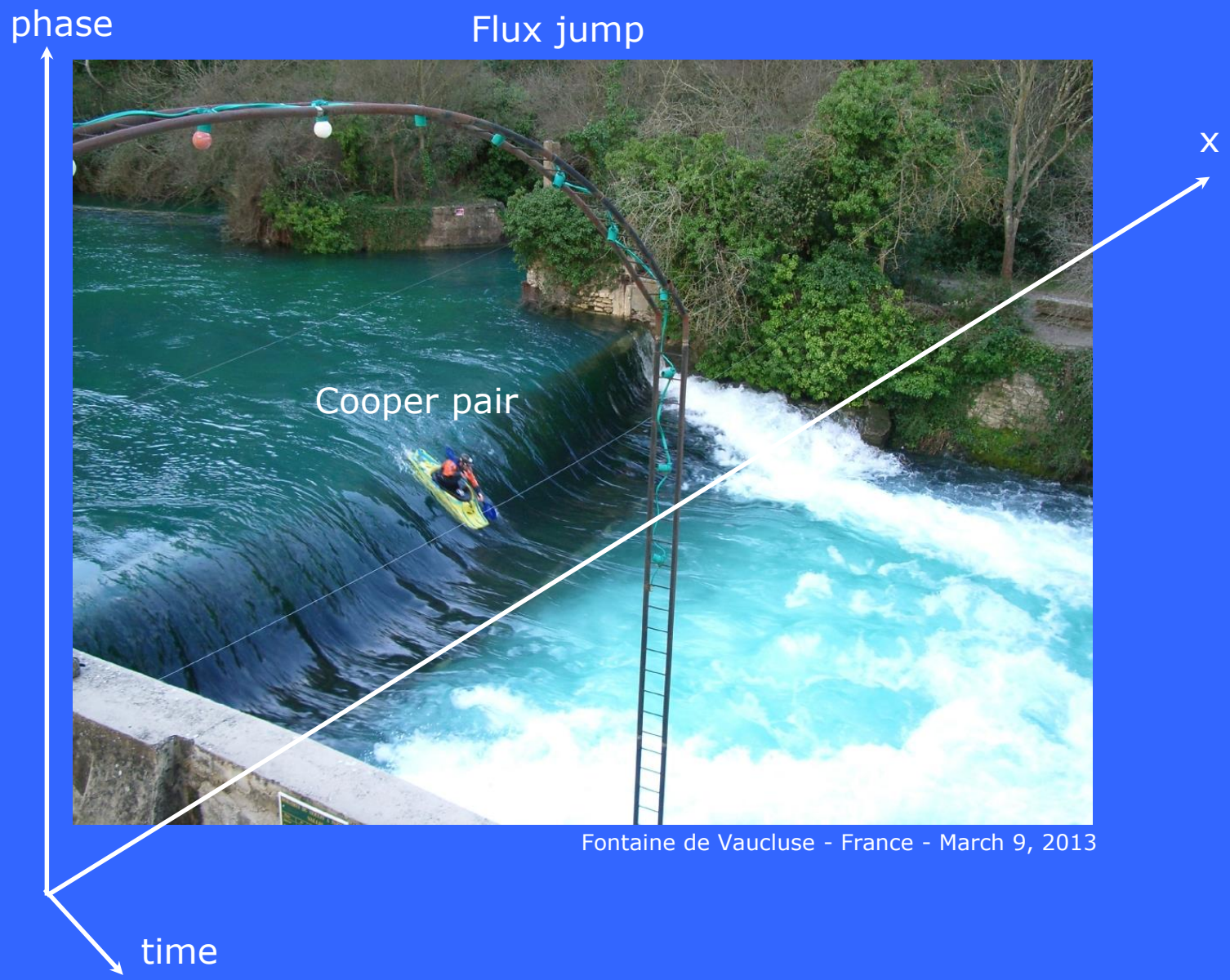

Fontaine de Vaucluse - France - March 9, 2013